

UNITED STATES DEPARTMENT OF THE INTERIOR
GEOLOGICAL SURVEY

Electrical-Resistivity Investigation
of the
Schofield High-Level Water Body, O'ahu, Hawai'i

by

Jim Kauahikaua
Honolulu, Hawaii

and

K. V. Shettigara
Department of Geology and Geophysics
University of Hawaii

Open-File Report 84-646

This report is preliminary and has not been reviewed for conformity with U.S. Geological Survey editorial standards and stratigraphic nomenclature.

1984

ABSTRACT

A total of 19 Schlumberger resistivity soundings and 3 resistivity gradient profiles were made to study the high-level water body beneath the Schofield plateau in central O'ahu. The soundings yield much detail on the thick weathered zone overlying unweathered rock over the entire area. They also delineate areas which are underlain by a conductor interpreted to be salt-water saturated rock outside the high-level aquifer. Within the aquifer, the basement conductor is not found. Secondly, the results indicate that the aquifer may be impounded by buried ridges of the Waianae volcano.

INTRODUCTION

The Schofield high-level water body is an important component of O'ahu's ground-water system. Within this body, ground-water levels are approximately 80 m above sea level whereas levels in immediately adjacent areas are less than 10 m above sea level. Leakage from this water body contributes an estimated 115 million gallons per day (mgd) of 200 to 250 mgd total input to the Pearl Harbor aquifer to the south and an estimated 18 of 55 mgd total input to the Waialua basal aquifer to the north (Dale and Takasaki, 1976). Although large municipal and agricultural demands are already made on these adjacent aquifers, increased demands are projected. More information about the location and nature of the structures bounding the Schofield water body is needed to estimate the size of the resource and the maximum level of utilization which will avoid permanent damage to the aquifer.

The Schofield high-level water body is located approximately beneath the highest part of the Schofield plateau on the island of O'ahu, which was formed by lavas from the younger Koolau volcano to the east flowing up to and being diverted along the front of the older Waianae volcano to the west (Stearns and Vaksvik, 1935); elevations within the study area exceed 225 m. No dikes or other geologic evidence are exposed in the gulches of the central plateau to help explain the high-level water there.

To provide subsurface information, a non-seismic geophysical survey was undertaken between April and June, 1982 covering the central Schofield plateau area. The largest obstacle for field surveys was expected to be interference (radio transmissions, pipe and power lines, unmapped underground installations, etc.) from intense military and municipal activity immediately over the high-level water; therefore the initial goal was to determine which of following techniques would be the most useful under these conditions: electrical-resistivity sounding and profiling, time-domain electromagnetic sounding, self-potential profiling, and total-field magnetic profiling.

Once the techniques were evaluated, the survey was to continue obtaining preliminary information with one or more of these techniques over the entire area. The goals of the project were to:

1. locate the northern and southern boundaries of the high-level aquifer more accurately,
2. determine the nature of the boundaries, and
3. study the regional, hydrogeologic setting of the high-level aquifer within the Schofield plateau.

Only the results of the electrical-resistivity sounding and profiling are presented in this report. The complete results of this study will be the subject of a second report.

DESCRIPTION OF RESISTIVITY TECHNIQUES USED

Resistivity is one of the most useful geophysical properties on which to base ground-water exploration because the resistivity of a rock varies with its water content and the quality of the contained water and because it is possible to determine the resistivities of deeply-buried rock units from surface measurements. Once the resistivity of the rock units are determined, gross physical properties like porosity, water quality, etc., can theoretically be estimated (Keller and Frischknecht, 1966). Resistivity methods are actually unique among surface geophysical methods in providing information concerning the presence and quality of water and are extensively used for determining the depth of fresh-salt water interfaces.

In resistivity prospecting, electrical current is passed into the earth through two electrodes, designated A and B. The difference in potential between any two points can then be measured using two more electrodes, designated M and N. For the electrode configurations described in this report, the electrodes are arranged in the order AMNB in a straight line. From the relative locations of the electrodes, a correction or geometrical factor can be computed which, when multiplied by the ratio of potential difference divided by the current through electrodes A and B, would produce a value identical to any which is produced by any other electrode configuration over a homogeneous halfspace and which is corrected similarly. For a homogeneous halfspace, that value is equal to the resistivity of the halfspace. For the more general case, the value is called an 'apparent resistivity' and it is the field data to be interpreted. Data are gathered by moving the electrodes and remaking the measurements, in one of two modes - sounding or profiling.

Resistivity Sounding

A resistivity sounding consists of a series of apparent resistivity measurements taken at several different electrode positions created by expanding the electrode array symmetrically about a central point, preferably along a straight line. Larger AB (current electrode) separations generally force deeper current penetration; thus, it is possible to control the depth of investigation by varying the current electrode separation.

Several configurations can be used for sounding; the best known is the Schlumberger electrode array used in this study in which the distance between electrodes M and N is kept smaller than one-fifth of the AB separation. Anomalies due to local inhomogeneities are minimized by moving either the MN pair of electrodes or the AB pair between readings, but not both at the same time. In practice, the MN electrode pair is moved once for every four or five AB electrode pair moves and the apparent resistivity is remeasured. For this survey, electrodes A and B were placed at logarithmically larger distances outward from the center (i.e. ... 10, 13, 16, 20, 25, 30, 40, 50, 65, 80, 100, 130, ...) while electrodes M and N were moved only when the distance $AB/2$ equalled decimal multiples of 10 and 30 (i.e., ... 10, 30, 100, 300, 1000, ...). At those points the distance $MN/2$ would be the same decimal multiple of 2 and 6, respectively. Expansion of the MN electrode pair is necessary in order to increase the voltage measured between them and to make the measurement more accurate. Values measured for the same AB separation with two different MN separations are almost always slightly different, perhaps due to small inhomogeneities around the electrodes; the data require reduction to remove this discrepancy before quantitative interpretation.

The reduction method used in this study involves multiplying each data segment (apparent resistivity values measured with the same MN electrode spacing) by a factor which may be different for different segments. Many conventions can be used for deciding to what base segment the rest will be shifted. For the Schofield data, all segments are shifted to the segment measured with the largest MN spacing; that is, the segment measured with the largest MN spacing is held fixed and the endpoints of the other segments are adjusted so that their endpoints match.

Application to the Schofield Area

Two previous resistivity sounding surveys have demonstrated that depth to the conductor, which is thought to represent salt-water saturated rock, 1) increases abruptly from outside the high-level aquifer going into it (Swartz, 1940), and 2) is quite deep just to the north of the high-level water body becoming shallower towards the coast (Zohdy and Jackson, 1969). More complete coverage with resistivity soundings in and around the target aquifer could map its boundaries and thereby fix the location of the impounding structures more accurately. In addition, the results could add information about shallower geologic features, like faults and weathered zones separating younger Koolau from older Waianae basalt formations.

Electrical-resistivity profiling

Lateral changes in resistivity can be found by moving a fixed electrode configuration from point to point along a line and generating a profile (normal profiling). A set of measurements represent an approximately-constant depth of investigation. For small depths of investigation, normal profiling can be fast and accurate. For larger depths of investigation (requiring larger current electrode separations), movement of the normal setup is difficult; for such cases, a variation on normal profiling known as gradient profiling is a good substitute. In gradient profiling, only the potential electrodes are moved within the central one-third of the distance between two stationary current electrodes. Even large current electrode separations can be measured quickly; however, the depth of investigation is different at each measurement station.

The primary focus of this study is the lateral change of the depths to salt-water saturated rock (represented in previous sounding studies by a low-resistivity layer at a depth usually greater than 400 m in this area); therefore, gradient profiles

Resistivity Investigation
Schofield, O'ahu

Kauahikaua & Shettigara

with current electrode separations of approximately 4 km were planned.

INTERPRETATION OF THE DATA

A total of 19 soundings and 3 profiles were conducted (see Figure 1 for locations) in the central Schofield plateau. Of these soundings, number 8 was not completed because the data appeared distorted, probably by a shallow, buried metal pipe known to be nearby. Nevertheless, all 19 soundings were interpreted with the aid of computer program MARQDCLAG_HP (see Appendix A) to find the closest matching horizontally-layered earth model; the structural interpretation of the Schofield area is based on a compilation of these layered-earth models. The interpretation of the profiling data presented in this report is of a very qualitative nature.

Electrical-Resistivity Sounding Data

The shifted sounding data sets were first interpreted using the manual curve-matching technique which involves finding the closest matching theoretical curve in a standard album of such curves. Catalogues of three-layer curves are readily available; curves for four or more layers may be graphically constructed from two- or three-layer curves using the 'auxiliary point method' (Bhattacharya and Patra, 1968). The resulting interpretation determines the model parameters corresponding to that theoretical curve. Results suggested that a minimum of 4 and as many as 7 layers may be required to adequately model the sounding data sets.

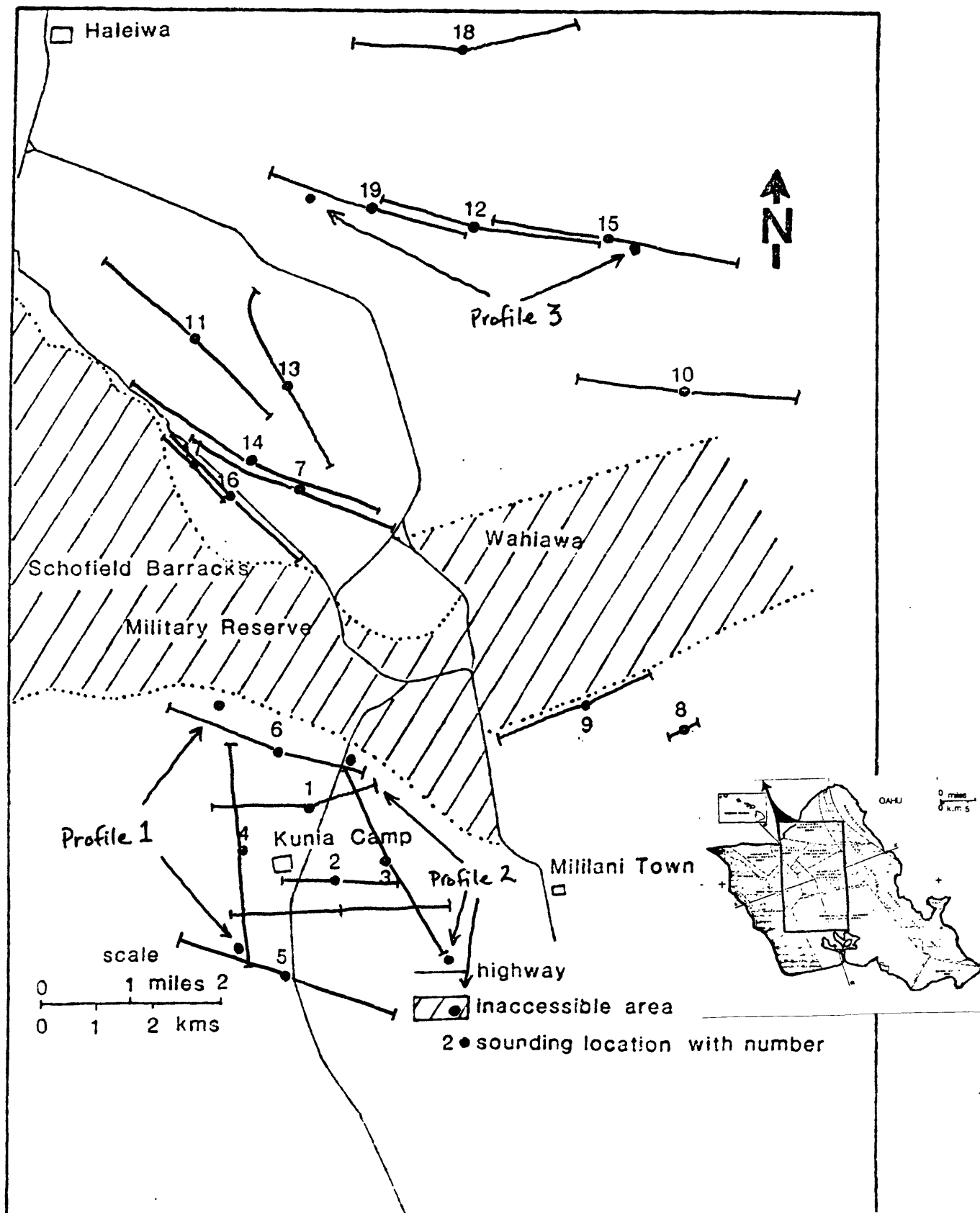


Figure 1

Map of central O'ahu, Hawai'i showing the Schofield plateau area including Schofield Barracks and the town of Wahiawa. Superimposed on this are the locations of 19 Schlumberger soundings and three Gradient profiles.

TABLE I.
REDUCED CHI-SQUARED STATISTIC FOR INVERSIONS

SDG	4-layer	5-layer	6-layer	7-layer
1	12.16	<u>10.57</u>	11.92	
2		<u>18.73</u>	23.91	
3	44.76	4.99	<u>4.32</u>	4.85
4		<u>9.05</u>	14.33	
5		<u>32.86</u>	42.54	
6		<u>6.60</u>	9.19	
7		12.74	<u>5.23</u>	
9	<u>47.85</u>	55.04		
10	<u>13.37</u>	14.58		
11		<u>18.89</u>	25.06	
12		<u>50.31</u>	66.92	
13		<u>12.88</u>	13.90	
14		<u>12.93</u>	15.27	
15		<u>14.38</u>	17.73	
16		10.88	<u>6.63</u>	
17		10.35	<u>7.84</u>	
18		<u>26.38</u>	29.88	
19		<u>22.69</u>	32.42	

The models obtained by curve-matching were used as starting models for the computer inversion program MARQDCLAG_HP. Initially, no constraints were imposed on any of the geoelectric parameters and all the sounding data sets were interpreted using 4-, 5-, 6-, and/or 7-layer models. The decision regarding what order of complexity (number of layers) was warranted in each interpretation is based on the minimum reduced chi-square statistic (Appendix A) summarized in Table I for each sounding data set and the models that were fit to it. Normally, the chi-square statistic decreases as more layers are included in the model; at some point, however, adding layers to the model slows the decrease and actually causes the chi-square statistic to increase. We choose the warranted complexity to be the point at which the chi-square statistic is a minimum. Although not shown in Table I, the chi-square statistic normally decreases by almost one-order of magnitude for each layer added to an under-specified model. The chi-squared values for the chosen models are underlined in Table I. On this basis, four-layer models are chosen for soundings 9 and 10, five-layer models for soundings 1,

1
2, 4, 5, 6, 11, 12, 13, 14, 15, 18, and 19, , and six-layer models for soundings 3, 7, 16, and 17. The majority of the sounding interpretations had a relatively conductive first layer, slightly resistive second layer, relatively conductive third layer, resistive fourth layer, conductive fifth layer, and, where included, a resistive sixth layer. During the course of the computer inversions, several of the layer resistivities and thicknesses were assigned unrealistically high or low values by MARQDCLAG_HP. This phenomena is a property of the unconstrained inversion for parameters which cannot be resolved very well for one or more of the following reasons:

1. insufficient data for that depth range,
2. noise in the field measurements,
3. poor initial guess of model parameters prior to inversion,
4. incorrect assumptions about the layers being horizontal and homogeneous,
5. the layer is thin and its resistivity is much larger or smaller than the resistivities above it (the equivalence phenomena).

Good field technique can minimize the effects of the first two causes. Use of several different initial parameters guesses can eliminate the effects of the third item. As for the fourth item, the real earth is never a homogeneous, horizontally-layered halfspace, but for most purposes it can be usefully approximated as one. The effect of the differences between the real earth and this theoretical abstraction can be qualitatively assessed by conducting crossed soundings or comparison of several soundings in the same area. A set of soundings that have significant similarities, like the Schofield set, would indicate that the homogeneous, horizontally-layered halfspace is a good approximation to the actual geologic conditions in that area. Crossed soundings were not practical in this area.

The problem of equivalence is inherent to direct-current electrical prospecting methods (see Appendix B). Its effects are

1. sounding 13 actually could be fit by either a 5- or 6-layer model, depending on how one decides the distribution of data errors; the 5-layer model is chosen here.

a consequence of the prospecting technique used and cannot be eliminated during interpretation. The best that can be extracted for an 'equivalenced' parameter are its upper and/or lower bounds. By doing several computer inversions each with the parameter in question held fixed to a different value, an approximate range of values can be established for which the fit of model to data was not affected. Appendix C shows final inversion results for each sounding; equivalenced or poorly resolved parameters that were fixed during computer inversion are explicitly noted.

Resistivity Gradient Profile Data

Practical, quantitative methods for interpreting profiling data have not yet been developed; however, we can draw some tentative conclusions from comparison of the profiling data with a theoretical gradient profile over a layered halfspace with the same geoelectric parameters as interpreted from nearby soundings. Three gradient profiles were run in the study area (Figure 1).

Figure 2 compares profile 1 data with theoretical curves representing the models interpreted for soundings 1, 3, 4, and 6. For the central and northern sections of data, the closest matching theoretical curve corresponds to the model interpreted from sounding 6. The southern data section has apparent resistivities which are lower in value than the sounding 6 theoretical curve, suggesting a transition from a model like sounding 6 in the north to a model more like that interpreted from sounding 4 in the south.

Figures 3 and 4 compare profile 2a and 2b data with theoretical curves representing the models interpreted for soundings 1, 3, 4, and 6. Three different symbols are used to represent data taken on three different days demonstrating the lack of repeatability with the equipment used. Taking this into account, the closest match corresponds to the model interpreted from sounding 4. The theoretical curves for models from soundings 1, 3 (which is the closest), and 6 have apparent resistivity values which generally exceed the data values throughout the profile.

Figure 5 compares profile 3a with theoretical curves representing the models interpreted for soundings 12, 15, and 19. Again, different symbols represent measurements made on different days. For profile 3, repeatability is somewhat better than for profiles 2a and 2b. The data are generally below the theoretical curve for the sounding 15 model and above the theoretical curves for the sounding 12 and 19 models. In general, the impression one is left with is that the profile 3 data are closer to the sounding 12 and 19 theoretical curves, but with significant, narrow, resistive anomalies superimposed.

With the exception of sections of profile 1, the profiling data, like the sounding data, suggest that the studied areas are underlain by a conductor. Resolution is not sufficient to contribute any information on shallower structure.

Schofield, O'ahu: Gradient Profile 1

VES 1 MODEL:

RHO (ohm-m)	30.80	168.40	47.50	400.00	183.60
H(M)	2.90	10.30	85.10	82.70	

VES 3 MODEL:

RHO (ohm-m)	76.20	126.50	48.70	598.60	231.60	23.20
H(M)	3.20	10.10	68.60	95.60	823.60	

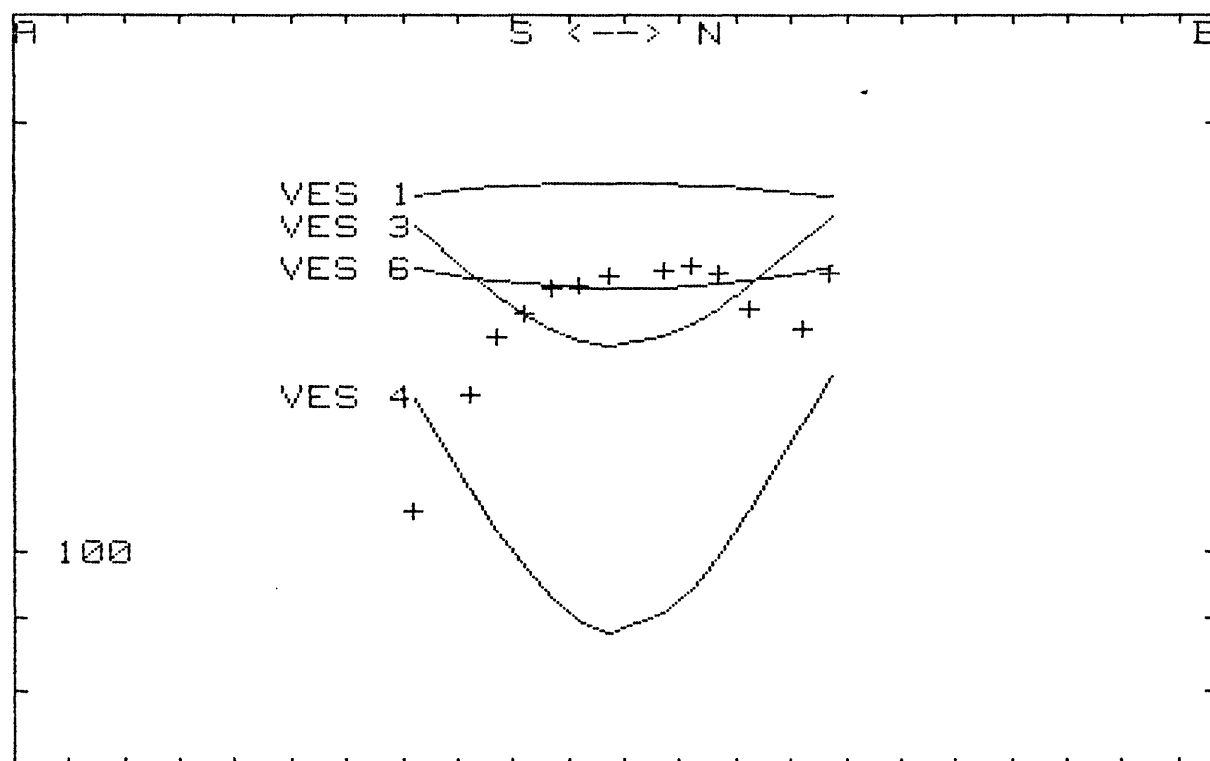
VES 4 MODEL:

RHO (ohm-m)	20.90	183.60	67.50	320.00	.30
H(M)	1.20	2.40	108.60	582.70	

VES 6 MODEL:

RHO (ohm-m)	49.40	173.00	72.70	400.00	145.20
H(M)	2.80	12.40	91.80	108.10	

AB= 4344 MN= 300



HORIZONTAL TICK INTERVAL = 200 M

APPARENT RESISTIVITY (OHM-M) PLOTTED AT CENTER OF MN PAIR

Figure 2 A semi-logarithmic plot of the apparent resistivity data from gradient profile 1. Current electrode separation was 4344 m and the potential electrode separation was 300 m. The potential electrodes were moved a distance of 100 m between measurements and the resulting apparent resistivity was plotted at the center of the potential array. Solid lines represent theoretical values over horizontally-layered models interpreted from nearby sounding data.

Schofield, O'ahu: Gradient Profile 2a

VES 1 MODEL:

RHO(ohm-m)	30.80	168.40	47.50	400.00	183.60
H(M)	2.90	10.30	85.10	82.70	

VES 3 MODEL:

RHO(ohm-m)	76.20	126.50	48.70	598.60	231.60	23.20
H(M)	3.20	10.10	68.60	95.60	823.60	

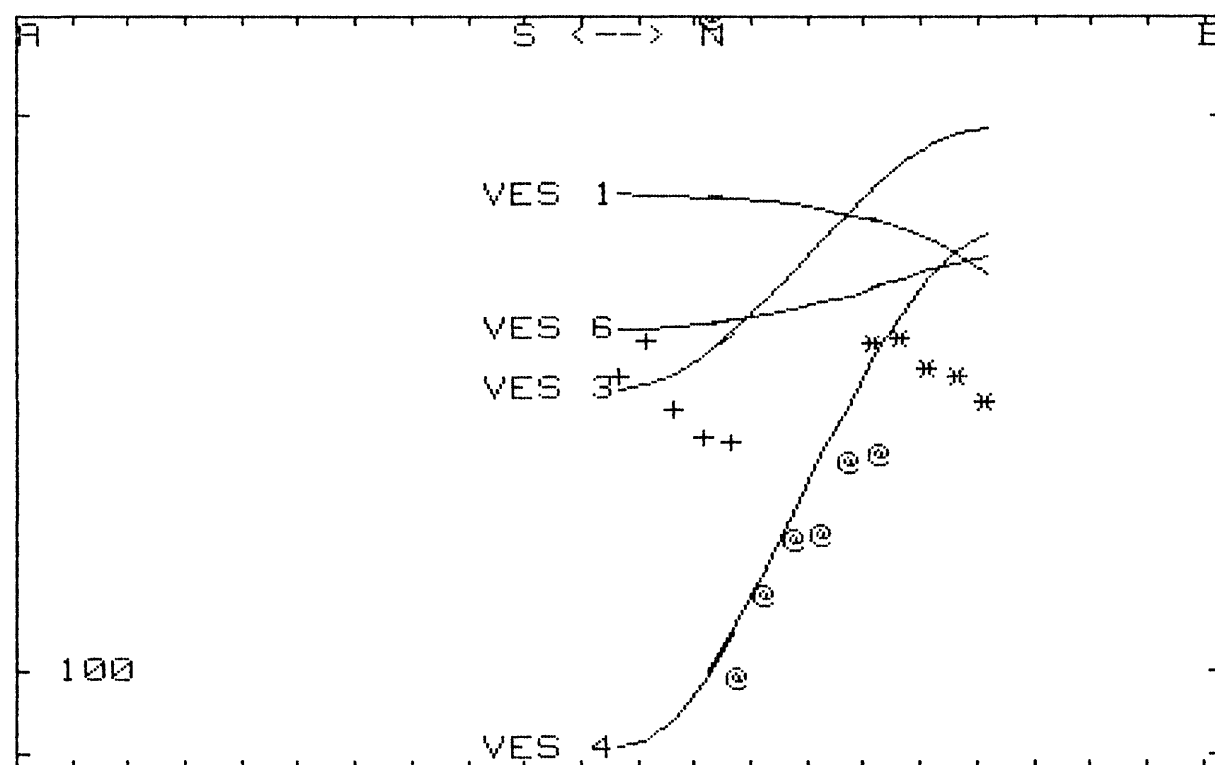
VES 4 MODEL:

RHO(ohm-m)	20.90	183.60	67.50	320.00	.30
H(M)	1.20	2.40	108.60	582.70	

VES 6 MODEL:

RHO(ohm-m)	49.40	173.00	72.70	400.00	145.20
H(M)	2.80	12.40	91.80	108.10	

AB= 4268 MN= 300



HORIZONTAL TICK INTERVAL = 200 M

APPARENT RESISTIVITY (OHM-M) PLOTTED AT CENTER OF MN PAIR

Figure 3

A semi-logarithmic plot of the apparent resistivity data from gradient profile 2a. Current electrode separation was 4268 m and the potential electrode separation was 300 m. The potential electrodes were moved a distance of 100 m between measurements and the resulting apparent resistivity was plotted at the center of the potential array. Solid lines represent theoretical values over horizontally-layered models interpreted from nearby sounding data.

Schofield, O'ahu: Gradient Profile 2b

VES 1 MODEL:

RHO(ohm-m)	30.80	168.40	47.50	400.00	183.60
H(M)	2.90	10.30	85.10	82.70	

VES 3 MODEL:

RHO(ohm-m)	76.20	126.50	48.70	598.60	231.60	23.20
H(M)	3.20	10.10	68.60	95.60	823.60	

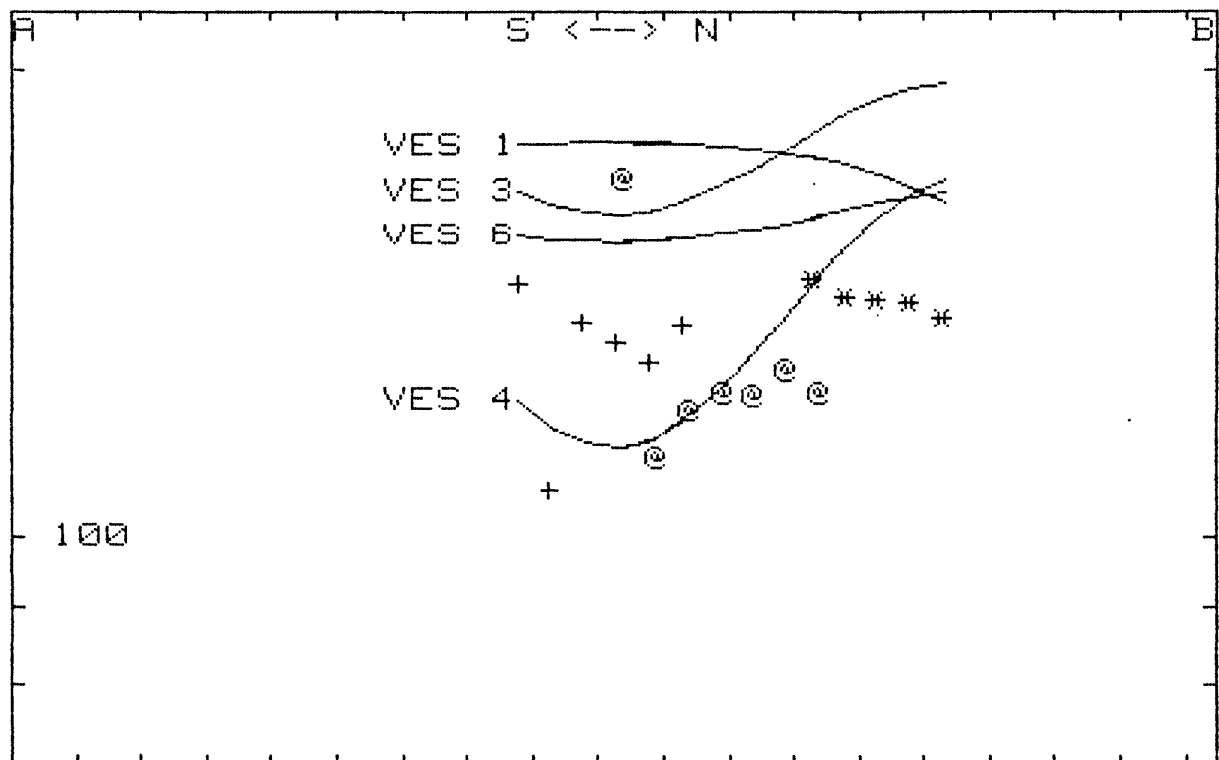
VES 4 MODEL:

RHO(ohm-m)	20.90	183.60	67.50	320.00	.30
H(M)	1.20	2.40	108.60	582.70	

VES 6 MODEL:

RHO(ohm-m)	49.40	173.00	72.70	400.00	145.20
H(M)	2.80	12.40	91.80	108.10	

AB= 3696 MN= 300



HORIZONTAL TICK INTERVAL = 200 M
 APPARENT RESISTIVITY (OHM-M) PLOTTED AT CENTER OF MN PAIR

Figure 4 A semi-logarithmic plot of the apparent resistivity data from gradient profile 2b. Current electrode separation was 3696 m and the potential electrode separation was 300 m. The potential electrodes were moved a distance of 100 m between measurements and the resulting apparent resistivity was plotted at the center of the potential array. Solid lines represent theoretical values over horizontally-layered models interpreted from nearby sounding data.

Schofield, O'ahu: Gradient Profile 3a

VES 12 MODEL:

RHO(ohm-m)	34.10	104.40	34.90	600.00	25.40
H(M)	1.40	16.30	83.00	373.80	

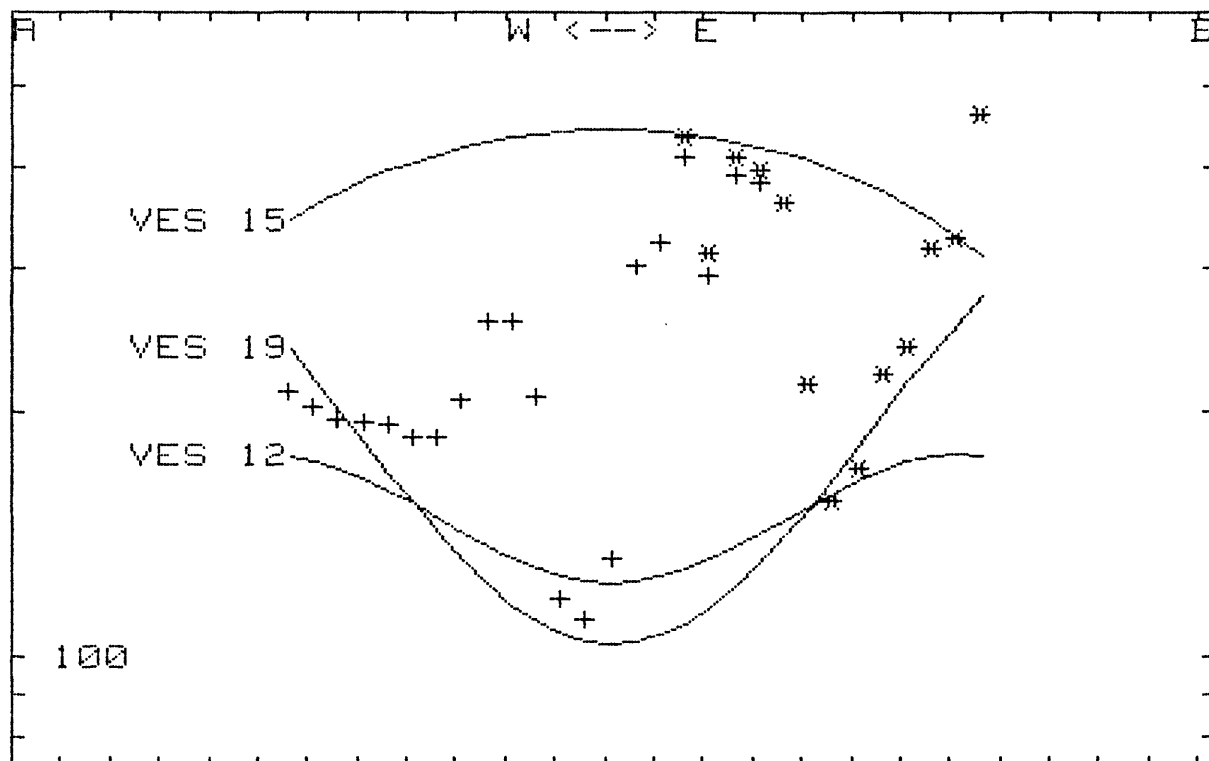
VES 15 MODEL:

RHO(ohm-m)	30.80	154.20	77.40	553.20
H(M)	4.20	24.60	109.60	

VES 19 MODEL:

RHO(ohm-m)	35.10	99.90	17.90	990.10	67.50
H(M)	3.00	18.40	8.90	200.10	

AB= 4870 MN= 300



HORIZONTAL TICK INTERVAL = 200 M
APPARENT RESISTIVITY (OHM-M) PLOTTED AT CENTER OF MN PAIR

Figure 5 A semi-logarithmic plot of the apparent resistivity data from gradient profile 3a. Current electrode separation was 4870 m and the potential electrode separation was 300 m. The potential electrodes were moved a distance of 100 m between measurements and the resulting apparent resistivity was plotted at the center of the potential array. Solid lines represent theoretical values over horizontally-layered models interpreted from nearby sounding data.

RESULTS AND DISCUSSION

The remainder of the interpretation is based only on the sounding survey results. The difference in quality between the quantitative sounding interpretations and the very qualitative profile interpretations is too great to make integration of the two practical.

With the exception of sounding 9, the first four layers of each of the soundings are quite similar. Layer one resistivities range from 5.6 to 96 ohm-m; thicknesses range from 0.1 to 4.2 m. Layer two resistivities range from 65 to 322 ohm-m; the corresponding thicknesses range from 2.2 to 40 m. Layer three was relatively conductive with resistivities between 18 and 111 ohm-m and thicknesses between 9 and 305 m. Layer four resistivities range from 309 to 990 ohm-m. Sounding 9 was unique in that each of the four layers that were resolved was more resistive than the one above.

This resistivity sequence correlates quite well with a shallow geologic section determined for the Kunia area with logs from a number of shallow borings (Mink, 1981). The section was composed of four layers, three of which are part of a complex weathered sequence. Mink's section is compared in detail with the geoelectric sequence derived from soundings 1 and 2 (Kunia) below:

Unit	<u>Geologic</u>			<u>Geoelectric</u>	
	thickness	description		resistivity	thickness
	(m)			(ohm-m)	(m)
1	3	soil & stiff		26 - 30	2.0 - 2.9
		red-brown clay			
2	6.2	unsat. saprolite		168 -322	5.9 -10.3
3	38.4	sat. saprolite		48 - 56	83 - 85
4		unweathered basalt		309 -400	

Geologic and geoelectric thicknesses correlate well for the

first two units, but the third geoelectric layer is at least twice as thick as the corresponding geologic unit. The geoelectric third layer thickness corresponds more closely with driller's logs for well 3-2703-01 at the same site as the shallow borings (USGS Water Resources Division, Hawaii District records, 1983) suggesting that perhaps the saturated saprolite was not completely penetrated by the shallow holes used in Mink's study. Although the resistivities cannot be directly compared to the listed rock types for appropriateness, the fact that geoelectric layer one and three are less resistive than layers two and four agrees well with their geologic description. The higher water content in soil, clay, or any saturated layer would generally cause resistivities to be lower in those layers.

The geoelectric section derived in Kunia is quite similar to sections derived from all other soundings in this study, with the exception of sounding 9. The widespread similarities lead us to believe that the geologic interpretation of each of the first four geoelectric layers in the Kunia area can be extrapolated to the entire northern and western portions of the study area. Specifically, the sounding results support (but do not, in themselves, confirm) the widespread presence of a saturated saprolite except in the southeastern part of the plateau. Figures 6, 7, and 8 are maps of the study area with the resistivity, thickness, and depth to the top of layer three, respectively, plotted.

By combined thickness, the fourth and deeper layers constitute most of the sounded section; however, with few exceptions, the resistivities and thicknesses of these deeper layers are not as well determined as those of the three geoelectric layers above them. Resolution is poorer because the layers are deeper and are prone to equivalence-type problems (Appendix B). Groupings must be used to discern any patterns that the data might have; in this case, individual parameter values are not as meaningful as the group or category they may belong in. Based on the resistivity values of these deeper layers, the soundings can be divided into four groups:

1. $\rho_4 > 450 \text{ ohm-m}$, $\rho_5 < 100 \text{ ohm-m}$, $\rho_6 > 350 \text{ ohm-m}$; soundings 7, 16, 17.
2. $\rho_4 > 450 \text{ ohm-m}$, $130 < \rho_5 < 230 \text{ ohm-m}$; soundings 1, 3, 6, 11, 13, 14.
3. $\rho_4 > 450 \text{ ohm-m}$, $\rho_5 < 70 \text{ ohm-m}$, no sixth layer; soundings 10, 12, 15, 19.

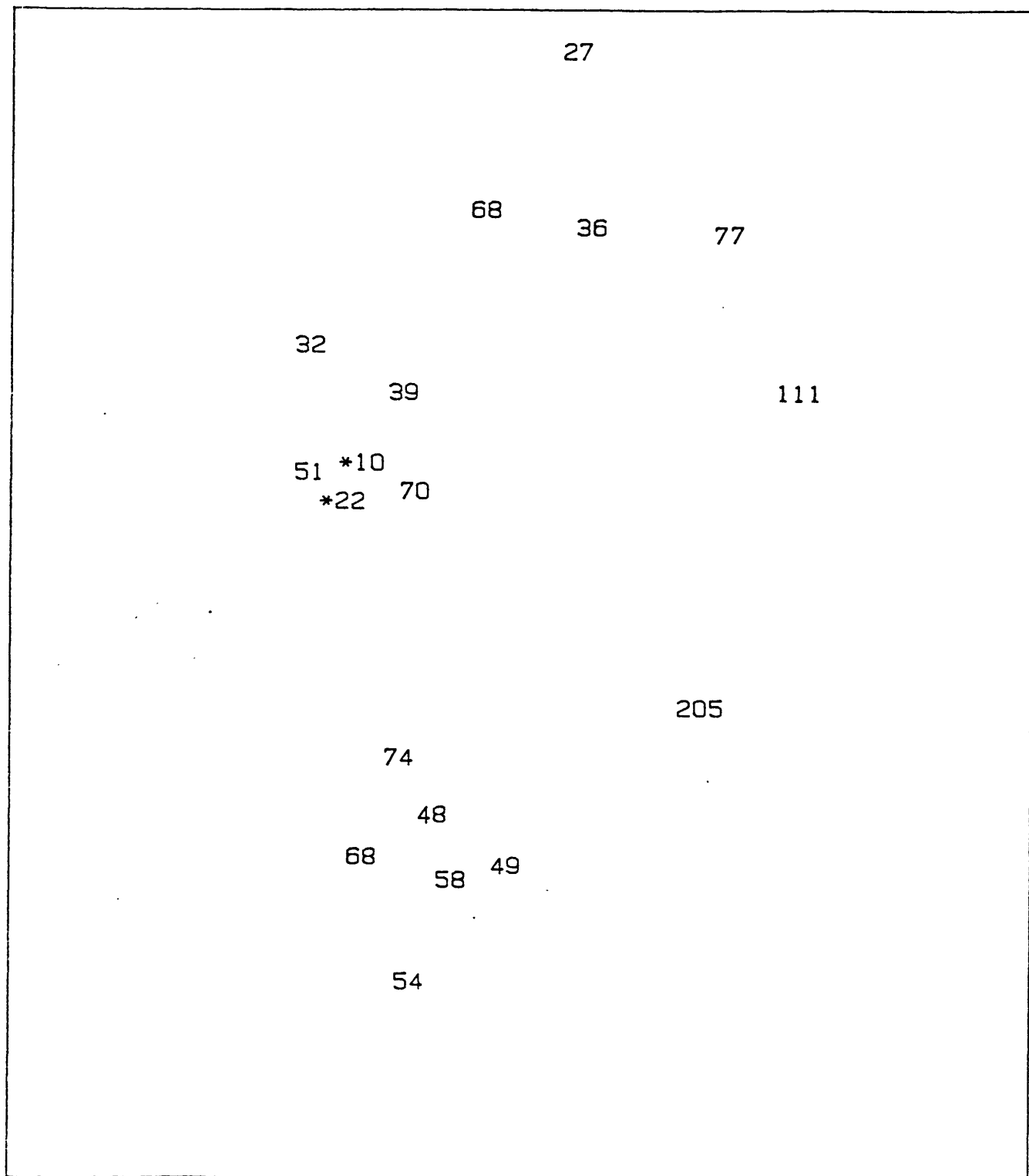


Figure 6

A map of the Schofield area showing the spatial distribution of the values determined for the third layer resistivity, in ohm-m. An asterisk precedes those values which are poorly resolved by the computer inversion.

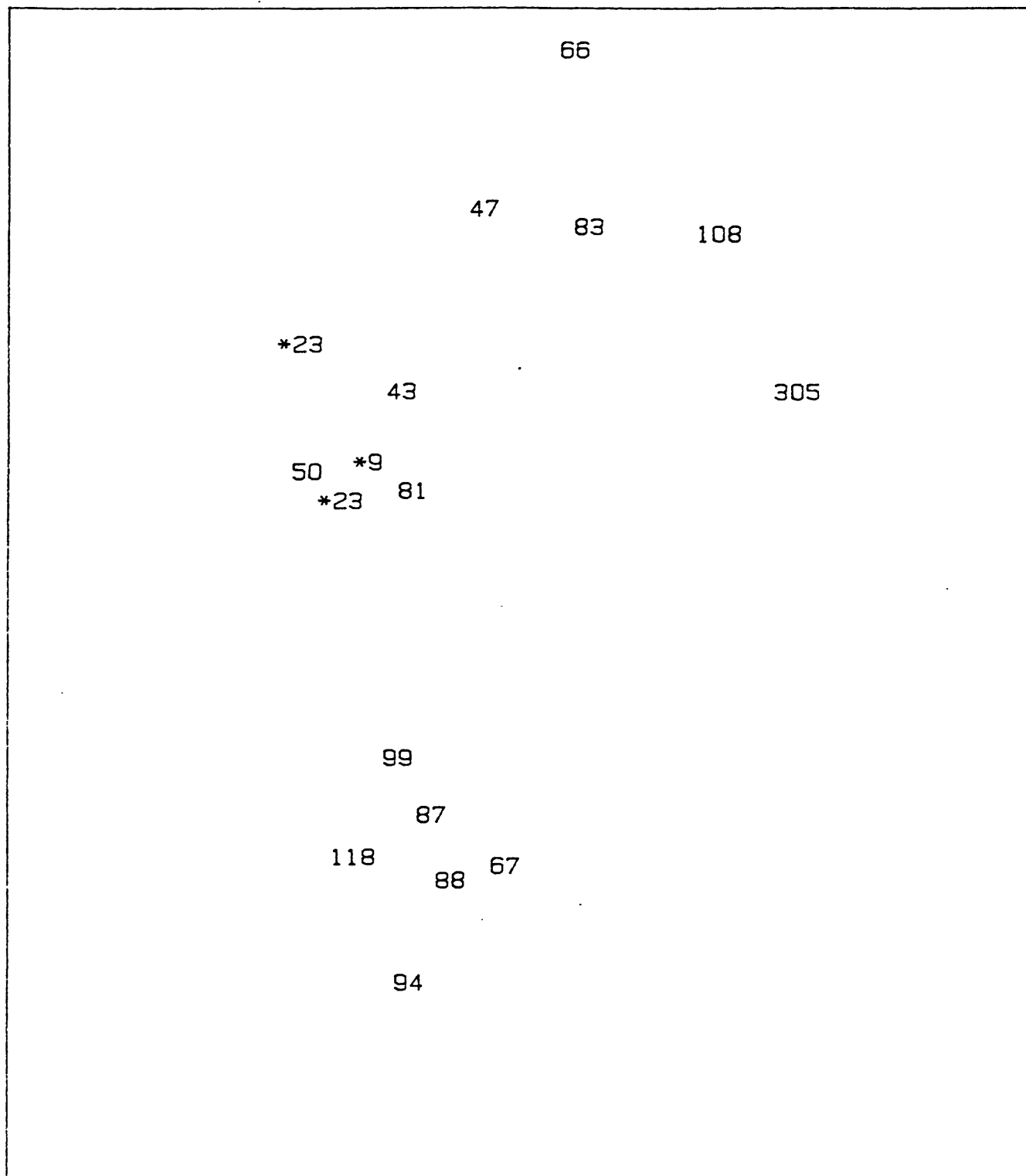


Figure 7

A map of the Schofield area showing the spatial distribution of the values determined for the third layer thickness, in meters. An asterisk precedes those values which are poorly resolved by the computer inversion.

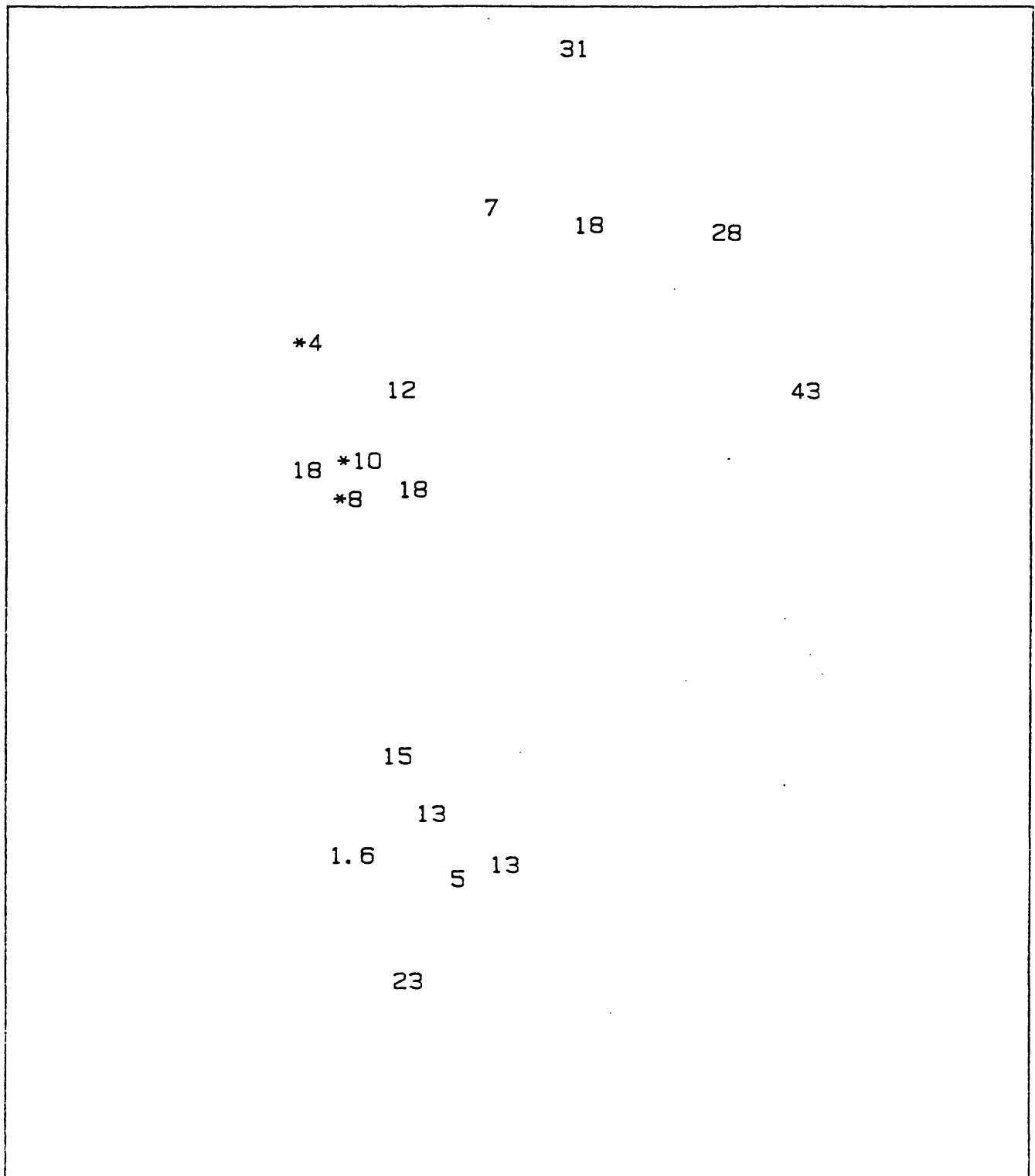


Figure 8

A map of the Schofield area showing the spatial distribution of the values determined for the depth from the ground surface to the top of layer 3, in meters. An asterisk precedes those values which are poorly resolved by computer inversion.

4. $180 < \rho_4 < 420$ ohm-m, $\rho_5 \leq 30$ ohm-m; soundings 2, 4, 5, 18.

The soundings in groups 1 and 2 are clustered together in the central western part of the study area, with those in group 3 located in the northeastern part. Group 4 soundings are found together in the Kunia area (southwest of Wahiawa). This grouping is summarized in map form in Figure 9.

One possible geologic interpretation of these groupings is that the fourth layer represents either the younger Koolau lavas ($\rho_4 > 450$ ohm-m in groups 1, 2, and 3) or the older Waianae lavas ($\rho_4 < 450$ ohm-m in group 4). In group 4, the Waianae lavas appear to be immediately beneath the weathered zone. The conductive fifth layer beneath the Waianae basalt in soundings 2, 4, and 5 is probably salt-water saturated basalt and represents the base of a fresh-water lens in that area. Note that the inclusion of sounding 18 from the northern part of the study area is probably due to noisy data and is not thought to imply the presence of Waianae lavas on the northeastern portion of the Schofield plateau.

Soundings in group 3 represent an analogous situation to those in group 4 except that the fourth layer is more resistive and probably represents Koolau basalts. Again, the conductive fifth layer is probably salt-water saturated basalt marking the base of the fresh-water lens. Sounding 10 is included in this group even though no basement conductor was detected because we believe that the fresh-water lens is thicker than the maximum depth (2 km below ground surface) that was sounded at this location.

Groups 1 and 2, located between the previously discussed groups, represent Koolau basalts overlaying Waianae basalts. In the soundings in group 1, a separate weathered zone mantling the buried Waianae is apparently visible as a thin, conductive fifth layer over a deeper resistive basement (the Waianae lavas). The buried weathered zone has resistivities that are less than 100 ohm-m. Those soundings in group 2 probably represent this same geologic situation, except that a separate weathered zone was not discernible; the entire Waianae section appears as a fifth layer of resistivity 130 to 230 ohm-m. The weathered zone may be thin to non-existent in these soundings. Sounding 3 in the Kunia area was unique in this group because a deep sixth layer was indicated and probably represents salt-water saturated basalts at the base of a fresh-water lens.

Alternatively, the fifth layer in Group 2 soundings might represent the fresh water saturated basalts directly. At least, the elevations interpreted for this layer correspond roughly to

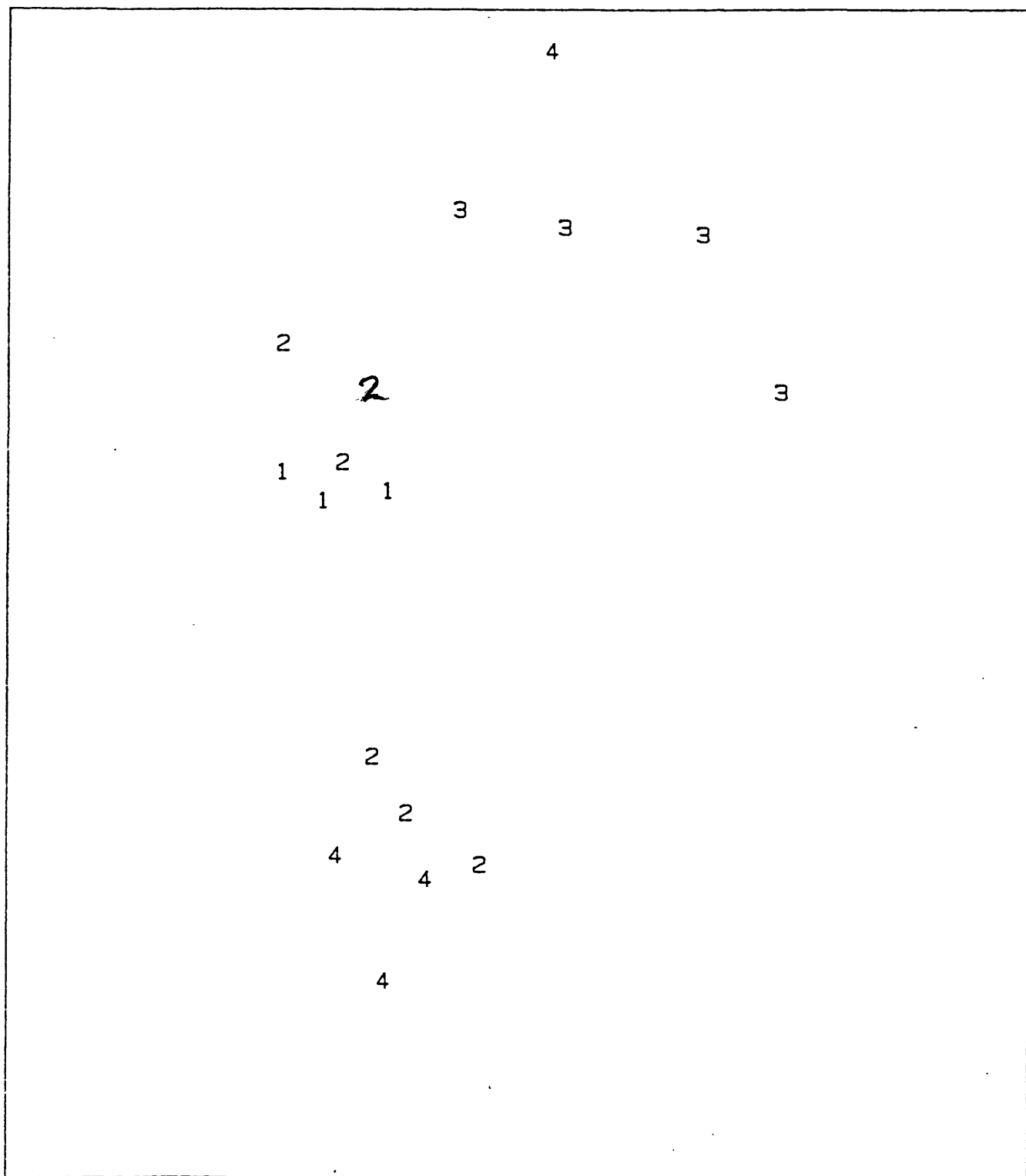


Figure 9

A map of the Schofield area showing the spatial distribution of the soundings categorized into groups 1 through 4 based on the resistivities determined for the fourth and deeper layers.

the known standing water level of approximately 80 m above sea level. If so, this would be one of the first geoelectric surveys to detect fresh-water saturated basalts directly.

In any event, the hydrologic significance of the Koolau/Waianae interpretation is readily apparent in Figure 10 which shows a map with the elevations of the interpreted Koolau-Waianae contact. The contact appears to be shallowest immediately to the north and south of Schofield Barracks (Figure 1) and may border the high-level aquifer, giving the strongest indication thus far that the water is impounded by buried ridges of the ancient Waianae volcano. Elevations within shaded portions of the map represent the interpreted salt water-fresh water interface. If estimates of the actual fresh-water lens thickness are desired at each of these locations, a more accurate value can be obtained by using Figure 11. This map shows values of the product of fourth layer resistivity and thickness. In most cases, this layer is not resolved well enough to allow independent estimation of both resistivity and thickness. The product of the two can be obtained more accurately than either parameter independently (Appendix B). The thickness of the fourth layer can then be estimated by dividing the resistivity-thickness product by a representative resistivity. Fresh-water lens thickness is approximately equal to the depth to the bottom of the fourth layer minus the elevation. Table II lists lens thickness estimates for assumed resistivities of 600 ohm-m for Koolau basalts and 400 ohm-m for Waianae basalts.

TABLE II. Estimated Fresh-Water Lens Thicknesses

Sounding	thickness
2	399 m
3	462
4	190
5	314
12	135
15	1560
18	--
19	115

No estimate is listed for sounding 18 because the salt/fresh-water interface would be above sea level for the assumed resistivity of 600 ohm-m. A basalt resistivity lower than 600 ohm-m is strongly indicated for sounding 18. The 1560 m estimate for sounding 15 is too thick to represent basal water,

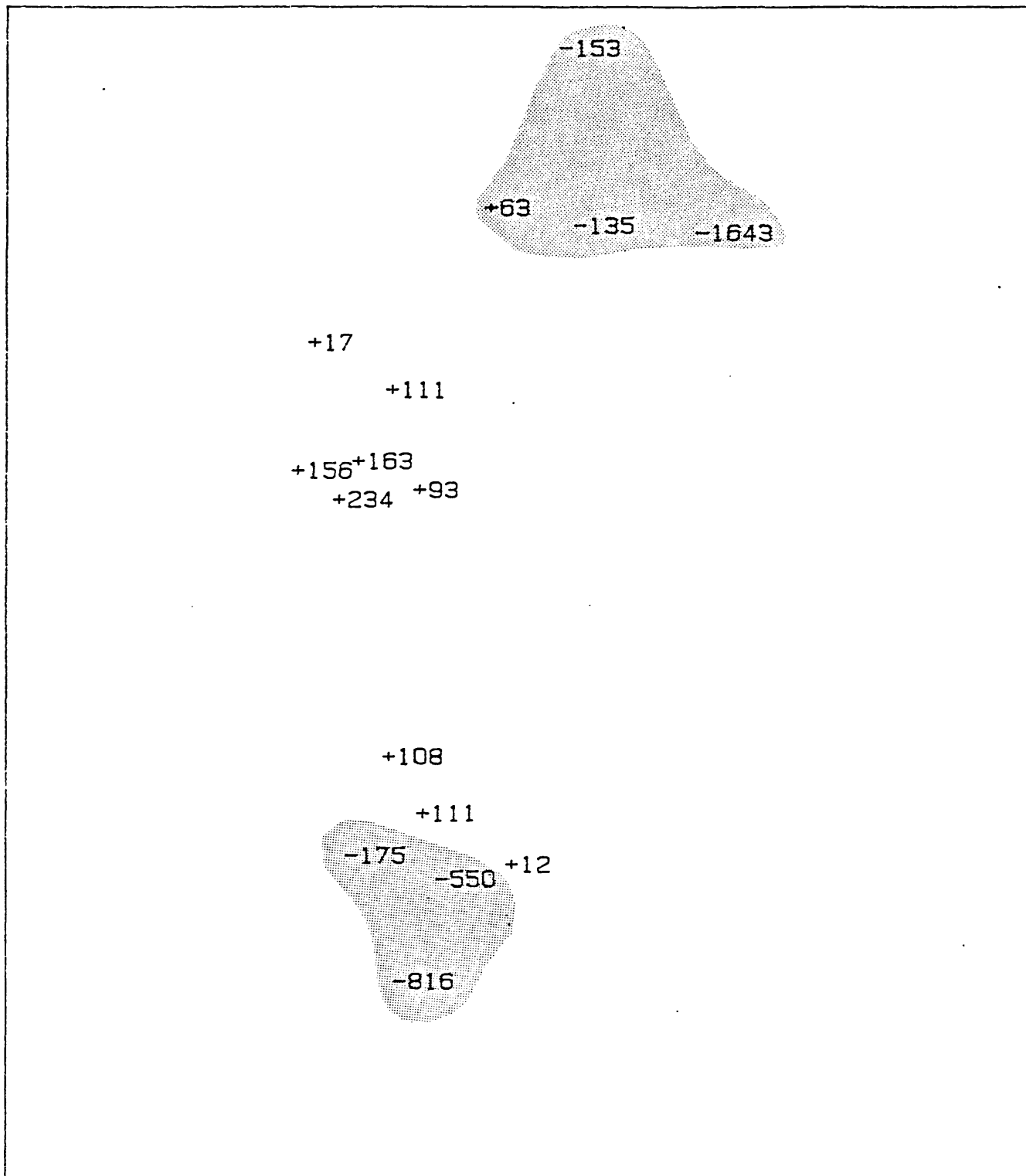


Figure 10

A map of the Schofield area showing the spatial distribution of the elevation (with respect to sea level) of the base of the fourth layer, in meters. Values within the shaded portions of the map are interpreted to represent the elevation of the fresh/salt water interface at the base of the fresh water lens at those locations.

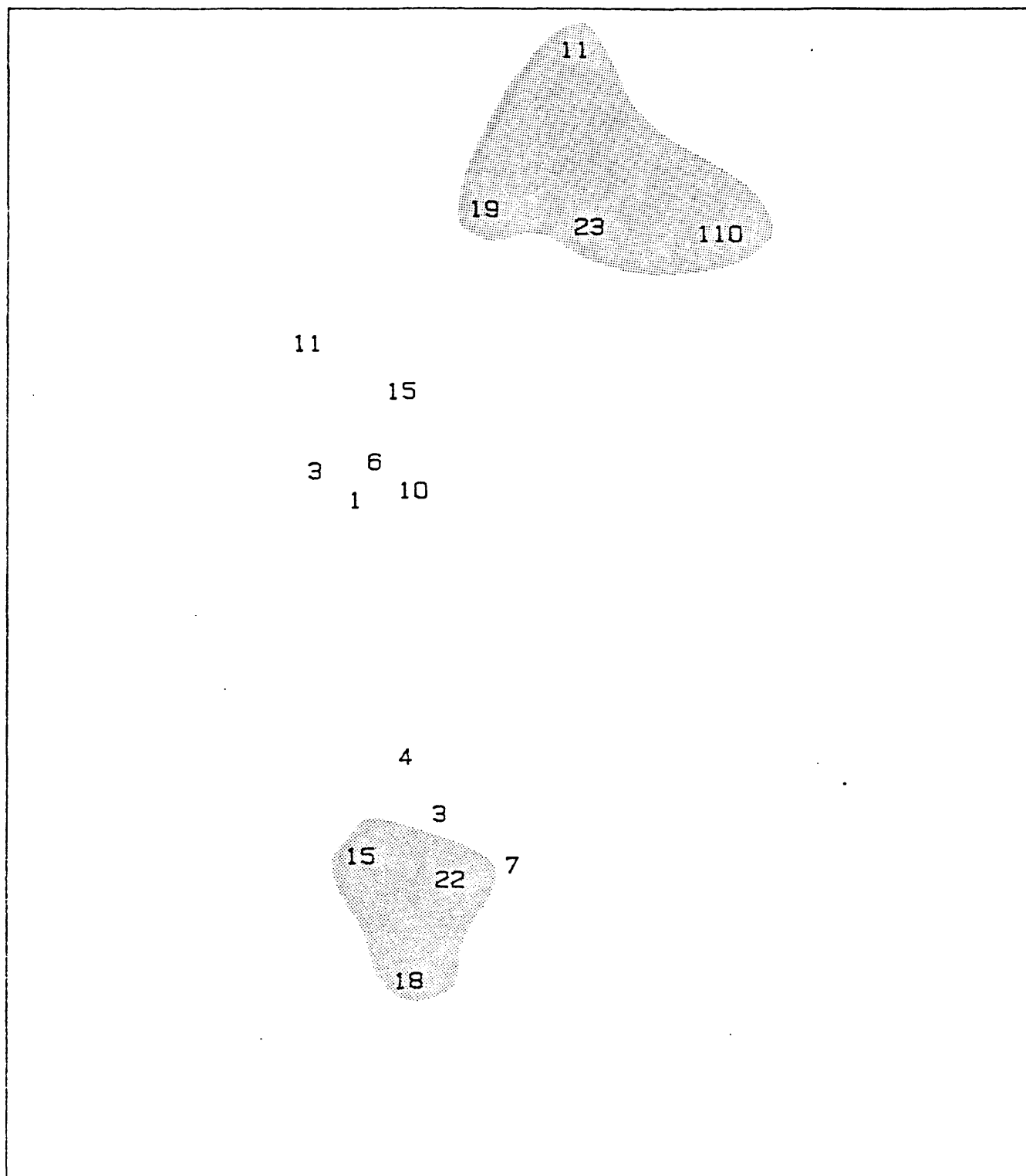


Figure 11

A map of the Schofield area showing the spatial distribution of the product of the resistivity and thickness (divided by 10,000) of the fourth

2

layer, in ohm-m. The shaded portion of the map represents those soundings which are interpreted to have penetrated a fresh water lens floating on salt water.

at least as it most commonly occurs in Hawai'i. The thick estimate probably does not actually indicate basal water at all, but may indicate high-level water. The same may be said for sounding 10 which did not detect the base of fresh water even though the sounding probably penetrated nearly 1500 m below sea level.

CONCLUSIONS

The nineteen Schlumberger resistivity soundings obtained on the central Schofield plateau have been modeled as horizontally-layered halfspaces with either four, five, or six layers. The shallowest three layers can be identified as components of a weathered zone atop unweathered basalt. The layer immediately above this unweathered rock may be a saturated saprolite observed in shallow test borings in the Kunia area (Mink, 1981). One possible interpretation of the deeper layers is that the Waianae basalts are distinctly visible to resistivity sounding techniques because they are of lower resistivity than the younger Koolau lavas and because, in some areas, they are mantled with a buried weathered zone. In this way, the Waianae basalts can be mapped as they dip beneath the Koolau basalts going eastward across the plateau. The Waianae rocks are very shallow to the north and south of the high-level water body and may represent buried ridges which impound water to anomalously high levels beneath Wahiawa. The soundings may be used to estimate fresh-water lens thicknesses in the northeastern and southwestern parts of the study area.

An alternative interpretation of the deep geoelectric layers is that fresh water saturated basalts underlay the unsaturated Koolau basalts. That is, the fifth layer may represent the water table directly and not Waianae basalts.

APPENDIX A: Schlumberger Sounding Computer Inversion

Computer programs such as MARQDCLAG (Anderson, 1979) offer an automatic means by which sounding data sets can be inverted to their best-fitting horizontally-layered model parameters. These parameters are the resistivities and thicknesses of each of the layers in the earth model. Of course, approximate matching can be done by manually comparing the sounding data to theoretical curves in a standard album; however, the computer inversion offers an additional advantage, besides speed and automation, of parameter resolution estimates. They offer a means of assessing the reliability of parameters they estimate.

When input with the sounding data set and an initial guess of the model parameters, program MARQDCLAG_HP (a version of MARQDCLAG written for a Hewlett-Packard 9826 microcomputer used in this study) automatically minimizes the following quantity:

$$\text{PHI} = \sum_{i=1}^N \left[\frac{y_i - f(x_i)}{w_i} \right]^2$$

where

N is the number of data in the sounding data set,
th

x_i is the i th electrode spacing,

y_i is the apparent resistivity measured at x_i ,

w_i is the apparent resistivity measurement error ($=y_i/100$), and

$f(x)$ is the theoretical calculated apparent resistivities.

The number of layers cannot be automatically varied by the program so it is a common practice to invert each sounding data set for several models, each having a different number of layers (as for example in Table I). The best-fitting model is chosen to

$$X^2 = PHI / (N - 2 * m)$$

During the inversions of the Schofield data sets, the natural logarithm of the parameters were manipulated to avoid use negative resistivities or thicknesses and to more accurately reflect the logarithmic resolution of these values. A detailed description of the headings and identifying terms used in the program output (listed in Appendix C) follows:

REDUCED CHI-SQUARED
= PHI / (N - 2 * m).

$B-SD \quad \exp^2 (PARAMETER-ERROR),$
 $B \quad \exp (PARAMETER),$
 $B+SD \quad \exp (PARAMETER+ERROR),$

FINAL UNSCALED PARAMETERS:

RESISTIVITY resistivity of layer i, in ohm-meters, and
DEPTH depth from surface to bottom of layer i, in
 meters.

2. $\exp(x)$ represents e, the base of the natural logarithms,
raised to the x power.

APPENDIX B: Equivalence and Suppression Phenomena

Under certain circumstances, it is possible for a layered medium with extremely different layer resistivities and thicknesses to yield apparent resistivity curves that do not differ from one another by more than average measurement error. The sets of layering parameters giving rise to the practically indistinguishable curves are said to be 'equivalent' and the phenomenon is called 'equivalence'. The exact conditions under which this phenomenon occurs are difficult to describe explicitly, but from a practical point of view, it is possible to distinguish two simple cases each involving three layers. The first case is that of an ascending type of resistivity sequence in which the middle layer (of three) is underlain by a more resistive one. If the middle layer is relatively thin, then its resistivity and thickness can be varied so that the ratio of thickness over resistivity is constant and the corresponding apparent resistivity curve will not vary significantly. The thicker the middle layer becomes, the more the range of the equivalent parameters is reduced.

The second case is that of a descending type of resistivity sequence in which the middle layer is underlain by a more conductive one. Again, if the layer is relatively thin and if the layer resistivity and thickness are varied such that their product remains constant, then the corresponding curves will not vary significantly. As with the first case, the thicker the middle layer becomes, the more the range of equivalent parameters is reduced.

These relationships become very important for interpreting the results of computer inversions for Schlumberger sounding data. Even when an inversion result consists of more than three layers, equivalenced sequences can usually be isolated and analyzed in terms of the simple three-layer models described above. Very often, layers were found which had highly correlated resistivities and thicknesses, and which had astronomically high estimated errors. The inversion found it impossible to determine values for the two parameters individually because the effect of changes in their values on the apparent resistivity curves were very similar. The two parameters were equivalenced and the inversion could only determine the ratio of the two (positive correlation coefficient) or the product of the two (negative

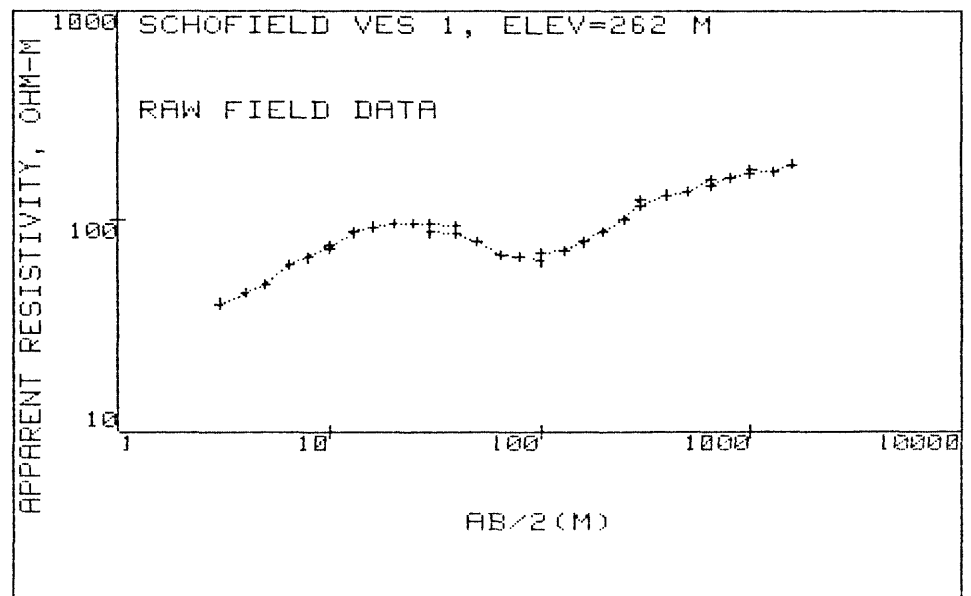
correlation coefficient).

Although we can't determine either the layer resistivity or thickness individually, we can establish a useful range for either by trial and error. The procedure is to run the inversion program several times, each with the equivalenced resistivity fixed to a different value. As long as both parameters lay within the range of equivalence of the layer, the reduced chi-squared statistic (Appendix A) will remain fairly constant.

A related effect that also complicates sounding interpretation is the 'suppression' phenomenon whereby the middle layer or layers in an ascending or descending sequence may be totally suppressed. If the layer is thickened, then its presence becomes more noticeable. The effect is significant when one is trying to correlate a geologic sequence of layers to the geoelectric layers determined by sounding.

APPENDIX C: Raw Data and Computer Inversion Listings

In this appendix, there are three pages of information for each of the eighteen soundings. First of the three is a plot and a listing of the raw field data. The second and third pages are the relevant portions of the computer inversion output. The headings are defined and the inversion process is briefly described in Appendix A.



AB/2 (M)	APP RHO
3.0	40.0
4.0	44.9
5.0	49.0
6.5	60.5
8.0	65.8
10.0	76.0
10.0	73.0
13.0	87.0
16.0	92.5
20.0	96.4
25.0	96.0
30.0	95.4
40.0	93.8
30.0	87.0
40.0	85.6
50.0	79.0
65.0	67.5
80.0	66.0
100.0	63.0
100.0	68.6
130.0	71.3
160.0	78.0
200.0	88.0
250.0	100.0
300.0	124.0
300.0	117.0
400.0	130.6
500.0	134.0
650.0	153.0
650.0	145.0
800.0	156.0
1000.0	165.0
1000.0	172.0
1300.0	168.0
1593.0	184.0

	X	OBSERVED	PREDICTED	%RESIDUALS	WEIGHT FN
1	+3.0000E+00	+3.5580E+01	+3.5435E+01	+4.0710E-01	+4.0283E+00
2	+4.0000E+00	+3.9930E+01	+3.9733E+01	+4.9239E-01	+3.1985E+00
3	+5.0000E+00	+4.3580E+01	+4.4725E+01	-2.6270E+00	+2.6851E+00
4	+6.5000E+00	+5.3810E+01	+5.2447E+01	+2.5324E+00	+1.7612E+00
5	+8.0000E+00	+5.8520E+01	+5.9665E+01	-1.9566E+00	+1.4891E+00
6	+1.0000E+01	+6.7590E+01	+6.7979E+01	-5.7592E-01	+1.1163E+00
7	+1.3000E+01	+8.0560E+01	+7.7584E+01	+3.6944E+00	+7.8578E-01
8	+1.6000E+01	+8.5650E+01	+8.4203E+01	+1.6890E+00	+6.9516E-01
9	+2.0000E+01	+8.9260E+01	+8.9375E+01	-1.2850E-01	+6.4007E-01
10	+2.5000E+01	+8.8890E+01	+9.1619E+01	-3.0702E+00	+6.4541E-01
11	+3.0000E+01	+8.8340E+01	+9.0865E+01	-2.8587E+00	+6.5347E-01
12	+4.0000E+01	+8.6850E+01	+8.5178E+01	+1.9257E+00	+6.7608E-01
13	+5.0000E+01	+8.0190E+01	+7.8281E+01	+2.3812E+00	+7.9305E-01
14	+6.5000E+01	+6.8510E+01	+7.0109E+01	-2.3336E+00	+1.0865E+00
15	+8.0000E+01	+6.6990E+01	+6.5551E+01	+2.1482E+00	+1.1364E+00
16	+1.0000E+02	+6.3950E+01	+6.3914E+01	+5.6200E-02	+1.2470E+00
17	+1.3000E+02	+6.6460E+01	+6.7052E+01	-8.9075E-01	+1.1546E+00
18	+1.6000E+02	+7.2710E+01	+7.3365E+01	-9.0079E-01	+9.6461E-01
19	+2.0000E+02	+8.2030E+01	+8.3369E+01	-1.6320E+00	+7.5787E-01
20	+2.5000E+02	+9.3210E+01	+9.5803E+01	-2.7815E+00	+5.8697E-01
21	+3.0000E+02	+1.1560E+02	+1.0700E+02	+7.4435E+00	+3.8161E-01
22	+4.0000E+02	+1.2900E+02	+1.2508E+02	+3.0411E+00	+3.0645E-01
23	+5.0000E+02	+1.3240E+02	+1.3842E+02	-4.5473E+00	+2.9091E-01
24	+6.5000E+02	+1.5120E+02	+1.5229E+02	-7.2371E-01	+2.2307E-01
25	+8.0000E+02	+1.6260E+02	+1.6136E+02	+7.6071E-01	+1.9288E-01
26	+1.0000E+03	+1.7200E+02	+1.6898E+02	+1.7538E+00	+1.7238E-01
27	+1.3000E+03	+1.6800E+02	+1.7525E+02	-4.3130E+00	+1.8068E-01
28	+1.5930E+03	+1.8400E+02	+1.7840E+02	+3.0427E+00	+1.5063E-01

CORRELATION MATRIX:

	1	2	3	5	6	7	8	9
1	+1.00	+.63	+.28	-.06	+.90	-.58	+.29	+.09
2	+.63	+1.00	+.65	-.15	+.88	-.98	+.64	+.22
3	+.28	+.65	+1.00	-.35	+.46	-.78	+.97	+.49
5	-.06	-.15	-.35	+1.00	-.10	+.20	-.49	-.90
6	+.90	+.88	+.46	-.10	+1.00	-.83	+.46	+.15
7	-.58	-.98	-.78	+.20	-.83	+1.00	-.75	-.28
8	+.29	+.64	+.97	-.49	+.46	-.75	+1.00	+.66
9	+.09	+.22	+.49	-.90	+.15	-.28	+.66	+1.00

REDUCED CHI-SQUARED=10.57

DCLAG: ***** END *****
COORDINATES: 0 0
ELEVATION : 262 METER
AZIMUTH :

SCHOFIELD VES 1, ELEV=262 M

B-SD	B	B+SD
2.806E+001	3.079E+001	3.379E+001
1.159E+002	1.684E+002	2.448E+002
4.137E+001	4.751E+001	5.456E+001
	4.000E+002	
1.667E+002	1.836E+002	2.022E+002
2.338E+000	2.904E+000	3.606E+000
5.807E+000	1.031E+001	1.829E+001
6.776E+001	8.510E+001	1.069E+002
4.087E+001	8.267E+001	1.672E+002

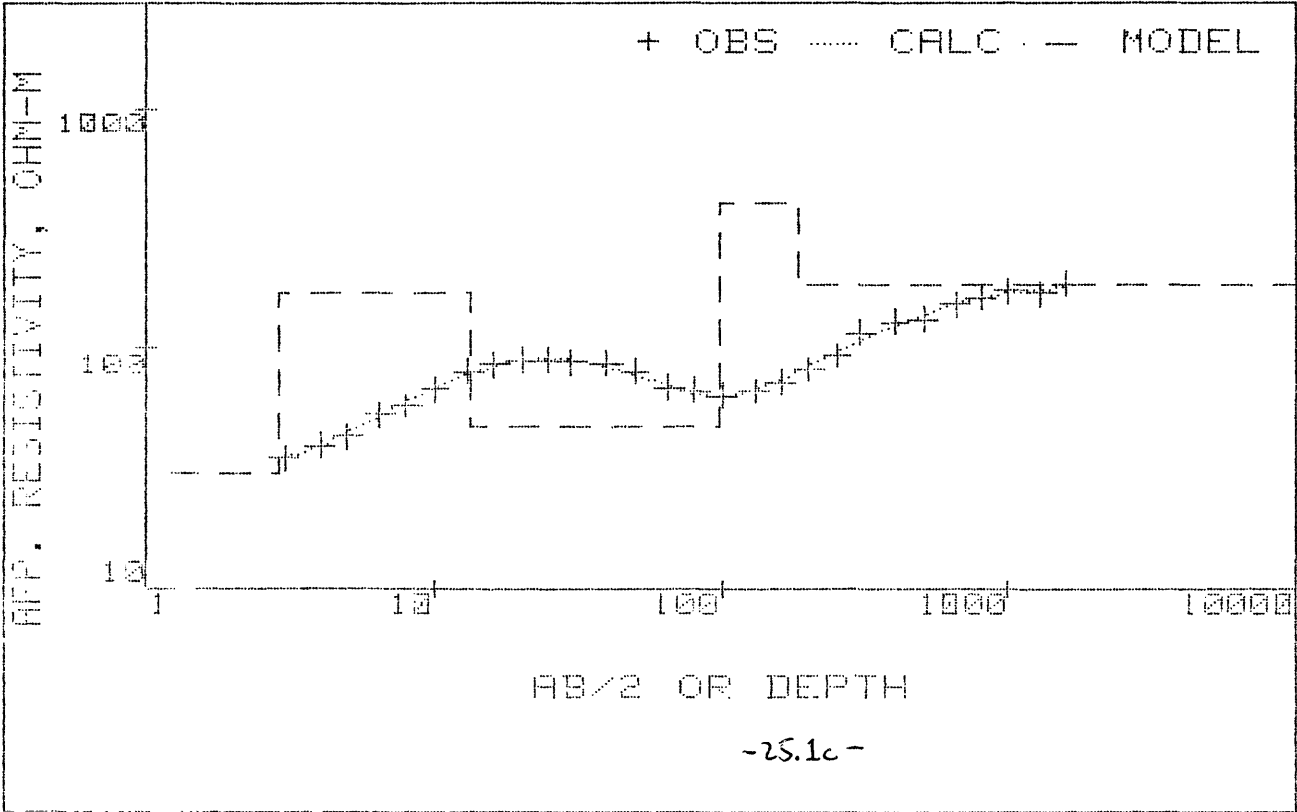
FINAL UNSCALED PARAMETERS--
(* denotes fixed value)

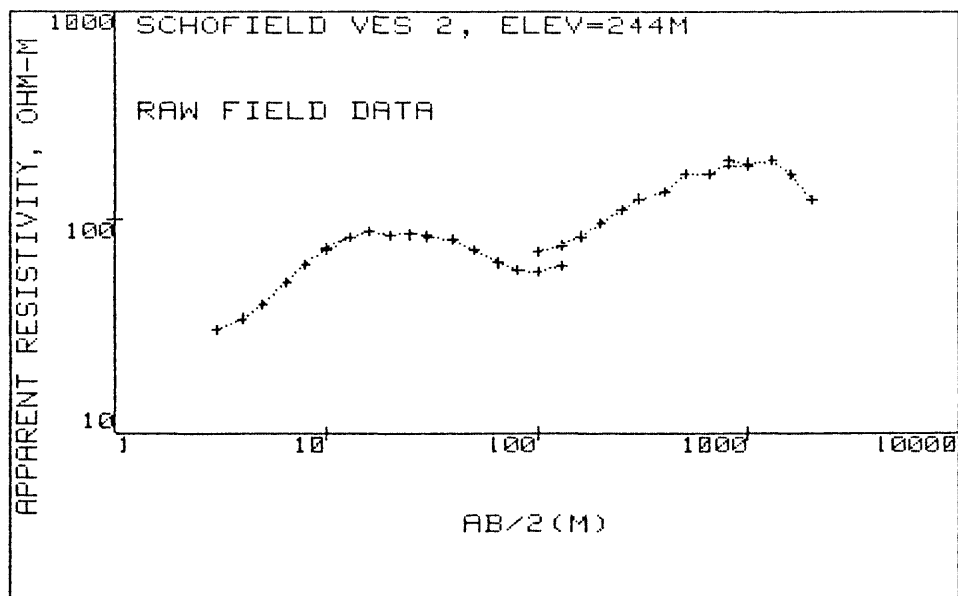
RESISTIVITY

DEPTH

1	3.07901960E+01	1	3.07901960E+01		
2	1.68438315E+02	2	1.68438315E+02		
3	4.75087085E+01	3	4.75087085E+01		
4	* 4.00000000E+02	4	4.00000000E+02		
5	1.83576023E+02	5	1.83576023E+02		
6	2.90365214E+00			1	2.90365214E+00
7	1.03057024E+01			2	1.32093545E+01
8	8.51038500E+01			3	9.83132045E+01
9	8.26733409E+01			4	1.80986545E+02

SCHOFIELD VES 1, ELEV=262 M





AB/2 (M) APP RHO

3.0	30.4
4.0	34.4
5.0	40.6
6.5	51.2
8.0	62.2
10.0	73.3
13.0	82.0
10.0	72.4
13.0	82.6
16.0	87.3
20.0	84.0
25.0	85.1
30.0	83.4
30.0	82.6
40.0	80.3
50.0	72.7
65.0	63.0
80.0	58.0
100.0	57.0
130.0	61.0
100.0	71.0
130.0	75.0
160.0	83.0
200.0	96.4
250.0	111.0
300.0	125.0
300.0	123.0
400.0	135.5
500.0	163.0
650.0	165.0
800.0	182.0
1000.0	180.0
800.0	194.0
1000.0	188.0
1300.0	196.0
1600.0	163.0
2000.0	124.0

	X	OBSERVED	PREDICTED	%RESIDUALS	WEIGHT FN
1	+3.0000E+00	+3.8590E+01	+3.7400E+01	+3.0833E+00	+4.7740E+00
2	+4.0000E+00	+4.3660E+01	+4.5634E+01	-4.5205E+00	+3.7296E+00
3	+5.0000E+00	+5.1530E+01	+5.4032E+01	-4.8558E+00	+2.6774E+00
4	+6.5000E+00	+6.4990E+01	+6.5749E+01	-1.1680E+00	+1.6832E+00
5	+8.0000E+00	+7.8950E+01	+7.5960E+01	+3.7867E+00	+1.1406E+00
6	+1.0000E+01	+9.3040E+01	+8.7197E+01	+6.2796E+00	+8.2128E-01
7	+1.3000E+01	+1.0410E+02	+9.9490E+01	+4.4280E+00	+6.5604E-01
8	+1.6000E+01	+1.1110E+02	+1.0726E+02	+3.4530E+00	+5.7597E-01
9	+2.0000E+01	+1.0690E+02	+1.1236E+02	-5.1075E+00	+6.2212E-01
10	+2.5000E+01	+1.0830E+02	+1.1306E+02	-4.3981E+00	+6.0614E-01
11	+3.0000E+01	+1.0610E+02	+1.1013E+02	-3.8003E+00	+6.3154E-01
12	+4.0000E+01	+1.0320E+02	+1.0022E+02	+2.8873E+00	+6.6753E-01
13	+5.0000E+01	+9.3410E+01	+9.0382E+01	+3.2417E+00	+8.1478E-01
14	+6.5000E+01	+8.0950E+01	+8.0134E+01	+1.0075E+00	+1.0849E+00
15	+8.0000E+01	+7.4520E+01	+7.5193E+01	-9.0320E-01	+1.2802E+00
16	+1.0000E+02	+7.3240E+01	+7.4141E+01	-1.2298E+00	+1.3254E+00
17	+1.3000E+02	+7.8380E+01	+7.8783E+01	-5.1396E-01	+1.1572E+00
18	+1.6000E+02	+8.6170E+01	+8.6666E+01	-5.7532E-01	+9.5745E-01
19	+2.0000E+02	+1.0010E+02	+9.8671E+01	+1.4280E+00	+7.0951E-01
20	+2.5000E+02	+1.1520E+02	+1.1349E+02	+1.4834E+00	+5.3570E-01
21	+3.0000E+02	+1.2980E+02	+1.2699E+02	+2.1618E+00	+4.2197E-01
22	+4.0000E+02	+1.4300E+02	+1.4938E+02	-4.4609E+00	+3.4766E-01
23	+5.0000E+02	+1.7200E+02	+1.6623E+02	+3.3523E+00	+2.4031E-01
24	+6.5000E+02	+1.7410E+02	+1.8306E+02	-5.1455E+00	+2.3455E-01
25	+8.0000E+02	+1.9200E+02	+1.9174E+02	+1.3398E-01	+1.9285E-01
26	+1.0000E+03	+1.8990E+02	+1.9364E+02	-1.9702E+00	+1.9714E-01
27	+1.3000E+03	+1.9600E+02	+1.8225E+02	+7.0153E+00	+1.8506E-01
28	+1.6000E+03	+1.6300E+02	+1.6124E+02	+1.0777E+00	+2.6758E-01
29	+2.0000E+03	+1.2400E+02	+1.2834E+02	-3.4975E+00	+4.6237E-01

CORRELATION MATRIX:

	1	2	3	4	5	6	7	8	9
1	+1.00	+.75	+.33	+.10	+.06	+.97	-.73	+.32	-.08
2	+.75	+1.00	+.61	+.21	+.12	+.88	-1.00	+.57	-.17
3	+.33	+.61	+1.00	+.52	+.29	+.43	-.66	+.93	-.40
4	+.10	+.21	+.52	+1.00	+.78	+.14	-.24	+.76	-.91
5	+.06	+.12	+.29	+.78	+1.00	+.08	-.13	+.48	-.96
6	+.97	+.88	+.43	+.14	+.08	+1.00	-.87	+.41	-.11
7	-.73	-1.00	-.66	-.24	-.13	-.87	+1.00	-.61	+.18
8	+.32	+.57	+.93	+.76	+.48	+.41	-.61	+1.00	-.62
9	-.08	-.17	-.40	-.91	-.96	-.11	+.18	-.62	+1.00

REDUCED CHI-SQUARED=18.73

DCLAE: ***** END *****
COORDINATES: 0 0
ELEVATION : 244 METER
AZIMUTH :

SCHOFIELD VES 2, ELEV=244M

B-SD	B	B+SD
1.914E+001	2.616E+001	3.575E+001
8.489E+001	3.218E+002	1.220E+003
5.023E+001	5.653E+001	6.363E+001
2.505E+002	3.088E+002	3.809E+002
6.030E-034	1.000E+000	1.658E+033
1.251E+000	2.041E+000	3.330E+000
1.282E+000	5.869E+000	2.686E+001
6.600E+001	8.292E+001	1.042E+002
4.064E+002	7.361E+002	1.333E+003

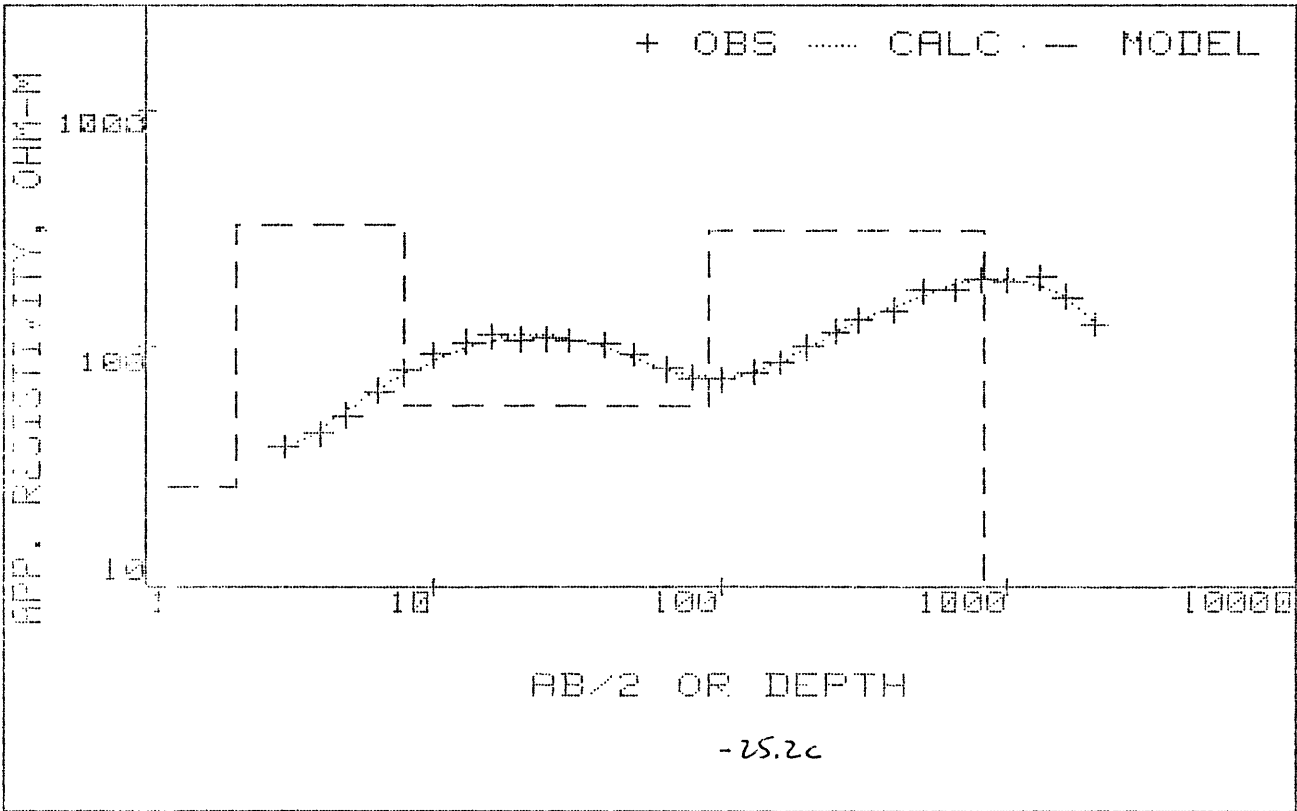
FINAL UNSCALED PARAMETERS--
(* denotes fixed value)

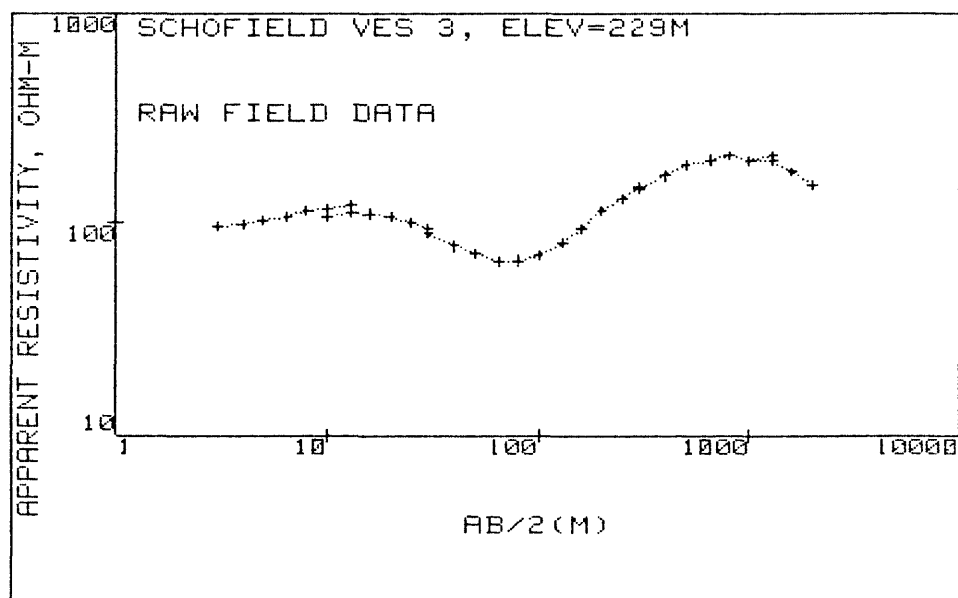
RESISTIVITY

DEPTH

1	2.61620239E+01	1	2.61620239E+01
2	3.21813773E+02	2	3.21813773E+02
3	5.65347181E+01	3	5.65347181E+01
4	3.08847321E+02	4	3.08847321E+02
5	1.00000000E+00	5	1.00000000E+00
6	2.04136964E+00	1	2.04136964E+00
7	5.86857183E+00	2	7.90994148E+00
8	8.29225324E+01	3	9.08324738E+01
9	7.36066046E+02	4	8.26898519E+02

SCHOFIELD VES 2, ELEV=244M





AB/2(M) APP RHO

3.0	95.3
4.0	97.2
5.0	101.6
6.5	106.0
8.0	113.0
10.0	117.0
13.0	121.0
10.0	106.4
13.0	111.0
16.0	110.0
20.0	106.0
25.0	99.5
30.0	93.0
30.0	89.0
40.0	78.0
50.0	72.0
65.0	66.7
80.0	67.0
100.0	71.0
100.0	71.0
130.0	81.0
160.0	94.0
200.0	113.0
250.0	130.0
300.0	146.0
300.0	144.0
400.0	166.0
500.0	189.0
650.0	201.0
800.0	213.5
800.0	211.0
1000.0	199.5
1300.0	210.0
1000.0	200.0
1300.0	201.0
1600.0	175.0
2000.0	151.0

	X	OBSERVED	PREDICTED	%RESIDUALS	WEIGHT FN
1	+3.0000E+00	+7.9540E+01	+7.8983E+01	+6.9980E-01	+1.4343E+00
2	+4.0000E+00	+8.1120E+01	+8.1663E+01	-6.6962E-01	+1.3789E+00
3	+5.0000E+00	+8.4800E+01	+8.4785E+01	+1.7281E-02	+1.2619E+00
4	+6.5000E+00	+8.8470E+01	+8.9486E+01	-1.1485E+00	+1.1593E+00
5	+8.0000E+00	+9.4310E+01	+9.3528E+01	+8.2942E-01	+1.0202E+00
6	+1.0000E+01	+9.7650E+01	+9.7423E+01	+2.3242E-01	+9.5161E-01
7	+1.3000E+01	+1.0100E+02	+1.0021E+02	+7.8448E-01	+8.8953E-01
8	+1.6000E+01	+1.0050E+02	+1.0017E+02	+3.2650E-01	+8.9840E-01
9	+2.0000E+01	+9.6860E+01	+9.7344E+01	-4.9942E-01	+9.6720E-01
10	+2.5000E+01	+9.0920E+01	+9.1618E+01	-7.6774E-01	+1.0977E+00
11	+3.0000E+01	+8.4980E+01	+8.5320E+01	-4.0054E-01	+1.2565E+00
12	+4.0000E+01	+7.4480E+01	+7.4598E+01	-1.5830E-01	+1.6358E+00
13	+5.0000E+01	+6.8750E+01	+6.7792E+01	+1.3939E+00	+1.9198E+00
14	+6.5000E+01	+6.3690E+01	+6.3611E+01	+1.2414E-01	+2.2370E+00
15	+8.0000E+01	+6.3970E+01	+6.3972E+01	-2.8741E-03	+2.2174E+00
16	+1.0000E+02	+6.7790E+01	+6.8236E+01	-6.5824E-01	+1.9746E+00
17	+1.3000E+02	+7.7340E+01	+7.8409E+01	-1.3823E+00	+1.5170E+00
18	+1.6000E+02	+8.9750E+01	+9.0156E+01	-4.5252E-01	+1.1265E+00
19	+2.0000E+02	+1.0790E+02	+1.0577E+02	+1.9734E+00	+7.7940E-01
20	+2.5000E+02	+1.2410E+02	+1.2355E+02	+4.4464E-01	+5.8920E-01
21	+3.0000E+02	+1.3940E+02	+1.3893E+02	+3.3487E-01	+4.6696E-01
22	+4.0000E+02	+1.6070E+02	+1.6313E+02	-1.5097E+00	+3.5138E-01
23	+5.0000E+02	+1.8300E+02	+1.8020E+02	+1.5308E+00	+2.7096E-01
24	+6.5000E+02	+1.9460E+02	+1.9600E+02	-7.2161E-01	+2.3962E-01
25	+8.0000E+02	+2.0670E+02	+2.0344E+02	+1.5749E+00	+2.1238E-01
26	+1.0000E+03	+1.9540E+02	+2.0467E+02	-4.7440E+00	+2.3766E-01
27	+1.3000E+03	+2.0570E+02	+1.9506E+02	+5.1735E+00	+2.1445E-01
28	+1.6000E+03	+1.7500E+02	+1.7810E+02	-1.7721E+00	+2.9630E-01
29	+2.0000E+03	+1.5100E+02	+1.5118E+02	-1.1971E-01	+3.9797E-01

CORRELATION MATRIX:

	1	2	3	4	5	6	7	8	9	10	11
1	+1.00	+.63	+.29	+.12	+.06	+.04	+.84	-.60	+.19	-.11	-.02
2	+.63	+1.00	+.66	+.30	+.16	+.10	+.92	-.97	+.45	-.28	-.06
3	+.29	+.66	+1.00	+.70	+.42	+.29	+.51	-.80	+.85	-.65	-.19
4	+.12	+.30	+.70	+1.00	+.83	+.63	+.22	-.41	+.97	-.99	-.53
5	+.06	+.16	+.42	+.83	+1.00	+.91	+.11	-.23	+.73	-.89	-.88
6	+.04	+.10	+.29	+.63	+.91	+1.00	+.07	-.15	+.53	-.70	-.99
7	+.84	+.92	+.51	+.22	+.11	+.07	+1.00	-.88	+.34	-.20	-.04
8	-.60	-.97	-.80	-.41	-.23	-.15	-.88	+1.00	-.57	+.38	+.09
9	+.19	+.45	+.85	+.97	+.73	+.53	+.34	-.57	+1.00	-.94	-.42
10	-.11	-.28	-.65	-.99	-.89	-.70	-.20	+.38	-.94	+1.00	+.61
11	-.02	-.06	-.19	-.53	-.88	-.99	-.04	+.09	-.42	+.61	+1.00

REDUCED CHI-SQUARED=4.324

DCLAG: ***** END *****
 COORDINATES: 0 0
 ELEVATION : 229 METER
 AZIMUTH :

SCHOFIELD VES 3, ELEV=229M

B-SD	B	B+SD
7.375E+001	7.616E+001	7.866E+001
1.130E+002	1.265E+002	1.415E+002
4.472E+001	4.870E+001	5.303E+001
6.246E+000	5.986E+002	5.737E+004
8.947E+001	2.316E+002	5.996E+002
4.953E-002	2.316E+001	1.083E+004
2.577E+000	3.235E+000	4.059E+000
7.666E+000	1.009E+001	1.327E+001
4.531E+001	6.860E+001	1.039E+002
5.693E-002	9.564E+001	1.606E+005
1.952E+002	8.236E+002	3.475E+003

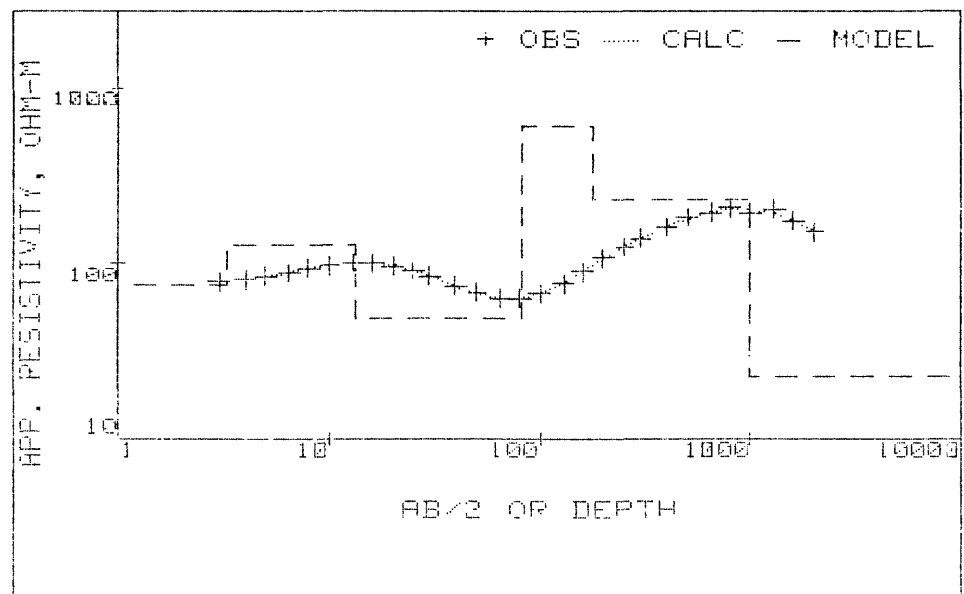
FINAL UNSCALED PARAMETERS--
 (* denotes fixed value)

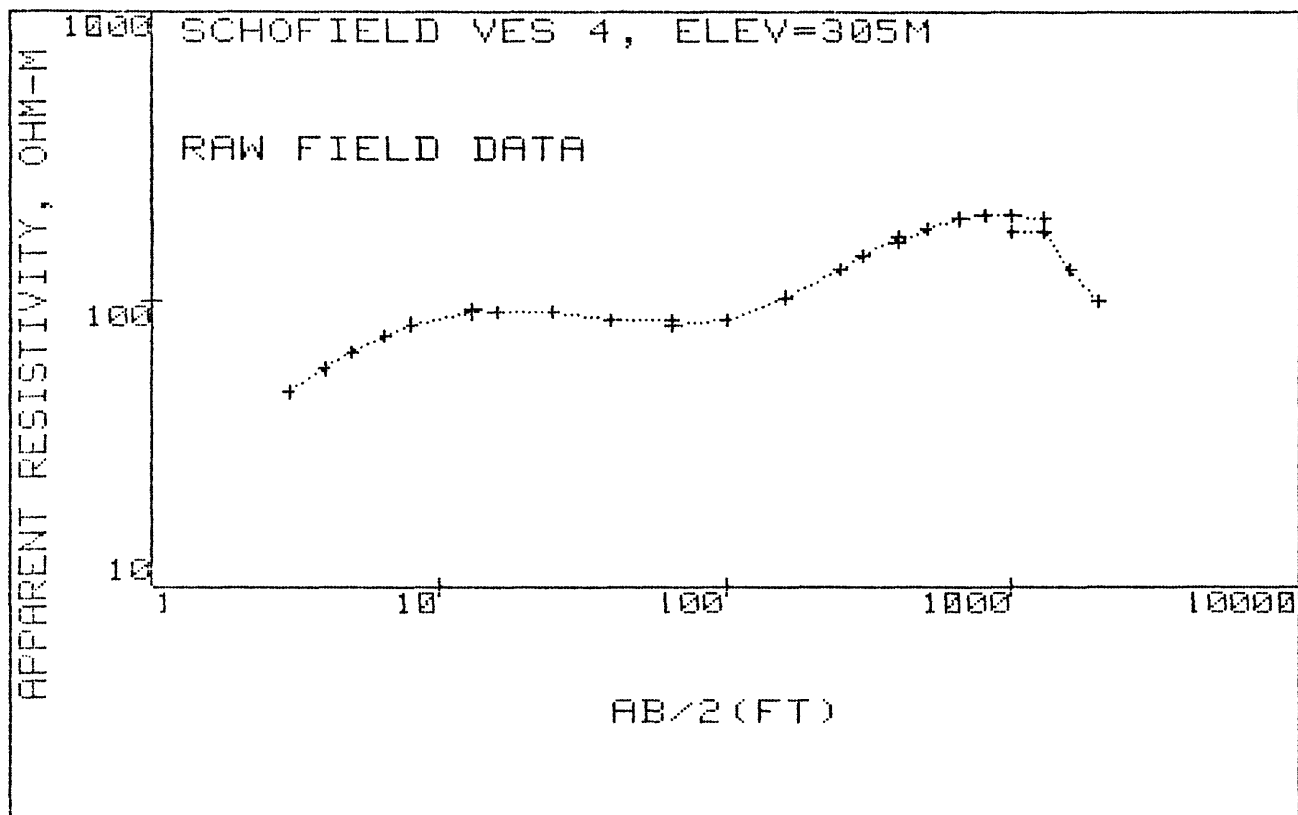
RESISTIVITY

DEPTH

1	7.61629416E+01	1	7.61629416E+01
2	1.26464434E+02	2	1.26464434E+02
3	4.86976475E+01	3	4.86976475E+01
4	5.98616878E+02	4	5.98616878E+02
5	2.31624937E+02	5	2.31624937E+02
6	2.31648917E+01	6	2.31648917E+01
7	3.23458365E+00	1	3.23458365E+00
8	1.00852118E+01	2	1.33197954E+01
9	6.85984275E+01	3	8.19182229E+01
10	9.56358960E+01	4	1.77554119E+02
11	8.23621328E+02	5	1.00117545E+03

SCHOFIELD VES 3, ELEV=229M





AB/2 (M) APP RHO

3.0	47.6
4.0	57.7
5.0	66.0
6.5	76.0
8.0	83.0
13.0	90.8
13.0	94.0
16.0	92.0
25.0	92.0
40.0	86.0
65.0	85.0
65.0	83.0
100.0	85.7
160.0	102.5
160.0	103.0
250.0	130.0
300.0	145.0
400.0	167.0
400.0	160.0
500.0	178.0
650.0	193.0
800.0	200.0
1000.0	198.0
1300.0	195.0
1000.0	176.1
1300.0	175.0
1600.0	129.0
2000.0	100.0

MARQUARDT STATISTICS: SCHOFIELD VES 4, ELEV=305M

	X	OBSERVED	PREDICTED	%RESIDUALS	WEIGHT FN
1	+3.0000E+00	+4.1390E+01	+4.1516E+01	-3.0469E-01	+3.7486E+00
2	+4.0000E+00	+5.0170E+01	+5.0370E+01	-3.9815E-01	+2.5514E+00
3	+5.0000E+00	+5.7390E+01	+5.7577E+01	-3.2516E-01	+1.9498E+00
4	+6.5000E+00	+6.6080E+01	+6.5664E+01	+6.2922E-01	+1.4707E+00
5	+8.0000E+00	+7.2170E+01	+7.1179E+01	+1.3730E+00	+1.2330E+00
6	+1.3000E+01	+7.8950E+01	+7.8623E+01	+4.1386E-01	+1.0303E+00
7	+1.6000E+01	+7.7270E+01	+7.9108E+01	-2.3782E+00	+1.0756E+00
8	+2.5000E+01	+7.7270E+01	+7.6299E+01	+1.2571E+00	+1.0756E+00
9	+4.0000E+01	+7.2230E+01	+7.2310E+01	-1.1123E-01	+1.2309E+00
10	+6.5000E+01	+7.1390E+01	+7.1194E+01	+2.7451E-01	+1.2600E+00
11	+1.0000E+02	+7.3710E+01	+7.4603E+01	-1.2120E+00	+1.1820E+00
12	+1.6000E+02	+8.8160E+01	+8.7000E+01	+1.3162E+00	+8.2626E-01
13	+2.5000E+02	+1.1130E+02	+1.1074E+02	+4.9997E-01	+5.1841E-01
14	+3.0000E+02	+1.2410E+02	+1.2330E+02	+6.4238E-01	+4.1698E-01
15	+4.0000E+02	+1.4290E+02	+1.4448E+02	-1.1032E+00	+3.1448E-01
16	+5.0000E+02	+1.5900E+02	+1.6018E+02	-7.4374E-01	+2.5402E-01
17	+6.5000E+02	+1.7240E+02	+1.7480E+02	-1.3940E+00	+2.1607E-01
18	+8.0000E+02	+1.7870E+02	+1.8069E+02	-1.1112E+00	+2.0110E-01
19	+1.0000E+03	+1.7690E+02	+1.7836E+02	-8.2774E-01	+2.0521E-01
20	+1.3000E+03	+1.7420E+02	+1.6106E+02	+7.5410E+00	+2.1162E-01
21	+1.6000E+03	+1.2900E+02	+1.3606E+02	-5.4753E+00	+3.8591E-01
22	+2.0000E+03	+1.0000E+02	+1.0146E+02	-1.4613E+00	+6.4219E-01

CORRELATION MATRIX:

	1	2	3	4	5	6	7	8	9
1	+1.00	+.92	+.40	+.13	+.07	+1.00	-.92	+.47	-.11
2	+.92	+1.00	+.53	+.18	+.09	+.94	-1.00	+.58	-.15
3	+.40	+.53	+1.00	+.41	+.22	+.42	-.55	+.79	-.36
4	+.13	+.18	+.41	+1.00	+.77	+.14	-.13	+.82	-.95
5	+.07	+.09	+.22	+.77	+1.00	+.07	-.10	+.52	-.92
6	+1.00	+.94	+.42	+.14	+.07	+1.00	-.94	+.49	-.12
7	-.92	-1.00	-.55	-.18	-.10	-.94	+1.00	-.59	+.16
8	+.47	+.58	+.79	+.82	+.52	+.49	-.59	+1.00	-.73
9	-.11	-.15	-.36	-.95	-.92	-.12	+.16	-.73	+1.00

REDUCED CHI-SQUARED=9.051

DCLAG: ***** END *****
 COORDINATES: 0 0
 ELEVATION : 305 METER
 AZIMUTH :

SCHOFIELD VES 4, ELEV=305M

B-SD	B	B+SD
8.506E-001	2.087E+001	5.121E+002
3.489E+000	1.836E+002	9.661E+003
6.472E+001	6.748E+001	7.036E+001
2.549E+002	3.200E+002	4.016E+002
5.806E-047	3.000E-001	1.550E+045
2.126E-002	1.193E+000	6.699E+001
1.394E-002	2.368E+000	4.023E+002
9.303E+001	1.086E+002	1.267E+002
3.868E+002	5.827E+002	8.776E+002

FINAL UNSCALED PARAMETERS--
 (* denotes fixed value)

1	2.08719976E+01
2	1.83594212E+02
3	6.74827199E+01
4	3.19986137E+02
5	3.00000000E-01
6	1.19338345E+00
7	2.36817646E+00
8	1.08552662E+02
9	5.82673049E+02

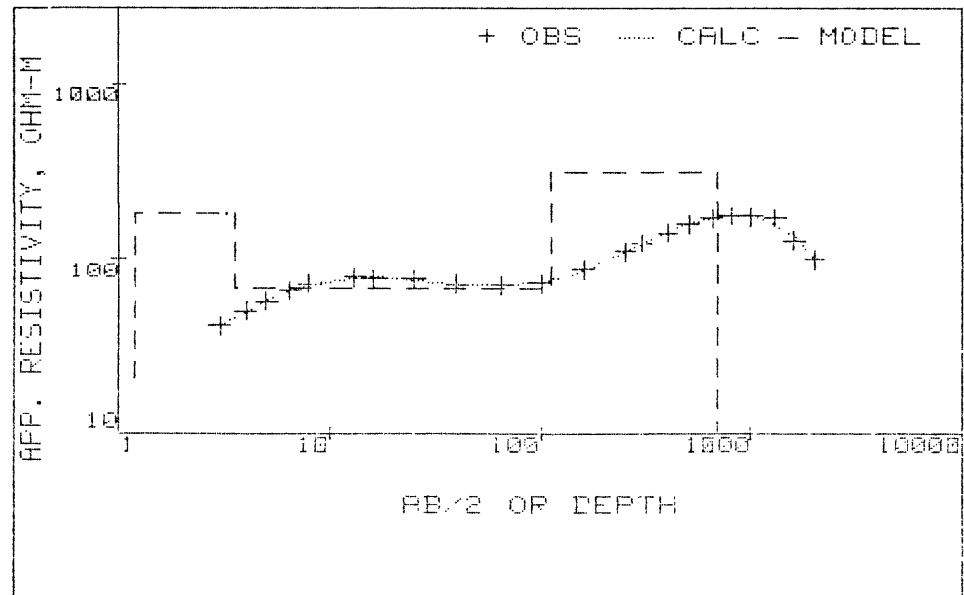
RESISTIVITY

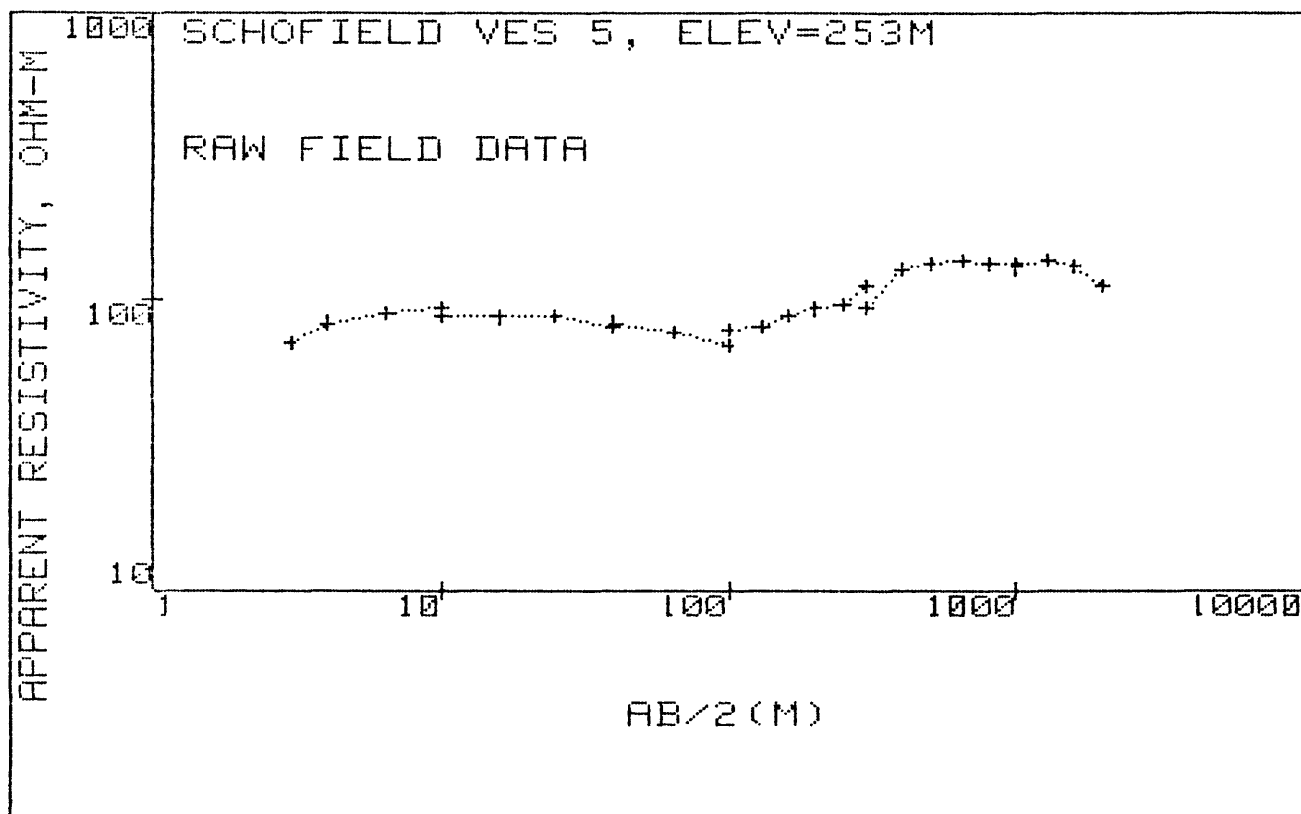
DEPTH

1	2.08719976E+01
2	1.83594212E+02
3	6.74827199E+01
4	3.19986137E+02
5	3.00000000E-01

1	1.19338345E+00
2	3.56155991E+00
3	1.12114222E+02
4	6.94787272E+02

SCHOFIELD VES 4, ELEV=305M





AB/2 (M) APP RHO

3.0	71.0
4.0	83.0
6.5	89.6
10.0	94.0
10.0	88.0
16.0	87.0
25.0	87.3
40.0	80.1
40.0	83.0
65.0	77.0
100.0	69.2
100.0	78.3
130.0	81.0
160.0	88.2
200.0	92.7
250.0	95.3
300.0	111.0
300.0	93.0
400.0	127.0
500.0	133.0
650.0	135.0
800.0	133.0
1000.0	131.0
1000.0	128.0
1300.0	135.0
1600.0	130.0
2000.0	111.0

	X	OBSERVED	PREDICTED	%RESIDUALS	WEIGHT FN
1	+3.0000E+00	+6.3800E+01	+6.5992E+01	-3.4350E+00	+1.8076E+00
2	+4.0000E+00	+7.4580E+01	+7.2011E+01	+3.4442E+00	+1.3228E+00
3	+6.5000E+00	+8.0510E+01	+7.9614E+01	+1.1124E+00	+1.1351E+00
4	+1.0000E+01	+8.4470E+01	+8.3580E+01	+1.0539E+00	+1.0312E+00
5	+1.6000E+01	+8.3510E+01	+8.5166E+01	-1.9835E+00	+1.0550E+00
6	+2.5000E+01	+8.3790E+01	+8.3761E+01	+3.4766E-02	+1.0480E+00
7	+4.0000E+01	+7.6880E+01	+7.8244E+01	-1.7744E+00	+1.2448E+00
8	+6.5000E+01	+7.1330E+01	+6.9741E+01	+2.2274E+00	+1.4461E+00
9	+1.0000E+02	+6.4100E+01	+6.5192E+01	-1.7034E+00	+1.7907E+00
10	+1.3000E+02	+6.6310E+01	+6.6044E+01	+4.0146E-01	+1.6733E+00
11	+1.6000E+02	+7.2200E+01	+6.9314E+01	+3.9970E+00	+1.4114E+00
12	+2.0000E+02	+7.5890E+01	+7.5679E+01	+2.7847E-01	+1.2775E+00
13	+2.5000E+02	+7.8020E+01	+8.4928E+01	-8.8538E+00	+1.2087E+00
14	+3.0000E+02	+9.0870E+01	+9.4181E+01	-3.6441E+00	+8.9104E-01
15	+4.0000E+02	+1.2410E+02	+1.1010E+02	+1.1280E+01	+4.7774E-01
16	+5.0000E+02	+1.3000E+02	+1.2163E+02	+6.4369E+00	+4.3536E-01
17	+6.5000E+02	+1.3190E+02	+1.3187E+02	+2.2271E-02	+4.2291E-01
18	+8.0000E+02	+1.3000E+02	+1.3608E+02	-4.6800E+00	+4.3536E-01
19	+1.0000E+03	+1.2800E+02	+1.3608E+02	-6.3092E+00	+4.4907E-01
20	+1.3000E+03	+1.3500E+02	+1.3046E+02	+3.3645E+00	+4.0371E-01
21	+1.6000E+03	+1.3000E+02	+1.2306E+02	+5.3390E+00	+4.3536E-01
22	+2.0000E+03	+1.1100E+02	+1.1417E+02	-2.8519E+00	+5.9716E-01

CORRELATION MATRIX:

	1	2	3	5	6	7	8	9
1	+1.00	+0.76	+0.30	-0.07	+1.00	-0.68	+0.35	+0.06
2	+0.76	+1.00	+0.48	-0.11	+0.76	-0.83	+0.53	+0.10
3	+0.30	+0.48	+1.00	-0.34	+0.30	-0.81	+0.97	+0.35
5	-0.07	-0.11	-0.34	+1.00	-0.07	+0.21	-0.46	-0.95
6	+1.00	+0.76	+0.30	-0.07	+1.00	-0.68	+0.35	+0.06
7	-0.68	-0.83	-0.81	+0.21	-0.68	+1.00	-0.82	-0.21
8	+0.35	+0.53	+0.97	-0.46	+0.35	-0.82	+1.00	+0.48
9	+0.06	+0.10	+0.35	-0.95	+0.06	-0.21	+0.48	+1.00

REDUCED CHI-SQUARED=32.86

DCLAG: ***** END *****
COORDINATES: 0 0
ELEVATION : 253 METER
AZIMUTH :

SCHOFIELD VES 5, ELEV=253M

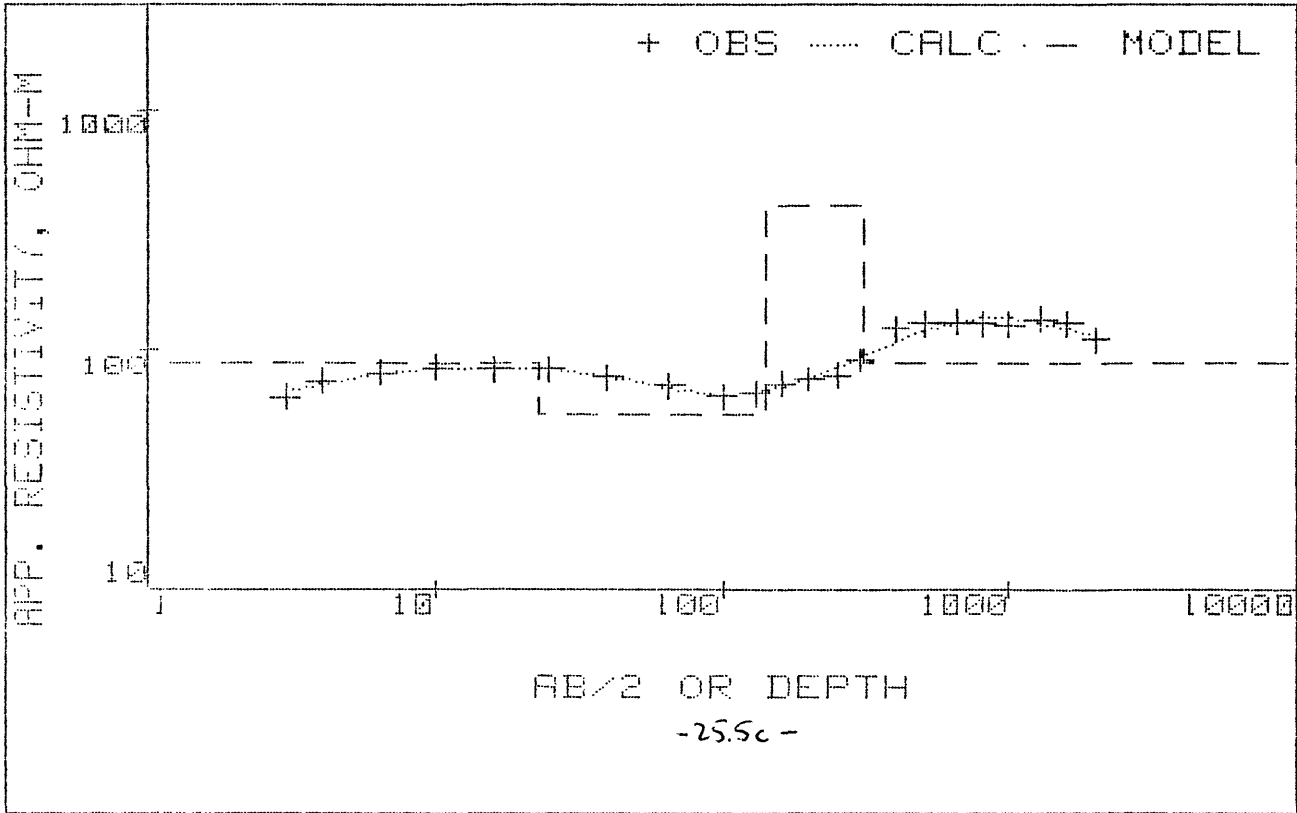
B-SD	B	B+SD
6.804E-044	5.579E+000	4.574E+044
8.102E+001	8.828E+001	9.619E+001
4.685E+001	5.476E+001	6.400E+001
	4.000E+002	
7.351E+001	8.928E+001	1.085E+002
1.074E-046	9.090E-002	7.696E+043
1.289E+001	2.312E+001	4.146E+001
8.822E+001	1.177E+002	1.570E+002
1.239E+002	1.678E+002	2.272E+002

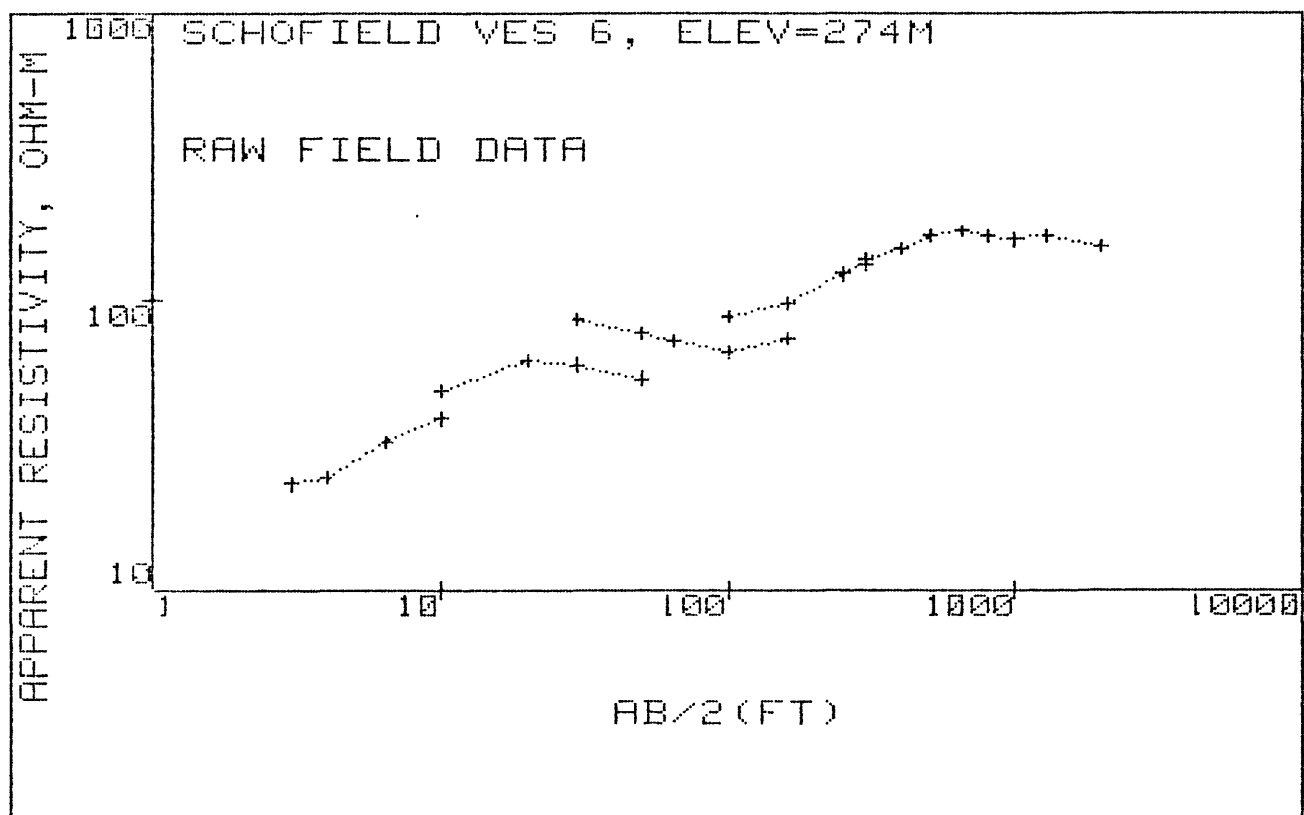
FINAL UNSCALED PARAMETERS--
(* denotes fixed value)

RESISTIVITY DEPTH

1	5.57872074E+00	1	5.57872074E+00		
2	8.82794751E+01	2	8.82794751E+01		
3	5.47554562E+01	3	5.47554562E+01		
4 *	4.00000000E+02	4	4.00000000E+02		
5	8.92847160E+01	5	8.92847160E+01		
6	9.08981323E-02			1	9.08981323E-02
7	2.31154970E+01			2	2.32063951E+01
8	1.17704349E+02			3	1.40910744E+02
9	1.67760555E+02			4	3.08671299E+02

SCHOFIELD VES 5, ELEV=253M





AB/2(M) APP RHO

3.0	23.4
4.0	24.6
6.5	32.6
10.0	39.2
10.0	48.8
20.0	62.0
30.0	60.2
50.0	54.0
30.0	86.1
50.0	76.7
65.0	72.0
100.0	65.9
160.0	73.5
100.0	87.7
160.0	97.7
250.0	122.7
300.0	132.5
300.0	137.5
400.0	151.4
500.0	168.0
650.0	176.0
800.0	167.0
1000.0	165.0
1000.0	162.6
1300.0	166.2
2000.0	154.0

	X	OBSERVED	PREDICTED	%RESIDUALS	WEIGHT FN
1	+3.0000E+00	+5.6470E+01	+5.5538E+01	+1.6499E+00	+3.2756E+00
2	+4.0000E+00	+5.9370E+01	+6.1114E+01	-2.9378E+00	+2.9635E+00
3	+6.5000E+00	+7.8680E+01	+7.7038E+01	+2.0863E+00	+1.6873E+00
4	+1.0000E+01	+9.4600E+01	+9.5409E+01	-8.5484E-01	+1.1672E+00
5	+2.0000E+01	+1.2020E+02	+1.1835E+02	+1.5382E+00	+7.2297E-01
6	+3.0000E+01	+1.1670E+02	+1.1890E+02	-1.8842E+00	+7.6699E-01
7	+5.0000E+01	+1.0470E+02	+1.0485E+02	-1.3989E-01	+9.5288E-01
8	+6.5000E+01	+9.7930E+01	+9.6388E+01	+1.5749E+00	+1.0892E+00
9	+1.0000E+02	+8.9630E+01	+9.0288E+01	-7.3419E-01	+1.3002E+00
10	+1.6000E+02	+9.9970E+01	+1.0054E+02	-5.7120E-01	+1.0452E+00
11	+2.5000E+02	+1.2550E+02	+1.2454E+02	+7.6812E-01	+6.6320E-01
12	+3.0000E+02	+1.3550E+02	+1.3588E+02	-2.8260E-01	+5.6892E-01
13	+4.0000E+02	+1.4920E+02	+1.5217E+02	-1.9933E+00	+4.6924E-01
14	+5.0000E+02	+1.6560E+02	+1.6163E+02	+2.3965E+00	+3.8090E-01
15	+6.5000E+02	+1.7340E+02	+1.6786E+02	+3.1959E+00	+3.4740E-01
16	+8.0000E+02	+1.6460E+02	+1.6894E+02	-2.6357E+00	+3.8554E-01
17	+1.0000E+03	+1.6260E+02	+1.6701E+02	-2.7115E+00	+3.9509E-01
18	+1.3000E+03	+1.6620E+02	+1.6234E+02	+2.3254E+00	+3.7816E-01
19	+2.0000E+03	+1.5400E+02	+1.5418E+02	-1.1587E-01	+4.4044E-01

CORRELATION MATRIX:

	1	2	3	5	6	7	8	9
1	+1.00	+.63	+.29	-.05	+.90	-.56	+.31	+.05
2	+.63	+1.00	+.64	-.12	+.88	-.95	+.66	+.12
3	+.29	+.64	+1.00	-.27	+.46	-.82	+.96	+.31
5	-.05	-.12	-.27	+1.00	-.08	+.17	-.40	-.87
6	+.90	+.88	+.46	-.08	+1.00	-.80	+.48	+.08
7	-.56	-.95	-.82	+.17	-.80	+1.00	-.81	-.18
8	+.31	+.66	+.96	-.40	+.48	-.81	+1.00	+.48
9	+.05	+.12	+.31	-.87	+.08	-.18	+.48	+1.00

REDUCED CHI-SQUARED=6.604

DCLAG: ***** END *****
COORDINATES: 0 0
ELEVATION : 274 METER
AZIMUTH :

SCHOFIELD VES 6, ELEV=274M

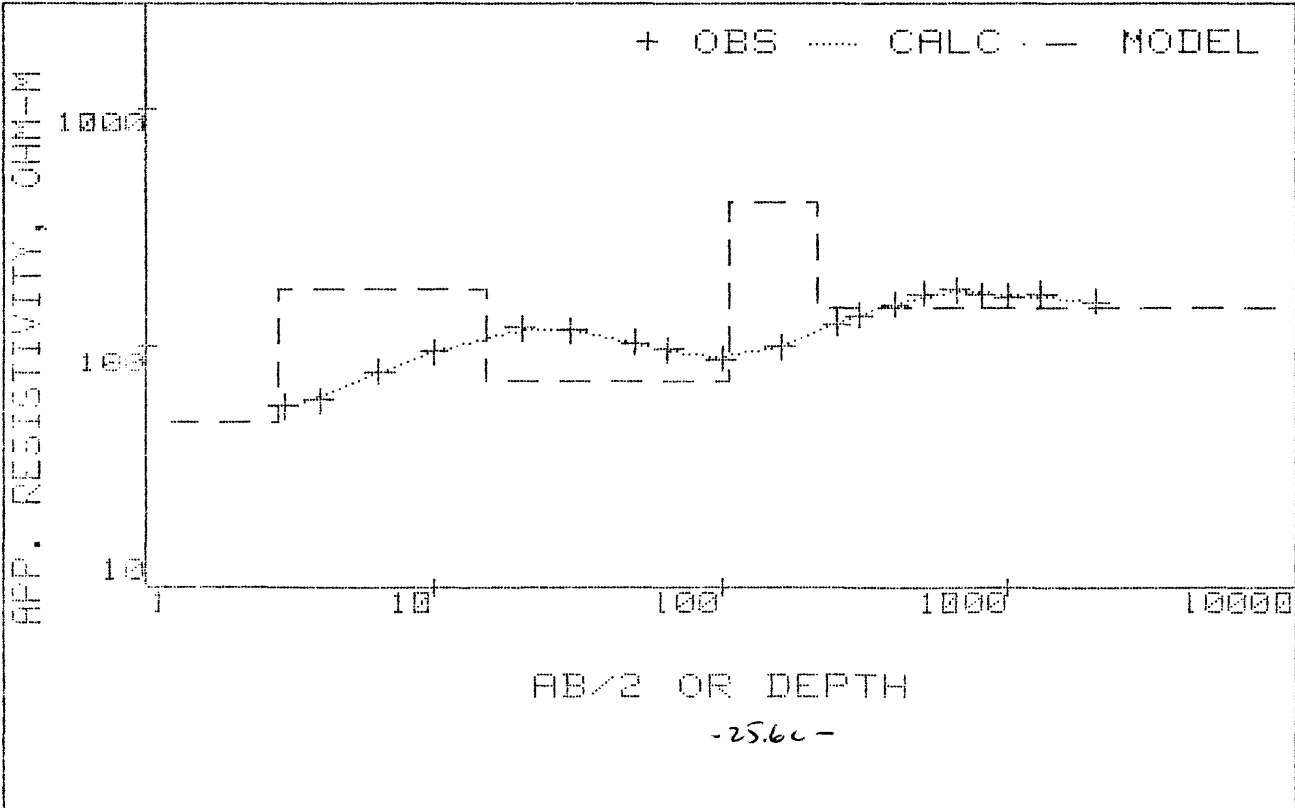
B-SD	B	B+SD
4.676E+001	4.937E+001	5.213E+001
1.475E+002	1.730E+002	2.029E+002
6.700E+001	7.272E+001	7.894E+001
	4.000E+002	
1.397E+002	1.452E+002	1.509E+002
2.426E+000	2.838E+000	3.321E+000
8.792E+000	1.241E+001	1.752E+001
7.977E+001	9.185E+001	1.058E+002
9.319E+001	1.081E+002	1.253E+002

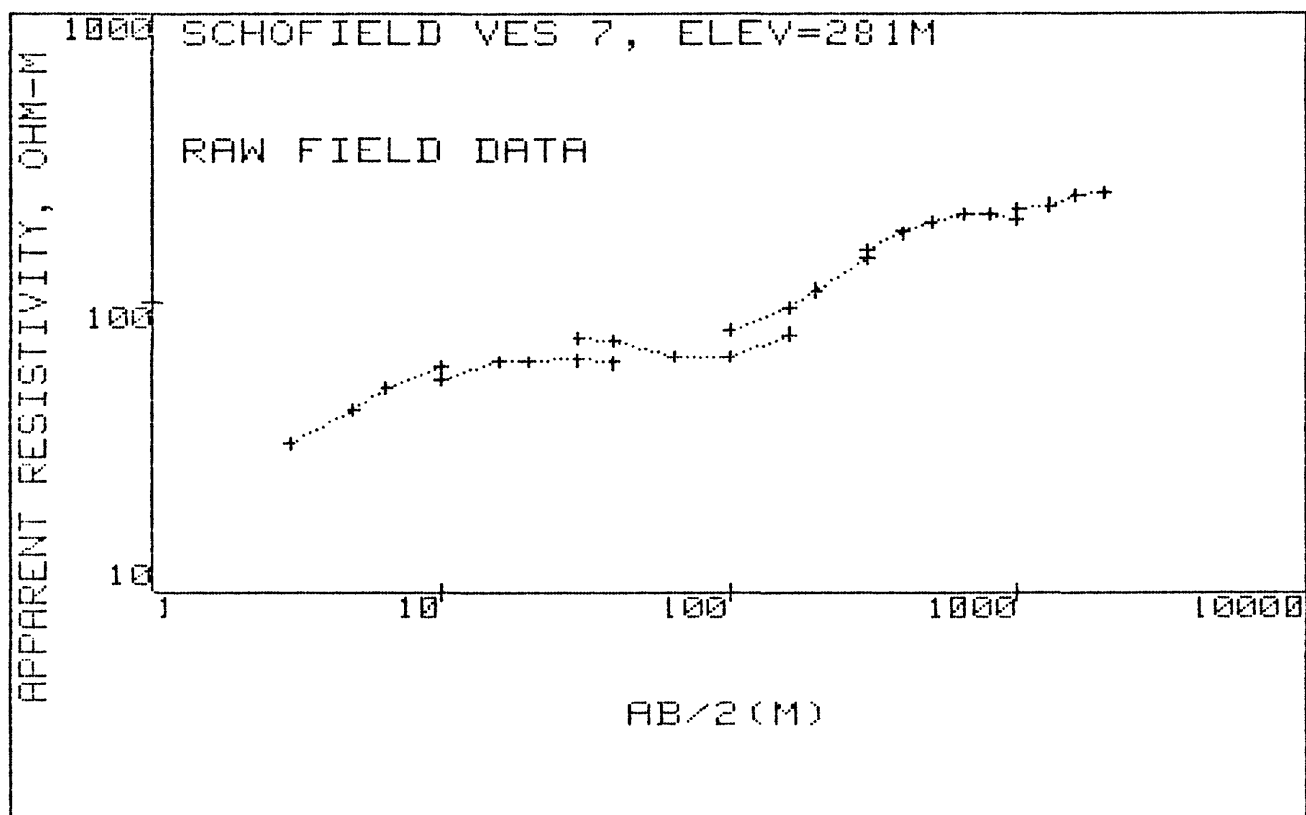
FINAL UNSCALED PARAMETERS--
(* denotes fixed value)

RESISTIVITY DEPTH

1	4.93709756E+01	1	4.93709756E+01		
2	1.73017805E+02	2	1.73017805E+02		
3	7.27241452E+01	3	7.27241452E+01		
4	* 4.00000000E+02	4	4.00000000E+02		
5	1.45161671E+02	5	1.45161671E+02		
6	2.83841883E+00			1	2.83841883E+00
7	1.24095808E+01			2	1.52479996E+01
8	9.18496512E+01			3	1.07097651E+02
9	1.08065807E+02			4	2.15163458E+02

SCHOFIELD VES 6, ELEV=274M





AB/2(M) APP RHO

3.0	32.7
5.0	42.2
6.5	50.0
10.0	59.0
10.0	53.7
16.0	62.0
20.0	62.6
30.0	63.0
40.0	61.7
30.0	75.7
40.0	73.6
65.0	64.9
100.0	65.0
160.0	77.9
100.0	80.7
160.0	96.4
200.0	110.0
300.0	142.0
300.0	150.9
400.0	173.0
500.0	190.0
650.0	202.0
800.0	203.0
1000.0	195.0
1000.0	210.0
1300.0	219.0
1600.0	238.0
2000.0	241.0

	X	OBSERVED	PREDICTED	%RESIDUALS	WEIGHT FN
1	+3.0000E+00	+5.0550E+01	+5.0441E+01	+2.1634E-01	+4.4119E+00
2	+5.0000E+00	+6.5230E+01	+6.6382E+01	-1.7667E+00	+2.6496E+00
3	+6.5000E+00	+7.7290E+01	+7.5897E+01	+1.8018E+00	+1.8872E+00
4	+1.0000E+01	+9.1200E+01	+9.1180E+01	+2.1578E-02	+1.3554E+00
5	+1.6000E+01	+1.0530E+02	+1.0415E+02	+1.0915E+00	+1.0168E+00
6	+2.0000E+01	+1.0630E+02	+1.0769E+02	-1.3051E+00	+9.9771E-01
7	+3.0000E+01	+1.0700E+02	+1.0798E+02	-9.1163E-01	+9.8470E-01
8	+4.0000E+01	+1.0480E+02	+1.0336E+02	+1.3725E+00	+1.0265E+00
9	+6.5000E+01	+9.2060E+01	+9.2652E+01	-6.4297E-01	+1.3302E+00
10	+1.0000E+02	+9.2200E+01	+9.1774E+01	+4.6155E-01	+1.3262E+00
11	+1.6000E+02	+1.1050E+02	+1.1060E+02	-9.2016E-02	+9.2331E-01
12	+2.0000E+02	+1.2590E+02	+1.2687E+02	-7.7125E-01	+7.1125E-01
13	+3.0000E+02	+1.6250E+02	+1.6276E+02	-1.5768E-01	+4.2694E-01
14	+4.0000E+02	+1.8630E+02	+1.8724E+02	-5.0440E-01	+3.2482E-01
15	+5.0000E+02	+2.0460E+02	+2.0225E+02	+1.1470E+00	+2.6932E-01
16	+6.5000E+02	+2.1750E+02	+2.1324E+02	+1.9571E+00	+2.3832E-01
17	+8.0000E+02	+2.1860E+02	+2.1686E+02	+7.9576E-01	+2.3592E-01
18	+1.0000E+03	+2.1000E+02	+2.1790E+02	-3.7599E+00	+2.5564E-01
19	+1.3000E+03	+2.1900E+02	+2.2074E+02	-7.9495E-01	+2.3506E-01
20	+1.6000E+03	+2.3800E+02	+2.2858E+02	+3.9561E+00	+1.9903E-01
21	+2.0000E+03	+2.4100E+02	+2.4482E+02	-1.5858E+00	+1.9411E-01

CORRELATION MATRIX:

	1	2	3	5	6	7	8	9	10	11
1	+1.00	+.64	+.30	-.09	-.08	+.98	-.50	+.31	+.10	-.09
2	+.64	+1.00	+.64	-.21	-.17	+.75	-.88	+.63	+.21	-.21
3	+.30	+.64	+1.00	-.50	-.42	+.38	-.90	+.98	+.51	-.50
5	-.09	-.21	-.50	+1.00	+.97	-.12	+.36	-.64	-1.00	+1.00
6	-.08	-.17	-.42	+.97	+1.00	-.10	+.30	-.55	-.96	+.97
7	+.98	+.75	+.38	-.12	-.10	+1.00	-.60	+.38	+.12	-.12
8	-.50	-.88	-.90	+.36	+.30	-.60	+1.00	-.87	-.36	+.36
9	+.31	+.63	+.98	-.64	-.55	+.38	-.87	+1.00	+.65	-.64
10	+.10	+.21	+.51	-1.00	-.96	+.12	-.36	+.65	+1.00	-1.00
11	-.09	-.21	-.50	+1.00	+.97	-.12	+.36	-.64	-1.00	+1.00

REDUCED CHI-SQUARED=5.225

DCLAG: ***** END *****
 COORDINATES: 0 0
 ELEVATION : 281 METER
 AZIMUTH :

SCHOFIELD VES 7, ELEV=281M

B-SD	B	B+SD
3.120E+001	3.626E+001	4.213E+001
1.245E+002	1.320E+002	1.399E+002
6.122E+001	6.902E+001	7.781E+001
	7.000E+002	
2.098E-116	2.574E+001	3.159E+118
7.410E+001	4.826E+002	3.143E+003
1.340E+000	1.680E+000	2.105E+000
1.283E+001	1.679E+001	2.198E+001
6.268E+001	7.703E+001	9.467E+001
9.560E-001	1.490E+002	2.321E+004
3.411E-117	9.908E+001	2.878E+120

FINAL UNSCALED PARAMETERS--
 (* denotes fixed value)

1	3.62582502E+01
2	1.31979346E+02
3	6.90213657E+01
4 *	7.00000000E+02
5	2.57418010E+01
6	4.82610162E+02
7	1.67972770E+00
8	1.67904991E+01
9	7.70324305E+01
10	1.48958575E+02
11	9.90776113E+01

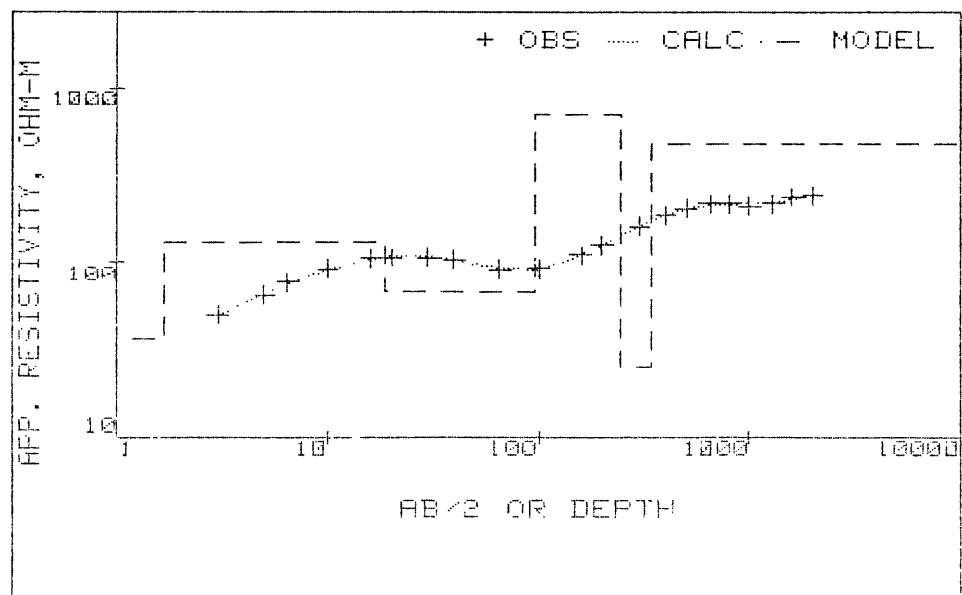
RESISTIVITY

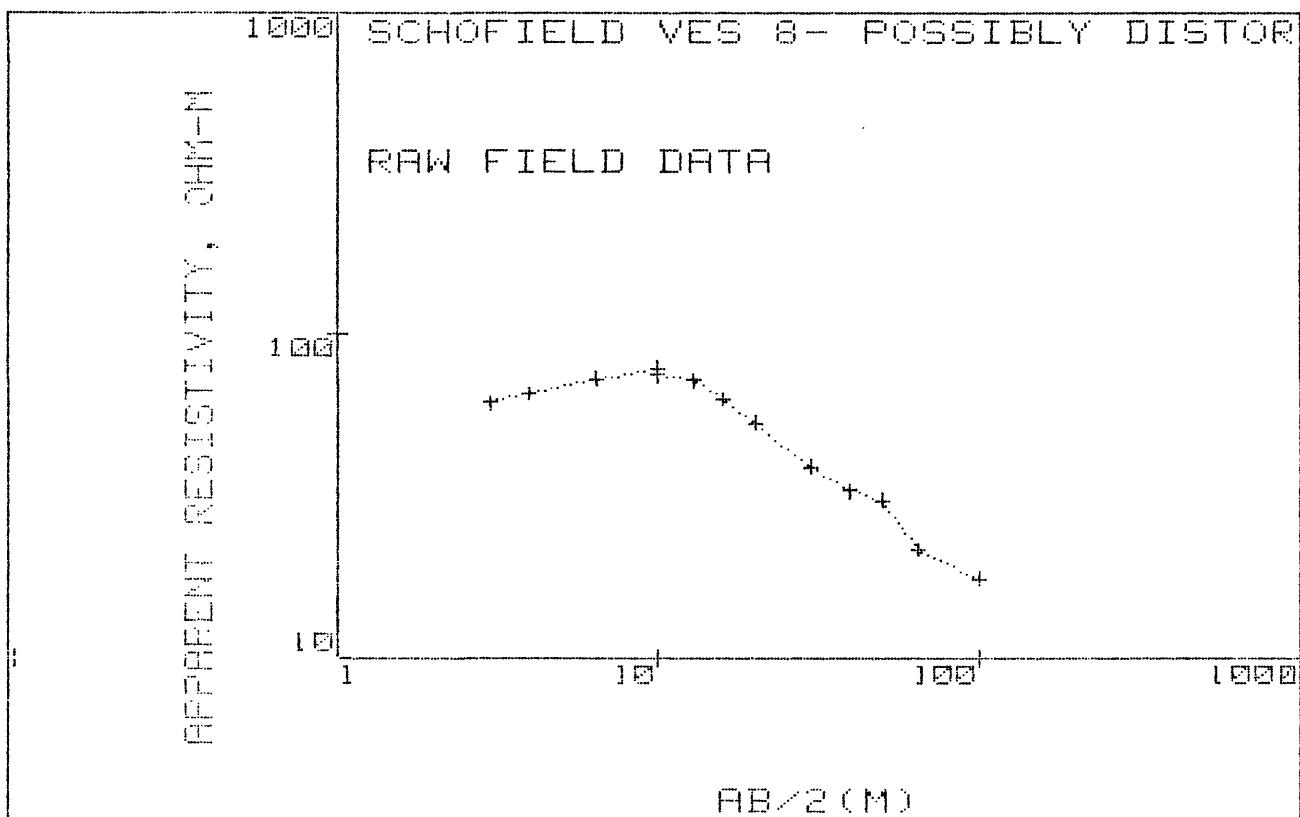
DEPTH

1	3.62582502E+01
2	1.31979346E+02
3	6.90213657E+01
4	7.00000000E+02
5	2.57418010E+01
6	4.82610162E+02

1	1.67972770E+00
2	1.84702268E+01
3	9.55026573E+01
4	2.44461233E+02
5	3.43538844E+02

SCHOFIELD VES 7, ELEV=281M





AB/2 (M) APP RHO

3.0	61.1
4.0	65.0
6.5	72.0
10.0	78.0
10.0	74.1
13.0	71.2
16.0	62.5
20.0	53.0
30.0	39.0
30.0	39.0
40.0	33.0
50.0	30.8
65.0	21.7
100.0	17.6

MARQUARDT STATISTICS: SCHOFIELD VES 8- POSSIBLY DISTORTED

	X	OBSERVED	PREDICTED	%RESIDUALS	WEIGHT FN
1	+3.0000E+00	+5.8045E+01	+5.8819E+01	-1.3340E+00	+3.6545E-01
2	+4.0000E+00	+6.1750E+01	+6.3253E+01	-2.4339E+00	+3.2291E-01
3	+6.5000E+00	+6.8400E+01	+6.8066E+01	+4.8866E-01	+2.6317E-01
4	+1.0000E+01	+7.4100E+01	+6.8622E+01	+7.3931E+00	+2.2424E-01
5	+1.3000E+01	+7.1200E+01	+6.6483E+01	+6.6249E+00	+2.4288E-01
6	+1.6000E+01	+6.2500E+01	+6.2993E+01	-7.8859E-01	+3.1521E-01
7	+2.0000E+01	+5.3000E+01	+5.7249E+01	-8.0168E+00	+4.3833E-01
8	+3.0000E+01	+3.9000E+01	+4.2731E+01	-9.5665E+00	+8.0952E-01
9	+4.0000E+01	+3.3000E+01	+3.2308E+01	+2.0967E+00	+1.1306E+00
10	+5.0000E+01	+3.0800E+01	+2.6115E+01	+1.5212E+01	+1.2979E+00
11	+6.5000E+01	+2.1700E+01	+2.1584E+01	+5.3349E-01	+2.6148E+00
12	+1.0000E+02	+1.7600E+01	+1.8666E+01	-6.0561E+00	+3.9749E+00

CORRELATION MATRIX:

	1	2	3	4	5
1	+1.00	+.60	-.84	+1.00	-.95
2	+.60	+1.00	-.34	+.60	-.78
3	-.84	-.34	+1.00	-.84	+.68
4	+1.00	+.60	-.84	+1.00	-.95
5	-.95	-.78	+.68	-.95	+1.00

REDUCED CHI-SQUARED=89.28

DCLAG: ***** END *****
COORDINATES: 0 0 UTM4
ELEVATION : 293 METER
AZIMUTH :

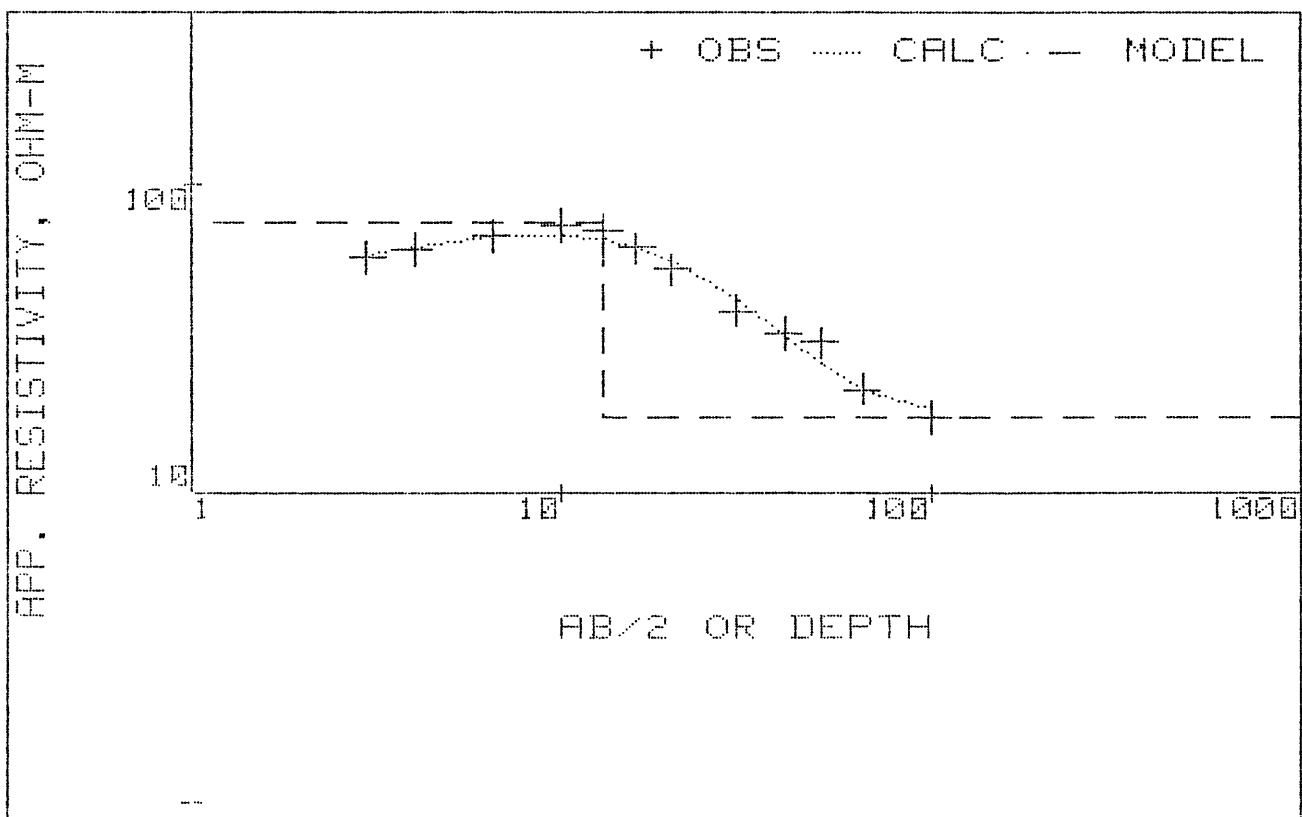
SCHOFIELD VES 8- POSSIBLY DISTORTED

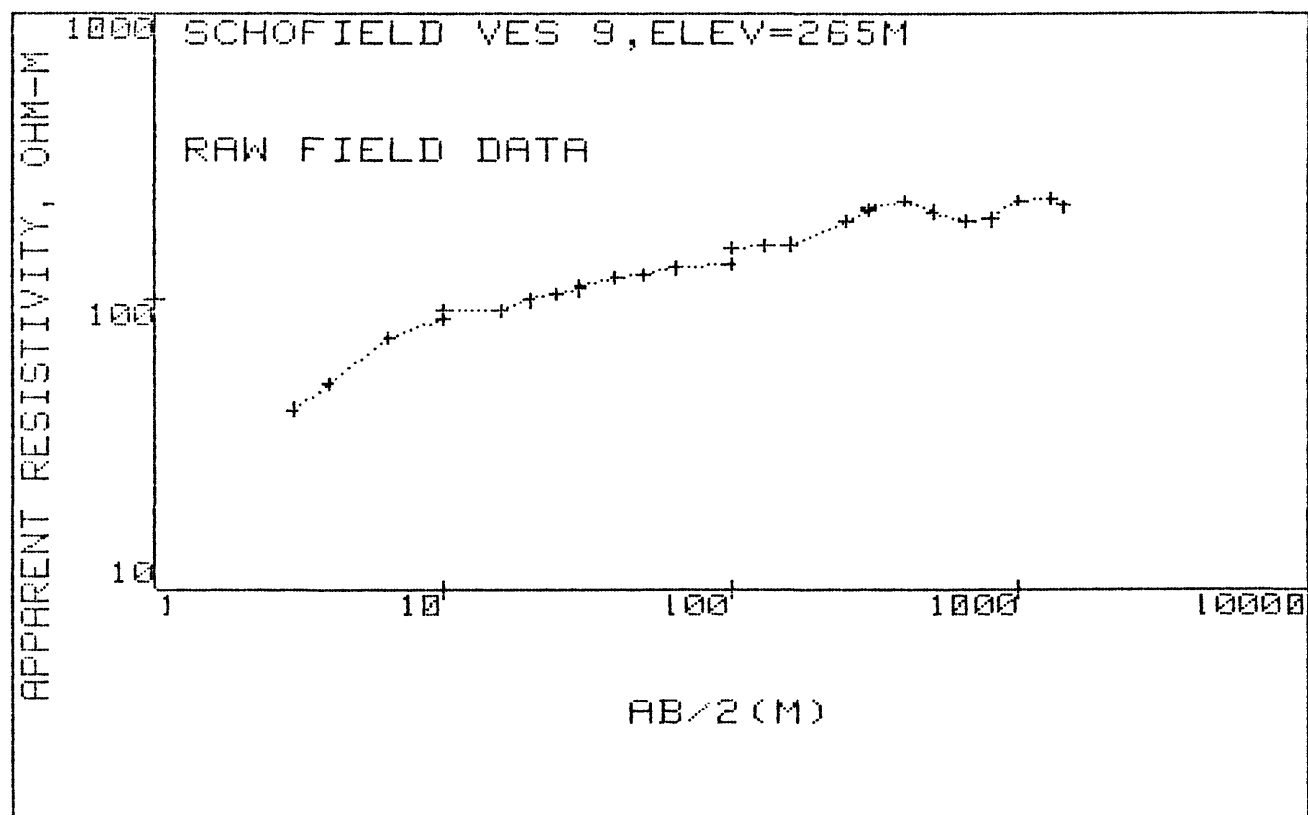
B-SD	B	B+SD
9.737E-054	2.000E+001	4.108E+055
5.569E+001	7.491E+001	1.008E+002
1.103E+001	1.745E+001	2.760E+001
6.089E-061	3.429E-001	1.931E+059
3.554E+000	1.261E+001	4.474E+001

FINAL UNSCALED PARAMETERS--
(* denotes fixed value)

RESISTIVITY		DEPTH	
1	2.00000000E+01	1	2.00000000E+01
2	7.49075051E+01	2	7.49075051E+01
3	1.74510853E+01	3	1.74510853E+01
4	3.42897315E-01	1	3.42897315E-01
5	1.26084790E+01	2	1.29513763E+01

SCHOFIELD VES 8- POSSIBLY DISTORTED





AB/2 (M) APP RHO

3.0	41.7
4.0	51.6
6.5	73.4
10.0	86.1
10.0	92.0
16.0	92.2
20.0	99.0
25.0	105.0
30.0	108.0
30.0	112.0
40.0	118.0
50.0	122.0
65.0	128.0
100.0	133.0
100.0	150.5
130.0	154.0
160.0	155.0
250.0	186.0
300.0	202.0
300.0	208.0
400.0	221.0
500.0	201.0
650.0	186.0
800.0	189.0
1000.0	220.0
1300.0	228.0
1442.0	210.0

	X	OBSERVED	PREDICTED	%RESIDUALS	WEIGHT FN
1	+3.0000E+00	+5.3840E+01	+5.6227E+01	-4.4339E+00	+5.2308E+00
2	+4.0000E+00	+6.6620E+01	+6.7275E+01	-9.8246E-01	+3.4164E+00
3	+6.5000E+00	+9.4770E+01	+8.6925E+01	+8.2775E+00	+1.6893E+00
4	+1.0000E+01	+1.1120E+02	+1.0347E+02	+6.9525E+00	+1.2262E+00
5	+1.6000E+01	+1.1140E+02	+1.1830E+02	-6.1899E+00	+1.2218E+00
6	+2.0000E+01	+1.1960E+02	+1.2380E+02	-3.5123E+00	+1.0600E+00
7	+2.5000E+01	+1.2690E+02	+1.2836E+02	-1.1507E+00	+9.4158E-01
8	+3.0000E+01	+1.3050E+02	+1.3151E+02	-7.7623E-01	+8.9035E-01
9	+4.0000E+01	+1.3750E+02	+1.3587E+02	+1.1822E+00	+8.0200E-01
10	+5.0000E+01	+1.4220E+02	+1.3925E+02	+2.0750E+00	+7.4987E-01
11	+6.5000E+01	+1.4910E+02	+1.4395E+02	+3.4519E+00	+6.8207E-01
12	+1.0000E+02	+1.5500E+02	+1.5498E+02	+1.5981E-02	+6.3113E-01
13	+1.3000E+02	+1.5860E+02	+1.6368E+02	-3.2039E+00	+6.0280E-01
14	+1.6000E+02	+1.5960E+02	+1.7101E+02	-7.1489E+00	+5.9527E-01
15	+2.5000E+02	+1.9150E+02	+1.8549E+02	+3.1390E+00	+4.1347E-01
16	+3.0000E+02	+2.0800E+02	+1.9031E+02	+8.5038E+00	+3.5047E-01
17	+4.0000E+02	+2.2100E+02	+1.9644E+02	+1.1114E+01	+3.1045E-01
18	+5.0000E+02	+2.0100E+02	+2.0008E+02	+4.5810E-01	+3.7531E-01
19	+6.5000E+02	+1.8600E+02	+2.0351E+02	-9.4149E+00	+4.3828E-01
20	+8.0000E+02	+1.8900E+02	+2.0599E+02	-8.9886E+00	+4.2448E-01
21	+1.0000E+03	+2.2000E+02	+2.0897E+02	+5.0133E+00	+3.1328E-01
22	+1.3000E+03	+2.2800E+02	+2.1400E+02	+6.1399E+00	+2.9168E-01
23	+1.4420E+03	+2.1000E+02	+2.1681E+02	-3.2425E+00	+3.4383E-01

CORRELATION MATRIX:

	1	2	3	4	5	6	7
1	+1.00	+.73	+.18	+.11	+1.00	+.38	+.12
2	+.73	+1.00	+.31	+.19	+.74	+.65	+.19
3	+.18	+.31	+1.00	+.78	+.19	+.77	+.79
4	+.11	+.19	+.78	+1.00	+.11	+.52	+1.00
5	+1.00	+.74	+.19	+.11	+1.00	+.38	+.12
6	+.38	+.65	+.77	+.52	+.38	+1.00	+.53
7	+.12	+.19	+.79	+1.00	+.12	+.53	+1.00

REDUCED CHI-SQUARED=47.85

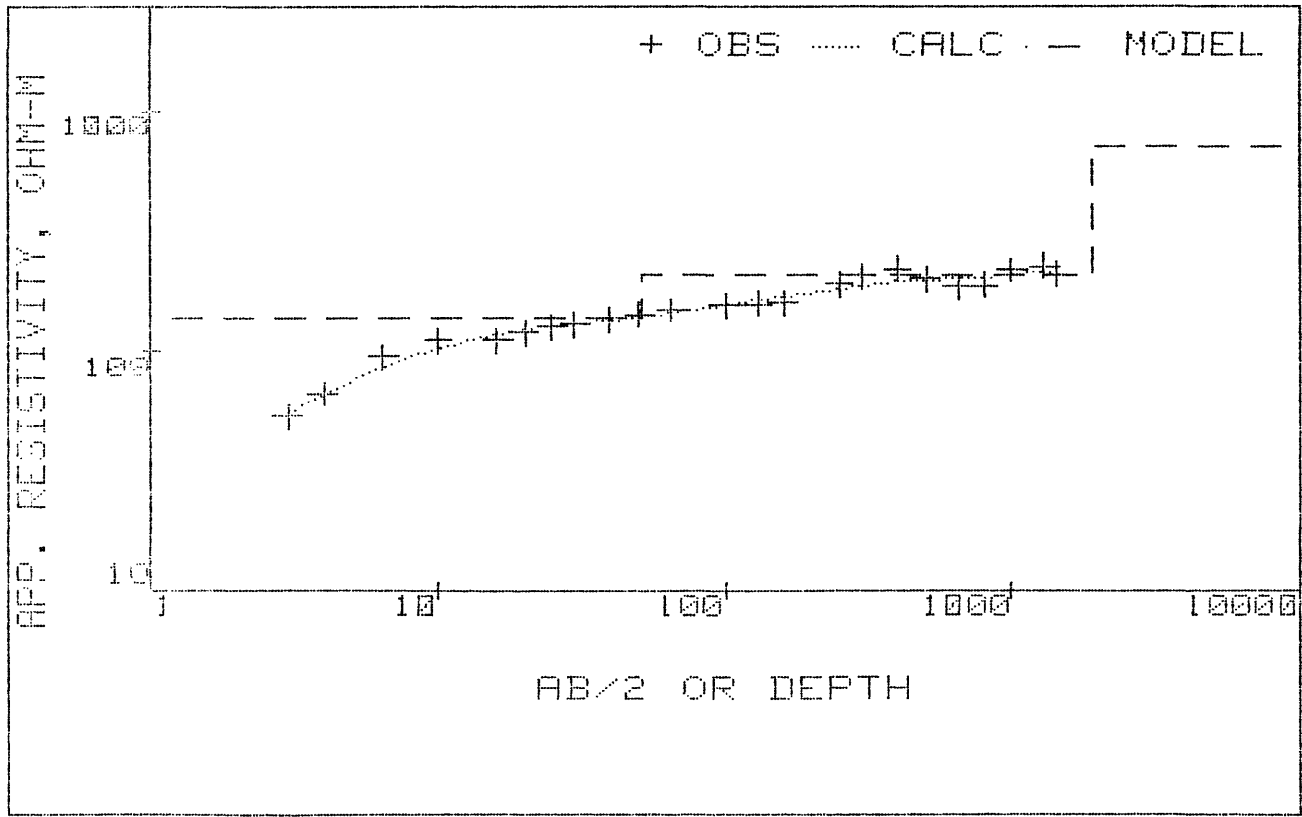
DCLAG: ***** END *****
SCHOFIELD VES 9,ELEV=265M
COORDINATES: 0 0
ELEVATION : 265 METER
AZIMUTH :

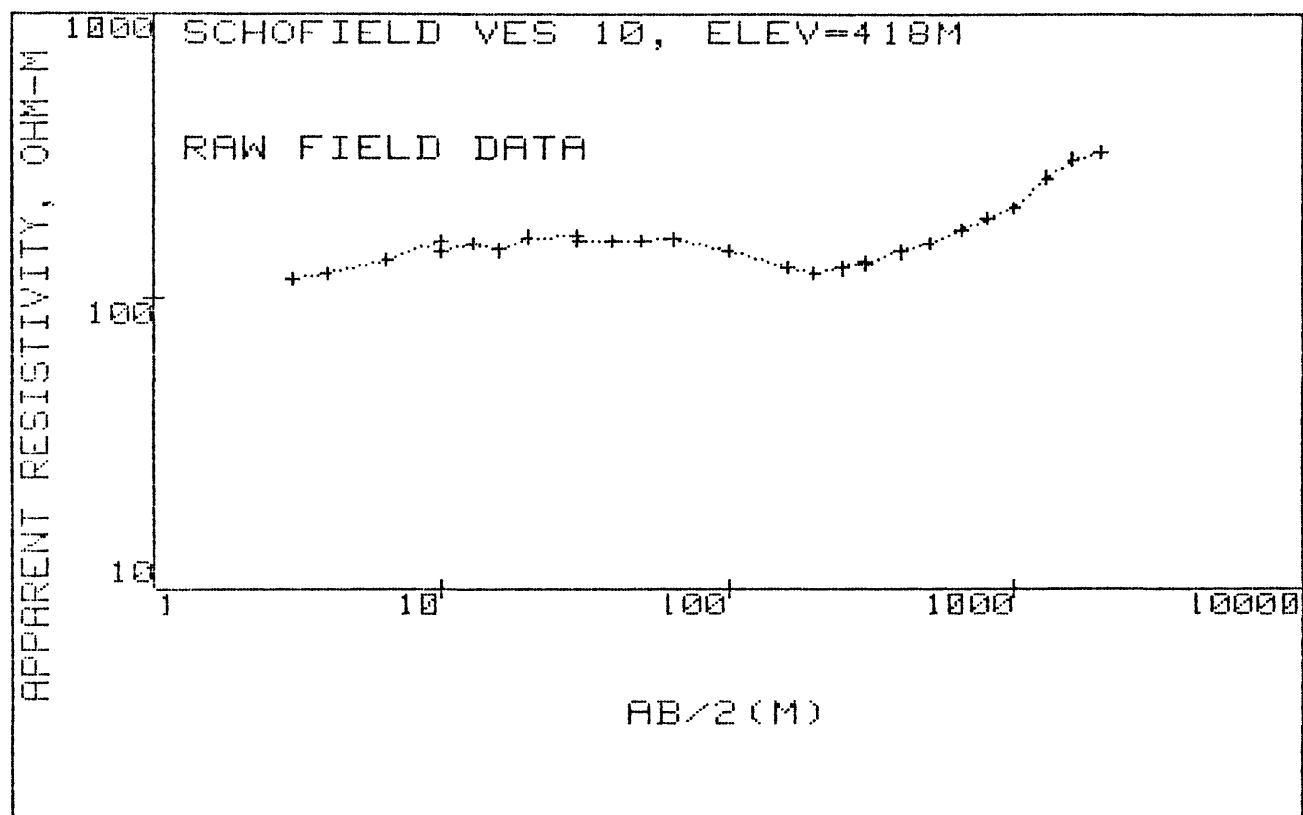
B-SD	B	B+SD
1.594E-006	1.405E+001	1.238E+008
1.322E+002	1.389E+002	1.459E+002
1.945E+002	2.074E+002	2.212E+002
3.034E-030	7.000E+002	1.615E+035
3.926E-008	4.927E-001	6.182E+006
3.757E+001	5.126E+001	6.993E+001
9.293E-007	1.849E+003	3.677E+012

FINAL UNSCALED PARAMETERS--
(* denotes fixed value)

RESISTIVITY		DEPTH	
1	1.40470869E+01	1	1.40470869E+01
2	1.38869937E+02	2	1.38869937E+02
3	2.07407133E+02	3	2.07407133E+02
4	7.00000000E+02	4	7.00000000E+02
5	4.92680484E-01	1	4.92680484E-01
6	5.12569154E+01	2	5.17495959E+01
7	1.84859034E+03	3	1.90033993E+03

SCHOFIELD VES 9,ELEV=265M





	X	OBSERVED	PREDICTED	%RESIDUALS	WEIGHT FN
1	+3.0000E+00	+1.0130E+02	+1.0133E+02	-2.9920E-02	+2.0294E+00
2	+4.0000E+00	+1.0570E+02	+1.0577E+02	-6.5530E-02	+1.8640E+00
3	+6.5000E+00	+1.1780E+02	+1.1826E+02	-3.9136E-01	+1.5007E+00
4	+1.0000E+01	+1.3510E+02	+1.3195E+02	+2.3328E+00	+1.1410E+00
5	+1.3000E+01	+1.4350E+02	+1.3958E+02	+2.7347E+00	+1.0113E+00
6	+1.6000E+01	+1.3610E+02	+1.4469E+02	-6.3115E+00	+1.1243E+00
7	+2.0000E+01	+1.5100E+02	+1.4908E+02	+1.2723E+00	+9.1335E-01
8	+3.0000E+01	+1.5280E+02	+1.5381E+02	-6.6087E-01	+8.9196E-01
9	+4.0000E+01	+1.5280E+02	+1.5435E+02	-1.0158E+00	+8.9196E-01
10	+5.0000E+01	+1.5280E+02	+1.5293E+02	-8.1893E-02	+8.9196E-01
11	+6.5000E+01	+1.5480E+02	+1.4901E+02	+3.7408E+00	+8.6906E-01
12	+1.0000E+02	+1.4120E+02	+1.3836E+02	+2.0145E+00	+1.0445E+00
13	+1.6000E+02	+1.2350E+02	+1.2691E+02	-2.7636E+00	+1.3654E+00
14	+2.0000E+02	+1.1950E+02	+1.2412E+02	-3.8660E+00	+1.4583E+00
15	+2.5000E+02	+1.2280E+02	+1.2402E+02	-9.9030E-01	+1.3810E+00
16	+3.0000E+02	+1.2900E+02	+1.2638E+02	+2.0274E+00	+1.2515E+00
17	+4.0000E+02	+1.4260E+02	+1.3578E+02	+4.7805E+00	+1.0241E+00
18	+5.0000E+02	+1.5300E+02	+1.4891E+02	+2.6714E+00	+8.8963E-01
19	+6.5000E+02	+1.7200E+02	+1.7163E+02	+2.1324E-01	+7.0394E-01
20	+8.0000E+02	+1.9200E+02	+1.9487E+02	-1.4939E+00	+5.6493E-01
21	+1.0000E+03	+2.0900E+02	+2.2397E+02	-7.1611E+00	+4.7676E-01
22	+1.3000E+03	+2.6600E+02	+2.6194E+02	+1.5258E+00	+2.9433E-01
23	+1.6000E+03	+3.0900E+02	+2.9366E+02	+4.9642E+00	+2.1811E-01
24	+2.0000E+03	+3.2400E+02	+3.2826E+02	-1.3148E+00	+1.9838E-01

CORRELATION MATRIX:

	1	2	3	4	5	6	7
1	+1.00	+.45	+.17	+.06	+.85	-.33	+.17
2	+.45	+1.00	+.47	+.15	+.74	-.77	+.46
3	+.17	+.47	+1.00	+.47	+.30	-.83	+.90
4	+.06	+.15	+.47	+1.00	+.10	-.31	+.76
5	+.85	+.74	+.30	+.10	+1.00	-.54	+.30
6	-.33	-.77	-.83	-.31	-.54	+1.00	-.76
7	+.17	+.46	+.90	+.76	+.30	-.76	+1.00

REDUCED CHI-SQUARED=13.37

DCLAG: ***** END *****
COORDINATES: 0 0
ELEVATION : 418 METER
AZIMUTH :

SCHOFIELD VES 10, ELEV=418M

B-SD	B	B+SD
9.297E+001	9.643E+001	1.000E+002
1.585E+002	1.625E+002	1.667E+002
1.073E+002	1.112E+002	1.154E+002
4.977E+002	5.369E+002	5.791E+002
2.518E+000	2.920E+000	3.388E+000
3.275E+001	3.997E+001	4.878E+001
2.775E+002	3.047E+002	3.346E+002

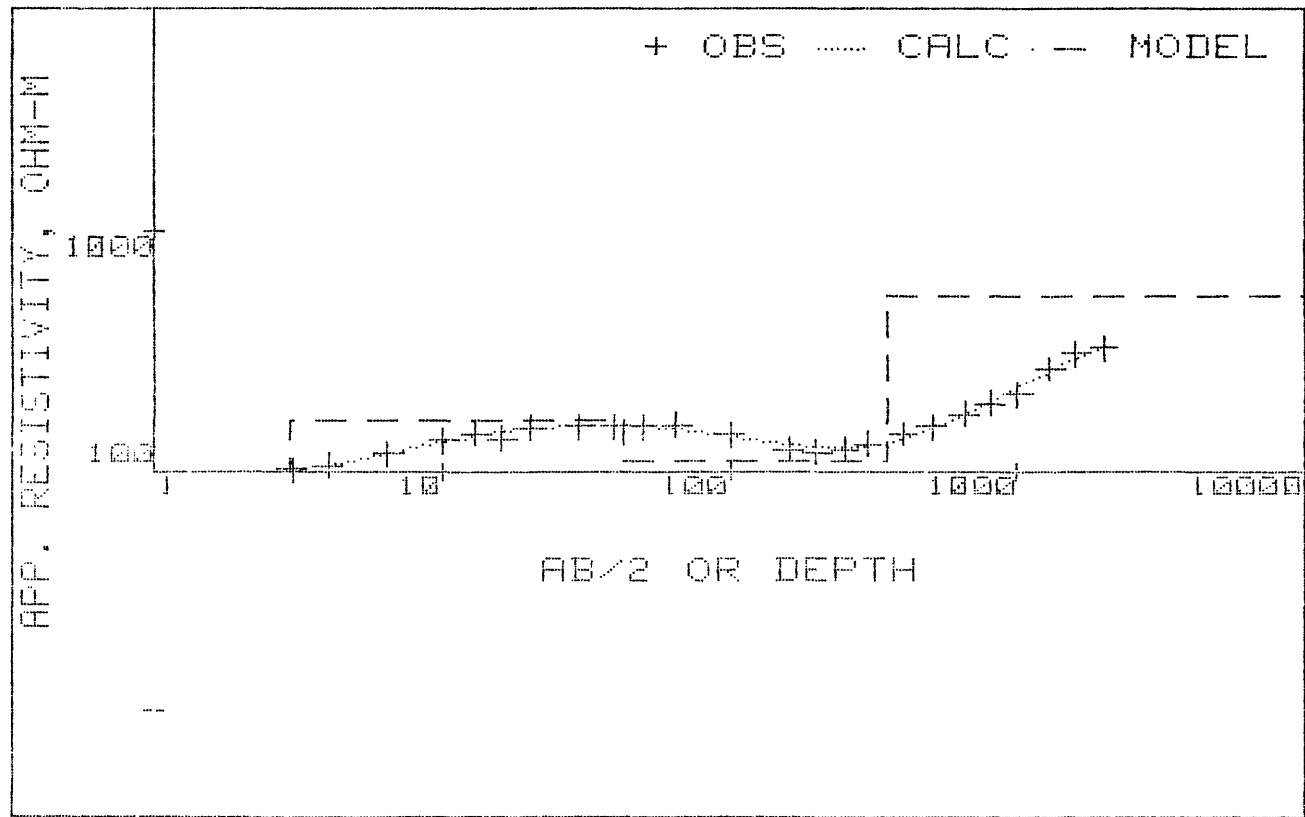
FINAL UNSCALED PARAMETERS--
(* denotes fixed value)

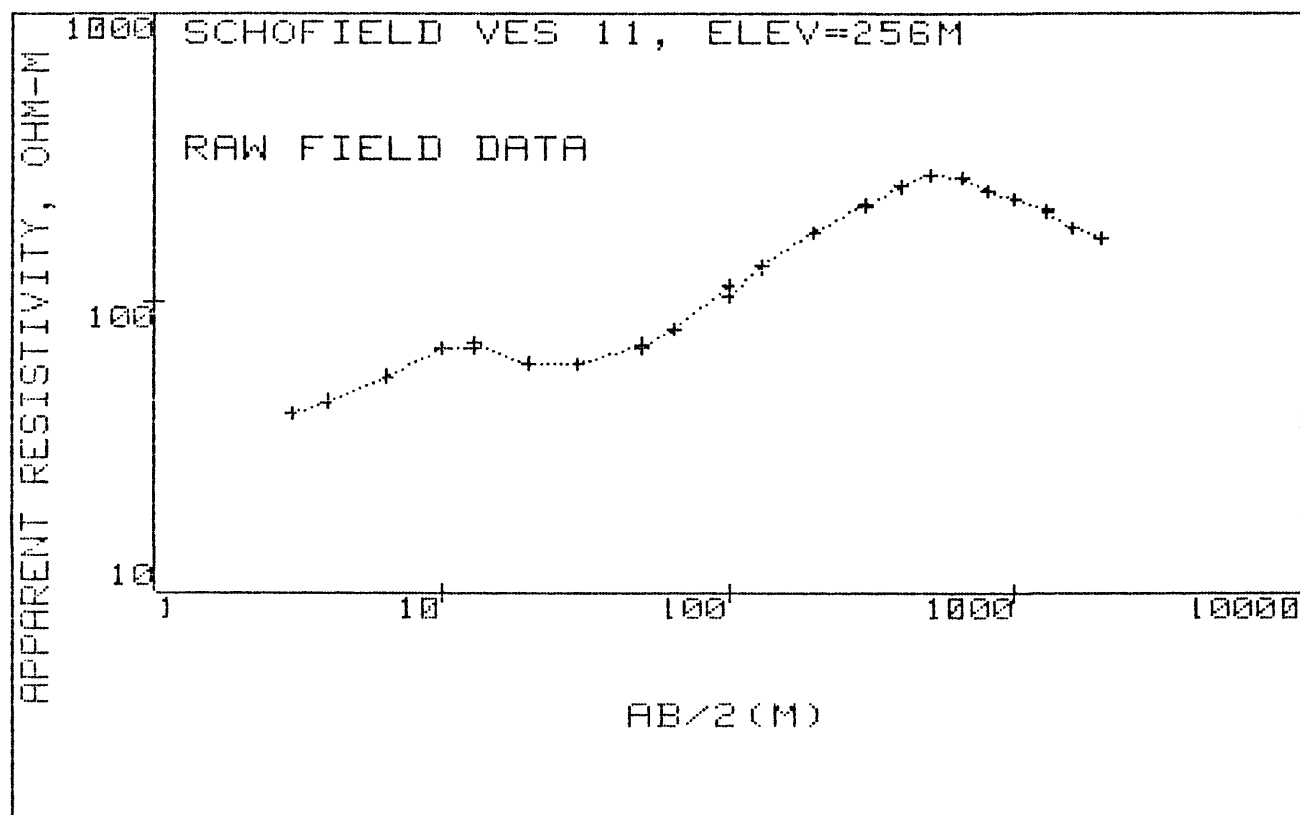
RESISTIVITY

DEPTH

1	9.64268676E+01	1	9.64268676E+01		
2	1.62534947E+02	2	1.62534947E+02		
3	1.11237818E+02	3	1.11237818E+02		
4	5.36855023E+02	4	5.36855023E+02		
5	2.92049881E+00			1	2.92049881E+00
6	3.99677437E+01			2	4.28882425E+01
7	3.04702068E+02			3	3.47590310E+02

SCHOFIELD VES 10, ELEV=418M





AB/2 (M) APP RHO

3.0	41.6
4.0	45.5
6.5	55.1
10.0	69.0
13.0	69.6
13.0	72.7
20.0	61.4
30.0	61.2
50.0	71.5
50.0	69.0
65.0	81.0
100.0	113.0
100.0	105.0
130.0	131.0
200.0	171.6
300.0	216.0
300.0	211.0
400.0	250.0
500.0	273.0
650.0	270.0
800.0	240.0
1000.0	226.0
1300.0	208.0
1300.0	205.0
1600.0	180.0
2000.0	164.5

	X	OBSERVED	PREDICTED	%RESIDUALS	WEIGHT FN
1	+3.0000E+00	+3.7510E+01	+3.7139E+01	+9.9025E-01	+3.9450E+00
2	+4.0000E+00	+4.1030E+01	+4.1474E+01	-1.0833E+00	+3.2971E+00
3	+6.5000E+00	+4.9690E+01	+5.1732E+01	-4.1103E+00	+2.2480E+00
4	+1.0000E+01	+6.2220E+01	+5.9029E+01	+5.1292E+00	+1.4338E+00
5	+1.3000E+01	+6.2760E+01	+6.0171E+01	+4.1255E+00	+1.4092E+00
6	+2.0000E+01	+5.3010E+01	+5.6296E+01	-6.1994E+00	+1.9753E+00
7	+3.0000E+01	+5.2840E+01	+5.1970E+01	+1.6461E+00	+1.9880E+00
8	+5.0000E+01	+6.1730E+01	+5.9956E+01	+2.8731E+00	+1.4566E+00
9	+6.5000E+01	+7.2460E+01	+7.2285E+01	+2.4085E-01	+1.0572E+00
10	+1.0000E+02	+1.0110E+02	+1.0256E+02	-1.4392E+00	+5.4304E-01
11	+1.3000E+02	+1.2610E+02	+1.2600E+02	+7.6083E-02	+3.4907E-01
12	+2.0000E+02	+1.6520E+02	+1.7089E+02	-3.4455E+00	+2.0338E-01
13	+3.0000E+02	+2.0800E+02	+2.1491E+02	-3.3227E+00	+1.2830E-01
14	+4.0000E+02	+2.4640E+02	+2.4054E+02	+2.3771E+00	+9.1423E-02
15	+5.0000E+02	+2.6910E+02	+2.5285E+02	+6.0376E+00	+7.6650E-02
16	+6.5000E+02	+2.6610E+02	+2.5520E+02	+4.0974E+00	+7.8388E-02
17	+8.0000E+02	+2.3650E+02	+2.4683E+02	-4.3659E+00	+9.9237E-02
18	+1.0000E+03	+2.2270E+02	+2.2924E+02	-2.9350E+00	+1.1192E-01
19	+1.3000E+03	+2.0500E+02	+2.0236E+02	+1.2866E+00	+1.3208E-01
20	+1.6000E+03	+1.8000E+02	+1.8131E+02	-7.3006E-01	+1.7131E-01
21	+2.0000E+03	+1.6450E+02	+1.6280E+02	+1.0332E+00	+2.0512E-01

CORRELATION MATRIX:

	1	3	4	5	6	7	8	9
1	+1.00	-.50	-.17	-.08	+.95	+.48	-.49	+.16
3	-.50	+1.00	+.50	+.23	-.67	-.98	+.99	-.46
4	-.17	+.50	+1.00	+.63	-.24	-.44	+.59	-.98
5	-.08	+.23	+.63	+1.00	-.11	-.20	+.27	-.76
6	+.95	-.67	-.24	-.11	+1.00	+.67	-.66	+.22
7	+.48	-.98	-.44	-.20	+.67	+1.00	-.96	+.40
8	-.49	+.99	+.59	+.27	-.66	-.96	+1.00	-.55
9	+.16	-.46	-.98	-.76	+.22	+.40	-.55	+1.00

REDUCED CHI-SQUARED=18.89

DCLAG: ***** END *****
 COORDINATES: 0 0
 ELEVATION : 256 METER
 AZIMUTH :

SCHOFIELD VES 11, ELEV=256M

B-SD	B	B+SD
2.739E+001	3.182E+001	3.698E+001
	2.000E+002	
1.673E+001	3.051E+001	5.564E+001
3.548E+002	5.287E+002	7.878E+002
1.165E+002	1.316E+002	1.486E+002
1.989E+000	2.657E+000	3.549E+000
1.457E+000	2.320E+000	3.676E+000
1.079E+001	2.167E+001	4.353E+001
1.214E+002	2.149E+002	3.804E+002

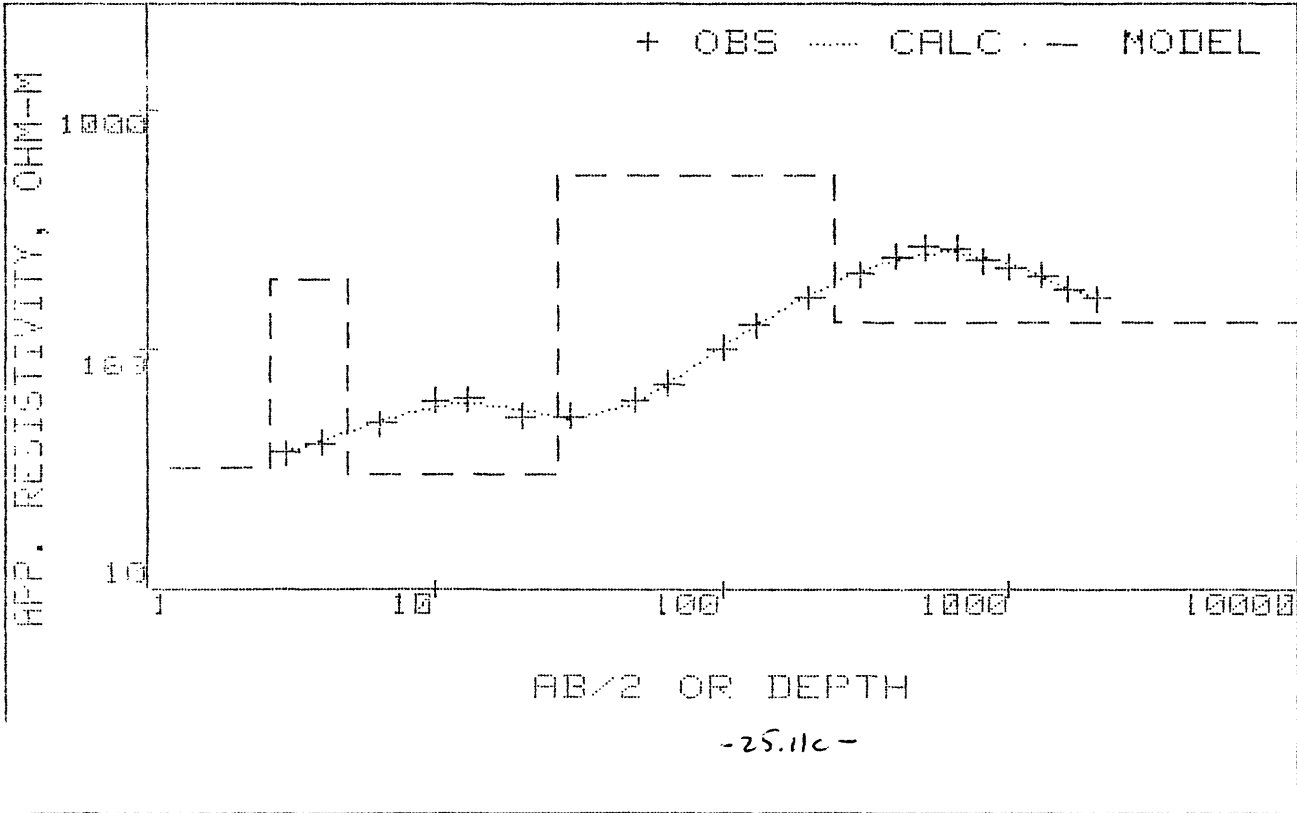
FINAL UNSCALED PARAMETERS--
 (* denotes fixed value)

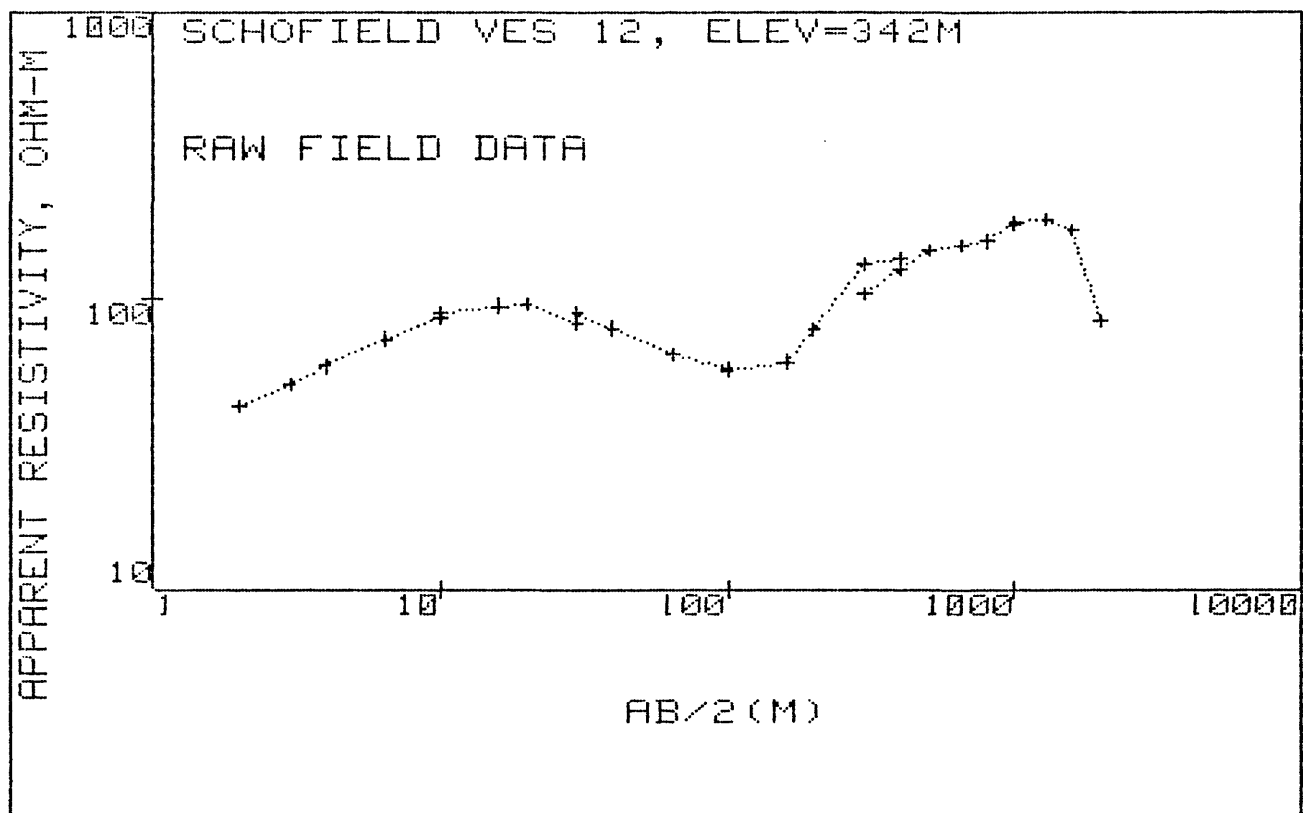
RESISTIVITY

DEPTH

1	3.18235102E+01	1	3.18235102E+01		
2	* 2.00000000E+02	2	2.00000000E+02		
3	3.05095278E+01	3	3.05095278E+01		
4	5.28713178E+02	4	5.28713178E+02		
5	1.31586517E+02	5	1.31586517E+02		
6	2.65701760E+00			1	2.65701760E+00
7	2.32018281E+00			2	4.97720041E+00
8	2.16682616E+01			3	2.66454620E+01
9	2.14923072E+02			4	2.41568534E+02

SCHOFIELD VES 11, ELEV=256M





AB/2 (M) APP RHO

2.0	43.2
3.0	51.5
4.0	59.0
6.5	73.0
10.0	85.7
10.0	88.9
16.0	94.6
20.0	96.4
30.0	82.0
30.0	89.0
40.0	79.6
65.0	65.0
100.0	58.0
100.0	57.2
160.0	61.5
200.0	79.2
300.0	132.0
400.0	137.0
300.0	104.0
400.0	127.0
500.0	148.0
650.0	154.0
800.0	159.0
1000.0	183.5
1000.0	187.0
1300.0	191.0
1600.0	176.0
2000.0	84.0

	X	OBSERVED	PREDICTED	%RESIDUALS	WEIGHT FN
1	+2.0000E+00	+4.1780E+01	+4.1693E+01	+2.0874E-01	+3.2252E+00
2	+3.0000E+00	+4.9800E+01	+4.9899E+01	-1.9836E-01	+2.2701E+00
3	+4.0000E+00	+5.7060E+01	+5.7465E+01	-7.1018E-01	+1.7291E+00
4	+6.5000E+00	+7.0590E+01	+7.1065E+01	-6.7246E-01	+1.1298E+00
5	+1.0000E+01	+8.2870E+01	+8.1373E+01	+1.8067E+00	+8.1979E-01
6	+1.6000E+01	+8.8190E+01	+8.7366E+01	+9.3393E-01	+7.2386E-01
7	+2.0000E+01	+8.9870E+01	+8.7097E+01	+3.0853E+00	+6.9705E-01
8	+3.0000E+01	+7.6440E+01	+7.9864E+01	-4.4798E+00	+9.6350E-01
9	+4.0000E+01	+6.8370E+01	+7.0070E+01	-2.4865E+00	+1.2044E+00
10	+6.5000E+01	+5.5830E+01	+5.3220E+01	+4.6749E+00	+1.8062E+00
11	+1.0000E+02	+4.9820E+01	+4.8666E+01	+2.3172E+00	+2.2682E+00
12	+1.6000E+02	+5.3560E+01	+5.9555E+01	-1.1193E+01	+1.9625E+00
13	+2.0000E+02	+6.8980E+01	+7.0224E+01	-1.8029E+00	+1.1832E+00
14	+3.0000E+02	+1.1500E+02	+9.7080E+01	+1.5583E+01	+4.2570E-01
15	+4.0000E+02	+1.1930E+02	+1.2047E+02	-9.8235E-01	+3.9556E-01
16	+5.0000E+02	+1.5080E+02	+1.3984E+02	+7.2703E+00	+2.4757E-01
17	+6.5000E+02	+1.5690E+02	+1.6177E+02	-3.1034E+00	+2.2869E-01
18	+8.0000E+02	+1.6200E+02	+1.7613E+02	-8.7239E+00	+2.1452E-01
19	+1.0000E+03	+1.8700E+02	+1.8564E+02	+7.2674E-01	+1.6099E-01
20	+1.3000E+03	+1.9100E+02	+1.8495E+02	+3.1690E+00	+1.5432E-01
21	+1.6000E+03	+1.7600E+02	+1.7328E+02	+1.5458E+00	+1.8175E-01
22	+2.0000E+03	+8.4000E+01	+1.5016E+02	-7.8759E+01	+7.9788E-03

CORRELATION MATRIX:

	1	2	3	5	6	7	8	9
1	+1.00	+.53	+.21	-.04	+.96	-.44	+.22	+.04
2	+.53	+1.00	+.54	-.11	+.70	-.86	+.55	+.12
3	+.21	+.54	+1.00	-.31	+.30	-.84	+.98	+.33
5	-.04	-.11	-.31	+1.00	-.06	+.21	-.40	-.99
6	+.96	+.70	+.30	-.06	+1.00	-.58	+.31	+.06
7	-.44	-.86	-.84	+.21	-.58	+1.00	-.83	-.22
8	+.22	+.55	+.98	-.40	+.31	-.83	+1.00	+.43
9	+.04	+.12	+.33	-.99	+.06	-.22	+.43	+1.00

REDUCED CH1-SQUARED=50.31

DCLAG: ***** END *****
COORDINATES: 0 0
ELEVATION : 342 METER
AZIMUTH ;

SCHOFIELD VES 12, ELEV=342M

B-SD	B	B+SD
2.467E+001	3.406E+001	4.702E+001
8.922E+001	1.044E+002	1.223E+002
2.562E+001	3.490E+001	4.755E+001
	6.000E+002	
1.476E-001	2.537E+001	4.361E+003
7.856E-001	1.397E+000	2.484E+000
1.057E+001	1.632E+001	2.518E+001
5.619E+001	8.298E+001	1.225E+002
1.791E+002	3.738E+002	7.799E+002

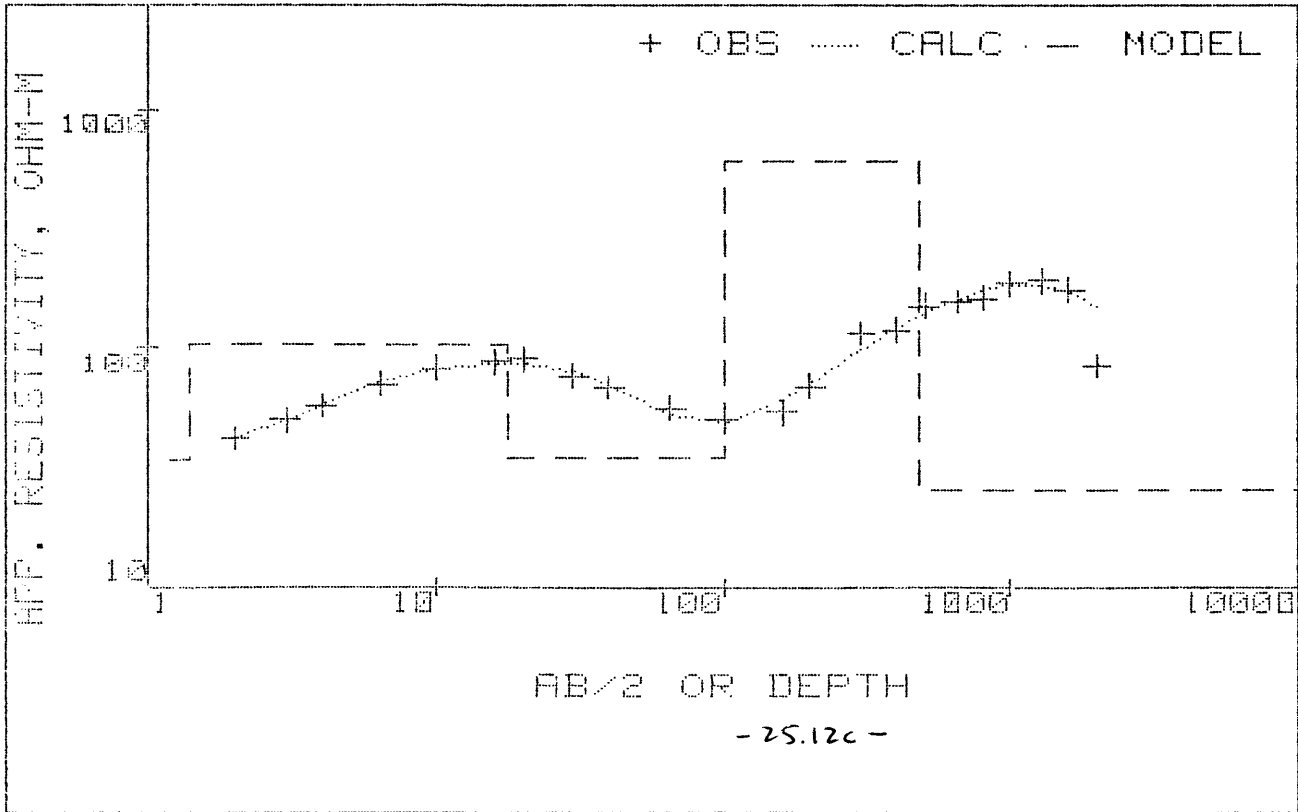
FINAL UNSCALED PARAMETERS--
(* denotes fixed value)

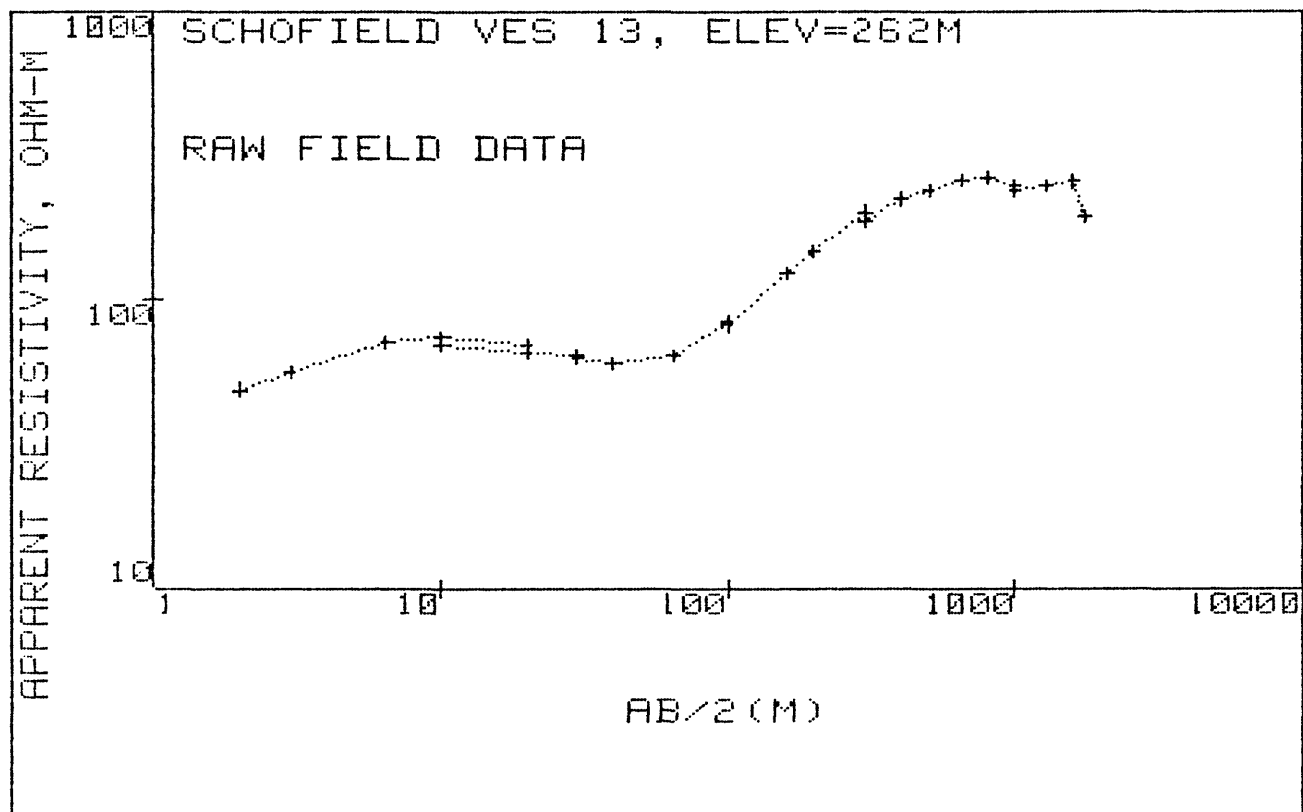
RESISTIVITY

DEPTH

1	3.40573310E+01	1	3.40573310E+01		
2	1.04448748E+02	2	1.04448748E+02		
3	3.48988719E+01	3	3.48988719E+01		
4 *	6.00000000E+02	4	6.00000000E+02		
5	2.53696041E+01	5	2.53696041E+01		
6	1.39681331E+00			1	1.39681331E+00
7	1.63171815E+01			2	1.77139948E+01
8	8.29847824E+01			3	1.00698777E+02
9	3.73794625E+02			4	4.74493402E+02

SCHOFIELD VES 12, ELEV=342M





AB/2 (M) APP RHO

2.0	48.5
3.0	56.0
6.5	71.0
10.0	73.2
20.0	69.0
10.0	69.2
20.0	65.2
30.0	63.0
30.0	62.0
40.0	60.0
65.0	63.5
100.0	83.2
100.0	81.6
160.0	124.0
200.0	148.0
300.0	201.0
300.0	187.0
400.0	224.0
500.0	241.0
650.0	264.0
800.0	267.0
1000.0	254.0
1000.0	242.0
1300.0	251.0
1600.0	261.0
1750.0	194.0

	X	OBSERVED	PREDICTED	%RESIDUALS	WEIGHT FN
1	+2.0000E+00	+3.9220E+01	+3.9142E+01	+1.9967E-01	+3.6285E+00
2	+3.0000E+00	+4.5280E+01	+4.5790E+01	-1.1267E+00	+2.7223E+00
3	+6.5000E+00	+5.7410E+01	+5.6170E+01	+2.1590E+00	+1.6934E+00
4	+1.0000E+01	+5.9190E+01	+5.9064E+01	+2.1293E-01	+1.5931E+00
5	+2.0000E+01	+5.5790E+01	+5.7458E+01	-2.9890E+00	+1.7932E+00
6	+3.0000E+01	+5.3900E+01	+5.3328E+01	+1.0613E+00	+1.9212E+00
7	+4.0000E+01	+5.2160E+01	+5.1168E+01	+1.9022E+00	+2.0515E+00
8	+6.5000E+01	+5.5200E+01	+5.5988E+01	-1.4273E+00	+1.8318E+00
9	+1.0000E+02	+7.2330E+01	+7.4303E+01	-2.7282E+00	+1.0669E+00
10	+1.6000E+02	+1.0990E+02	+1.0902E+02	+7.9740E-01	+4.6212E-01
11	+2.0000E+02	+1.3120E+02	+1.3000E+02	+9.1101E-01	+3.2425E-01
12	+3.0000E+02	+1.7820E+02	+1.7372E+02	+2.5125E+00	+1.7576E-01
13	+4.0000E+02	+2.1340E+02	+2.0618E+02	+3.3821E+00	+1.2256E-01
14	+5.0000E+02	+2.2960E+02	+2.2902E+02	+2.5266E-01	+1.0588E-01
15	+6.5000E+02	+2.5150E+02	+2.4877E+02	+1.0868E+00	+8.8241E-02
16	+8.0000E+02	+2.5440E+02	+2.5557E+02	-4.6085E-01	+8.6241E-02
17	+1.0000E+03	+2.4200E+02	+2.5167E+02	-3.9950E+00	+9.5305E-02
18	+1.3000E+03	+2.5100E+02	+2.3183E+02	+7.6378E+00	+8.8593E-02
19	+1.6000E+03	+2.6100E+02	+2.0720E+02	+2.0612E+01	+8.1934E-04
20	+1.7500E+03	+1.9400E+02	+1.9528E+02	-6.5841E-01	+1.4830E-01

CORRELATION MATRIX:

	1	2	3	4	5	6	7	8	9
1	+1.00	+.72	+.31	+.11	+.05	+1.00	-.52	+.33	-.10
2	+.72	+1.00	+.56	+.21	+.10	+.76	-.79	+.59	-.18
3	+.31	+.56	+1.00	+.58	+.30	+.34	-.93	+.99	-.53
4	+.11	+.21	+.58	+1.00	+.73	+.12	-.46	+.66	-.98
5	+.05	+.10	+.30	+.73	+1.00	+.06	-.23	+.35	-.85
6	+1.00	+.76	+.34	+.12	+.06	+1.00	-.56	+.36	-.10
7	-.52	-.79	-.93	-.46	-.23	-.56	+1.00	-.93	+.41
8	+.33	+.59	+.99	+.66	+.35	+.36	-.93	+1.00	-.60
9	-.10	-.18	-.53	-.98	-.85	-.10	+.41	-.60	+1.00

REDUCED CHI-SQUARED=12.88

DCLAG: ***** END *****
COORDINATES: 0 0
ELEVATION : 262 METER
AZIMUTH :

SCHOFIELD VES 13, ELEV=262M

B-SD	B	B+SD
9.581E+000	2.683E+001	7.515E+001
5.852E+001	6.446E+001	7.101E+001
2.088E+001	3.505E+001	5.885E+001
3.416E+002	6.000E+002	1.054E+003
6.218E+001	9.974E+001	1.600E+002
1.614E+001	7.919E+001	3.885E+000
6.355E+000	1.290E+001	2.619E+001
1.637E+001	3.478E+001	7.391E+001
1.297E+002	3.012E+002	6.994E+002

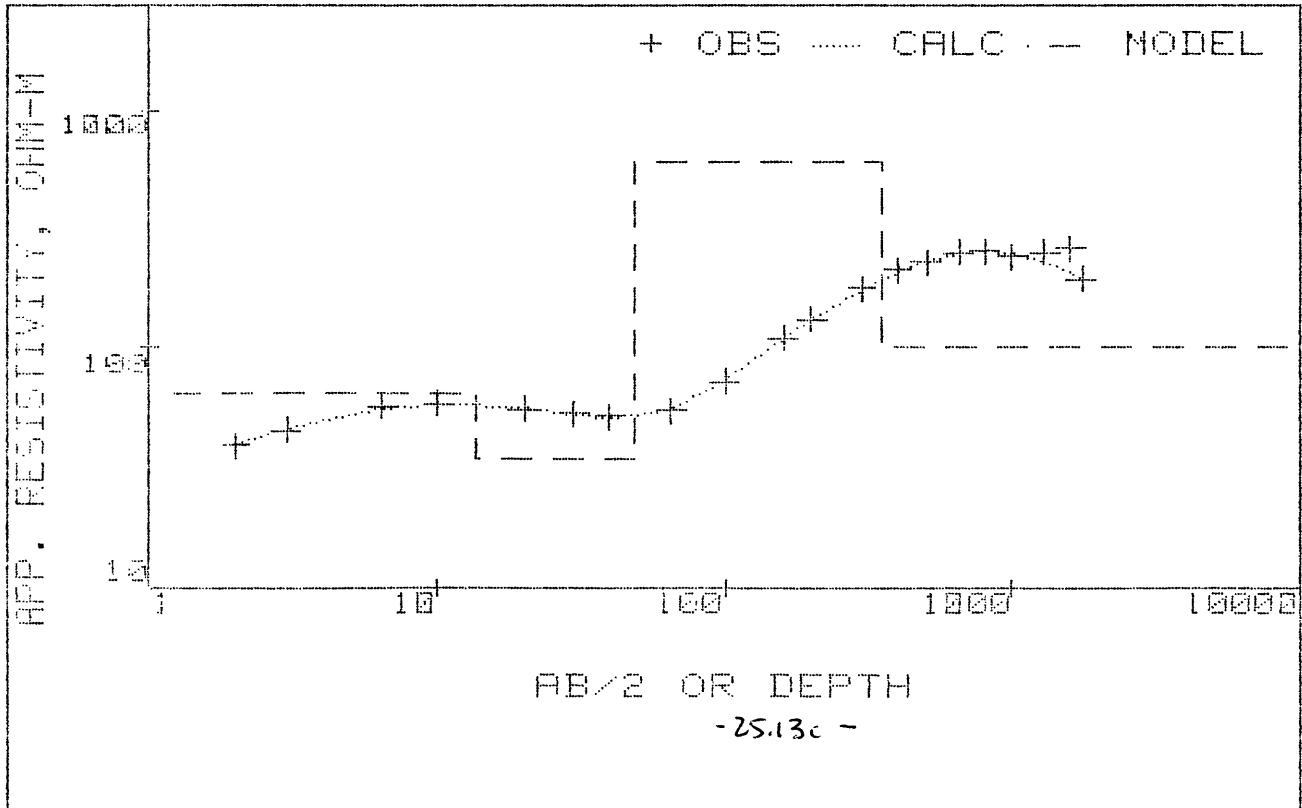
FINAL UNSCALED PARAMETERS--
(* denotes fixed value)

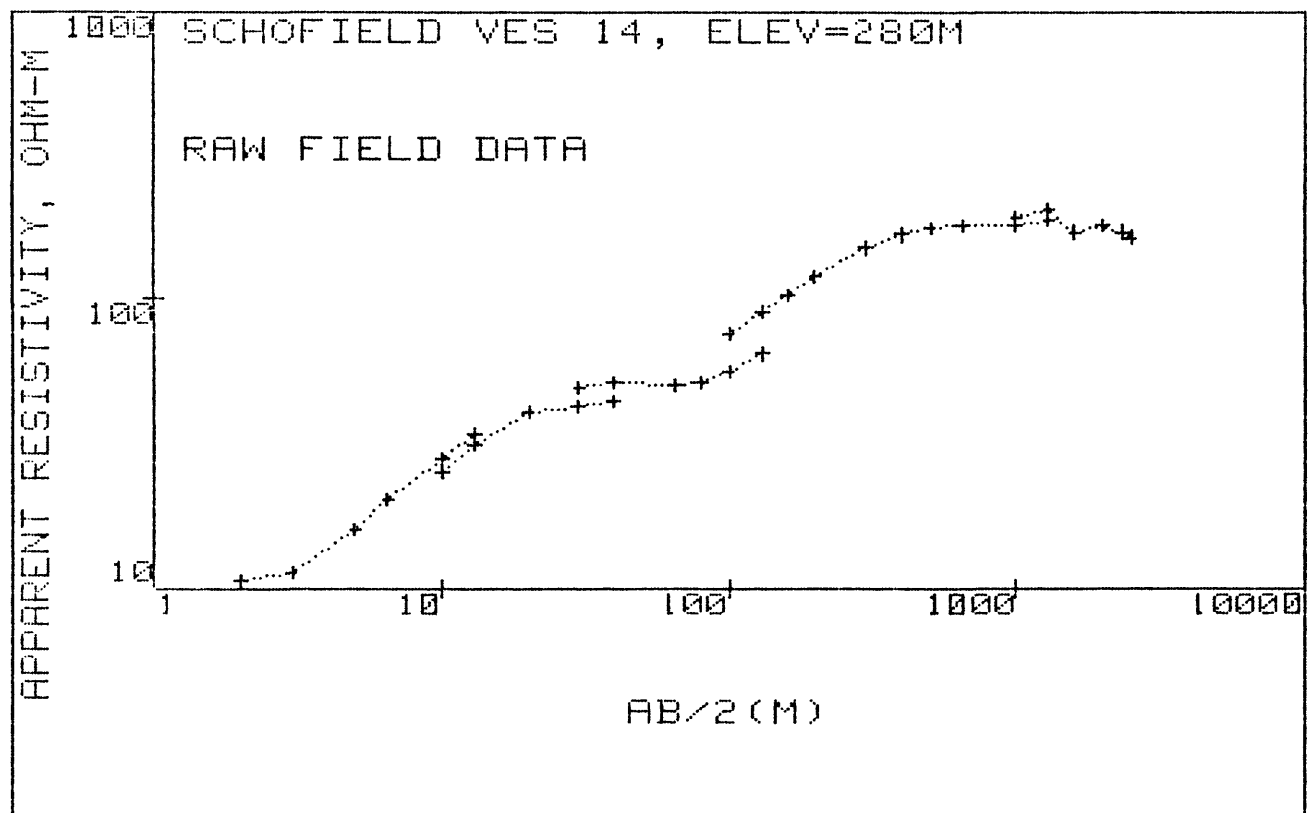
RESISTIVITY

DEPTH

1	2.68336946E+01	1	2.68336946E+01	
2	6.44599852E+01	2	6.44599852E+01	
3	3.50546548E+01	3	3.50546548E+01	
4	6.00000000E+02	4	6.00000000E+02	
5	9.97436793E+01	5	9.97436793E+01	
6	7.91898269E-01			1 7.91898269E-01
7	1.29013534E+01			2 1.36932516E+01
8	3.47842291E+01			3 4.84774807E+01
9	3.01223002E+02			4 3.49700483E+02

SCHOFIELD VES 13, ELEV=262M





AB/2 (M) APP RHO

2.0	10.7
3.0	11.4
5.0	16.1
6.5	20.2
10.0	28.2
13.0	34.3
10.0	25.4
13.0	31.2
20.0	40.4
30.0	42.0
40.0	44.4
30.0	49.0
40.0	51.0
65.0	50.1
80.0	51.0
100.0	56.0
130.0	64.4
100.0	76.0
130.0	89.2
160.0	102.5
200.0	119.0
300.0	151.0
300.0	149.0
400.0	166.0
500.0	175.0
650.0	178.0
1000.0	178.0
1300.0	188.0
1000.0	192.0
1300.0	205.0
1600.0	169.2
2000.0	179.0
2350.0	169.0
2500.0	162.0

	X	OBSERVED	PREDICTED	%RESIDUALS	WEIGHT FN
1	+2.0000E+00	+1.6450E+01	+1.5953E+01	+3.0218E+00	+7.5866E+00
2	+3.0000E+00	+1.7530E+01	+1.8229E+01	-3.9880E+00	+6.6806E+00
3	+5.0000E+00	+2.4750E+01	+2.5166E+01	-1.6820E+00	+3.3514E+00
4	+6.5000E+00	+3.1060E+01	+3.0991E+01	+2.2375E-01	+2.1280E+00
5	+1.0000E+01	+4.3350E+01	+4.3409E+01	-1.3692E-01	+1.0924E+00
6	+1.3000E+01	+5.2730E+01	+5.2024E+01	+1.3390E+00	+7.3835E-01
7	+2.0000E+01	+6.8620E+01	+6.5518E+01	+4.5207E+00	+4.3599E-01
8	+3.0000E+01	+7.1340E+01	+7.3632E+01	-3.2126E+00	+4.0338E-01
9	+4.0000E+01	+7.5410E+01	+7.5073E+01	+4.4631E-01	+3.6101E-01
10	+6.5000E+01	+7.3510E+01	+7.3788E+01	-3.7812E-01	+3.7991E-01
11	+8.0000E+01	+7.4830E+01	+7.5730E+01	-1.2032E+00	+3.6663E-01
12	+1.0000E+02	+8.2170E+01	+8.1885E+01	+3.4738E-01	+3.0405E-01
13	+1.3000E+02	+9.4490E+01	+9.5028E+01	-5.6942E-01	+2.2994E-01
14	+1.6000E+02	+1.0970E+02	+1.0911E+02	+5.3894E-01	+1.7059E-01
15	+2.0000E+02	+1.2730E+02	+1.2645E+02	+6.6703E-01	+1.2668E-01
16	+3.0000E+02	+1.6160E+02	+1.5935E+02	+1.3915E+00	+7.8613E-02
17	+4.0000E+02	+1.8000E+02	+1.7975E+02	+1.3865E-01	+6.3363E-02
18	+5.0000E+02	+1.8980E+02	+1.9140E+02	-8.4348E-01	+5.6988E-02
19	+6.5000E+02	+1.9300E+02	+1.9860E+02	-2.9023E+00	+5.5114E-02
20	+1.0000E+03	+1.9300E+02	+1.9486E+02	-9.6202E-01	+5.5114E-02
21	+1.3000E+03	+2.0390E+02	+1.8641E+02	+8.5761E+00	+4.9379E-02
22	+1.6000E+03	+1.6920E+02	+1.7904E+02	-5.8154E+00	+7.1710E-02
23	+2.0000E+03	+1.7900E+02	+1.7205E+02	+3.8822E+00	+6.4072E-02
24	+2.3500E+03	+1.6900E+02	+1.6803E+02	+5.7315E-01	+7.1879E-02
25	+2.5000E+03	+1.6200E+02	+1.6674E+02	-2.9288E+00	+7.8225E-02

CORRELATION MATRIX:

	1	3	4	5	6	7	8	9
1	+1.00	-.25	-.10	-.04	+.89	+.27	-.24	+.10
3	-.25	+1.00	+.68	+.29	-.49	-.98	+1.00	-.66
4	-.10	+.68	+1.00	+.63	-.21	-.60	+.74	-.99
5	-.04	+.29	+.63	+1.00	-.08	-.24	+.33	-.70
6	+.89	-.49	-.21	-.08	+1.00	+.54	-.47	+.20
7	+.27	-.98	-.60	-.24	+.54	+1.00	-.97	+.57
8	-.24	+1.00	+.74	+.33	-.47	-.97	+1.00	-.71
9	+.10	-.66	-.99	-.70	+.20	+.57	-.71	+1.00

REDUCED CHI-SQUARED=12.93

DCLAB: ***** END *****
COORDINATES: 0 0
ELEVATION : 280 METER
AZIMUTH :

SCHOFIELD VES 14, ELEV=280M

B-SD	B	B+SD
1.337E+001	1.470E+001	1.616E+001
	3.000E+002	
1.372E+000	2.771E+001	5.594E+002
8.263E+001	4.021E+002	1.956E+003
1.432E+002	1.569E+002	1.718E+002
2.380E+000	2.740E+000	3.156E+000
2.460E+000	6.129E+000	1.527E+001
8.289E-001	2.501E+001	7.546E+002
1.717E+001	1.666E+002	1.617E+003

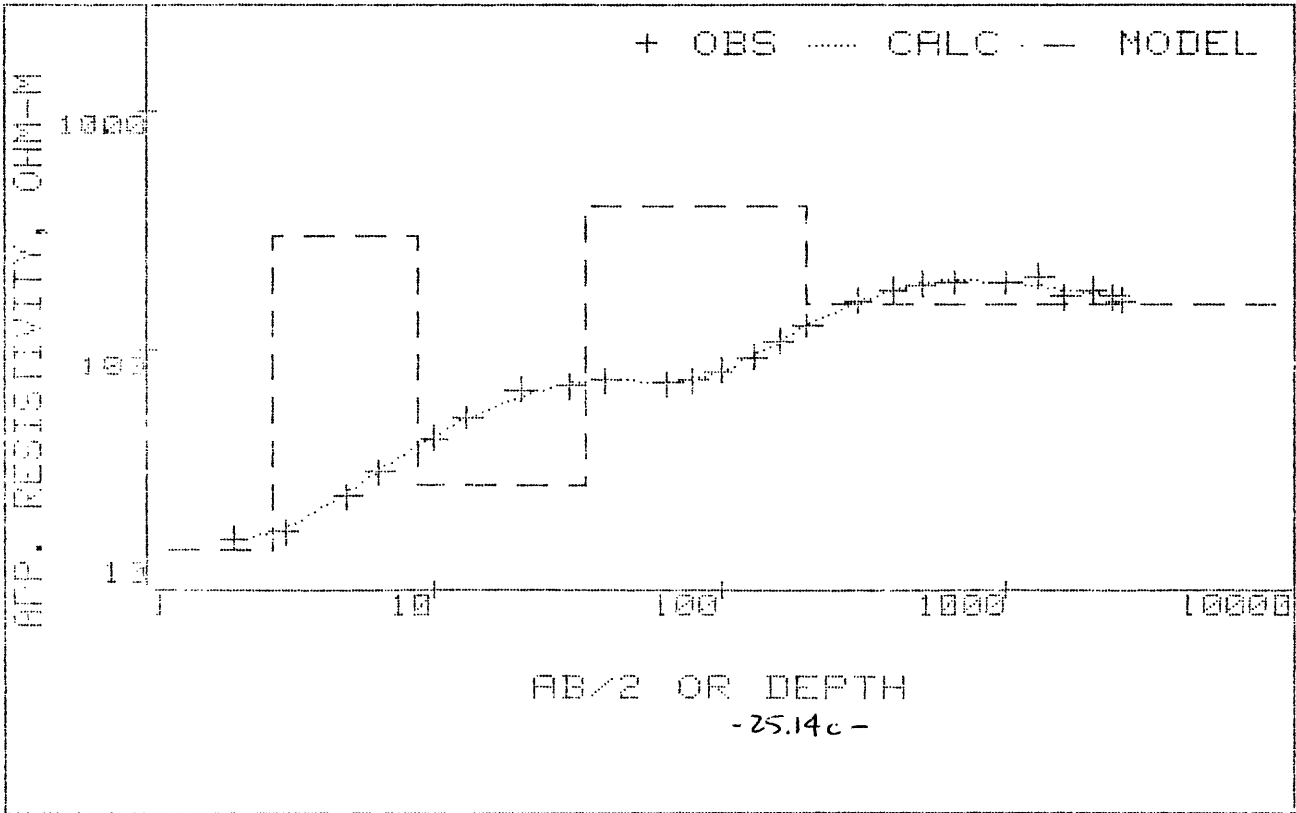
FINAL UNSCALED PARAMETERS--
(* denotes fixed value)

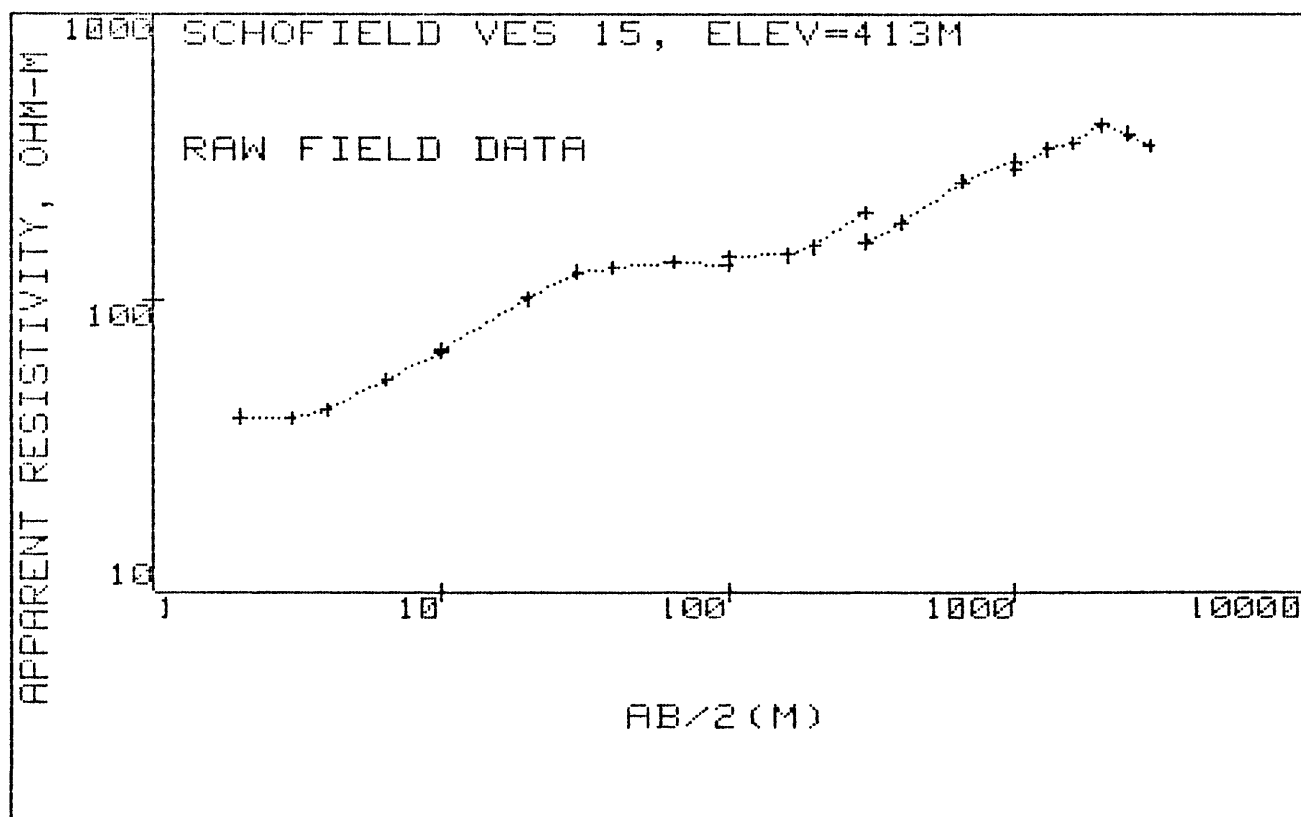
RESISTIVITY

DEPTH

1	1.46980532E+01	1	1.46980532E+01		
2	* 3.00000000E+02	2	3.00000000E+02		
3	2.77071483E+01	3	2.77071483E+01		
4	4.02062456E+02	4	4.02062456E+02		
5	1.56870150E+02	5	1.56870150E+02		
6	2.74031210E+00			1	2.74031210E+00
7	6.12888525E+00			2	8.86919734E+00
8	2.50103187E+01			3	3.38795160E+01
9	1.66640767E+02			4	2.00520283E+02

SCHOFIELD VES 14, ELEV=280M





AB/2 (M) APP RHO

2.0	40.0
3.0	39.8
4.0	42.5
6.5	53.2
10.0	66.7
10.0	67.5
20.0	101.0
30.0	125.0
30.0	124.0
40.0	129.0
65.0	136.0
100.0	132.5
100.0	141.0
160.0	142.5
200.0	152.0
300.0	198.0
300.0	158.5
400.0	184.0
650.0	260.0
1000.0	309.0
1000.0	289.0
1300.0	338.0
1600.0	354.0
2000.0	410.0
2488.0	383.0
2915.0	350.0

	X	OBSERVED	PREDICTED	%RESIDUALS	WEIGHT FN
1	+2.0000E+00	+3.1990E+01	+3.1317E+01	+2.1051E+00	+4.4872E+00
2	+3.0000E+00	+3.1830E+01	+3.2478E+01	-2.0366E+00	+4.5325E+00
3	+4.0000E+00	+3.3990E+01	+3.4391E+01	-1.1811E+00	+3.9747E+00
4	+6.5000E+00	+4.2550E+01	+4.1673E+01	+2.0612E+00	+2.5363E+00
5	+1.0000E+01	+5.3350E+01	+5.3809E+01	-8.5965E-01	+1.6134E+00
6	+2.0000E+01	+7.9830E+01	+8.0726E+01	-1.1227E+00	+7.2057E-01
7	+3.0000E+01	+9.8790E+01	+9.6058E+01	+2.7659E+00	+4.7052E-01
8	+4.0000E+01	+1.0280E+02	+1.0417E+02	-1.3361E+00	+4.3453E-01
9	+6.5000E+01	+1.0840E+02	+1.0885E+02	-4.1686E-01	+3.9080E-01
10	+1.0000E+02	+1.0560E+02	+1.0533E+02	+2.5569E-01	+4.1179E-01
11	+1.6000E+02	+1.0670E+02	+1.0666E+02	+3.6751E-02	+4.0335E-01
12	+2.0000E+02	+1.1380E+02	+1.1424E+02	-3.9047E-01	+3.5459E-01
13	+3.0000E+02	+1.4820E+02	+1.4337E+02	+3.2607E+00	+2.0908E-01
14	+4.0000E+02	+1.7210E+02	+1.7470E+02	-1.5093E+00	+1.5504E-01
15	+6.5000E+02	+2.4320E+02	+2.4040E+02	+1.1503E+00	+7.7639E-02
16	+1.0000E+03	+2.8900E+02	+3.0395E+02	-5.1738E+00	+5.4981E-02
17	+1.3000E+03	+3.3800E+02	+3.3944E+02	-4.2703E-01	+4.0195E-02
18	+1.6000E+03	+3.5400E+02	+3.6194E+02	-2.2423E+00	+3.6644E-02
19	+2.0000E+03	+4.1000E+02	+3.7636E+02	+8.2047E+00	+2.7317E-02
20	+2.4880E+03	+3.8300E+02	+3.7584E+02	+1.8693E+00	+3.1305E-02
21	+2.9150E+03	+3.5000E+02	+3.6362E+02	-3.8908E+00	+3.7486E-02

CORRELATION MATRIX:

	1	2	3	4	5	6	7	8	9
1	+1.00	+.37	+.14	+.04	+.03	+.69	-.26	+.16	-.03
2	+.37	+1.00	+.63	+.22	+.13	+.85	-.89	+.66	-.14
3	+.14	+.63	+1.00	+.56	+.35	+.41	-.89	+.99	-.38
4	+.04	+.22	+.56	+1.00	+.85	+.13	-.38	+.66	-.89
5	+.03	+.13	+.35	+.85	+1.00	+.08	-.23	+.44	-1.00
6	+.69	+.85	+.41	+.13	+.08	+1.00	-.67	+.44	-.09
7	-.26	-.89	-.89	-.38	-.23	-.67	+1.00	-.89	+.26
8	+.16	+.66	+.99	+.66	+.44	+.44	-.89	+1.00	-.47
9	-.03	-.14	-.38	-.89	-1.00	-.09	+.26	-.47	+1.00

REDUCED CHI-SQUARED=14.38

DCLAG: ***** END *****
COORDINATES: 0 0
ELEVATION : 413 METER
AZIMUTH :

SCHOFIELD VES 15, ELEV=413M

B-SD	B	B+SD
2.942E+001	3.076E+001	3.216E+001
1.181E+002	1.542E+002	2.014E+002
5.209E+001	7.744E+001	1.151E+002
4.100E+002	5.532E+002	7.464E+002
2.327E-243	1.000E+000	4.297E+242
3.609E+000	4.229E+000	4.955E+000
8.992E+000	2.460E+001	6.728E+001
5.740E+001	1.096E+002	2.091E+002
4.779E+001	1.973E+003	8.148E+004

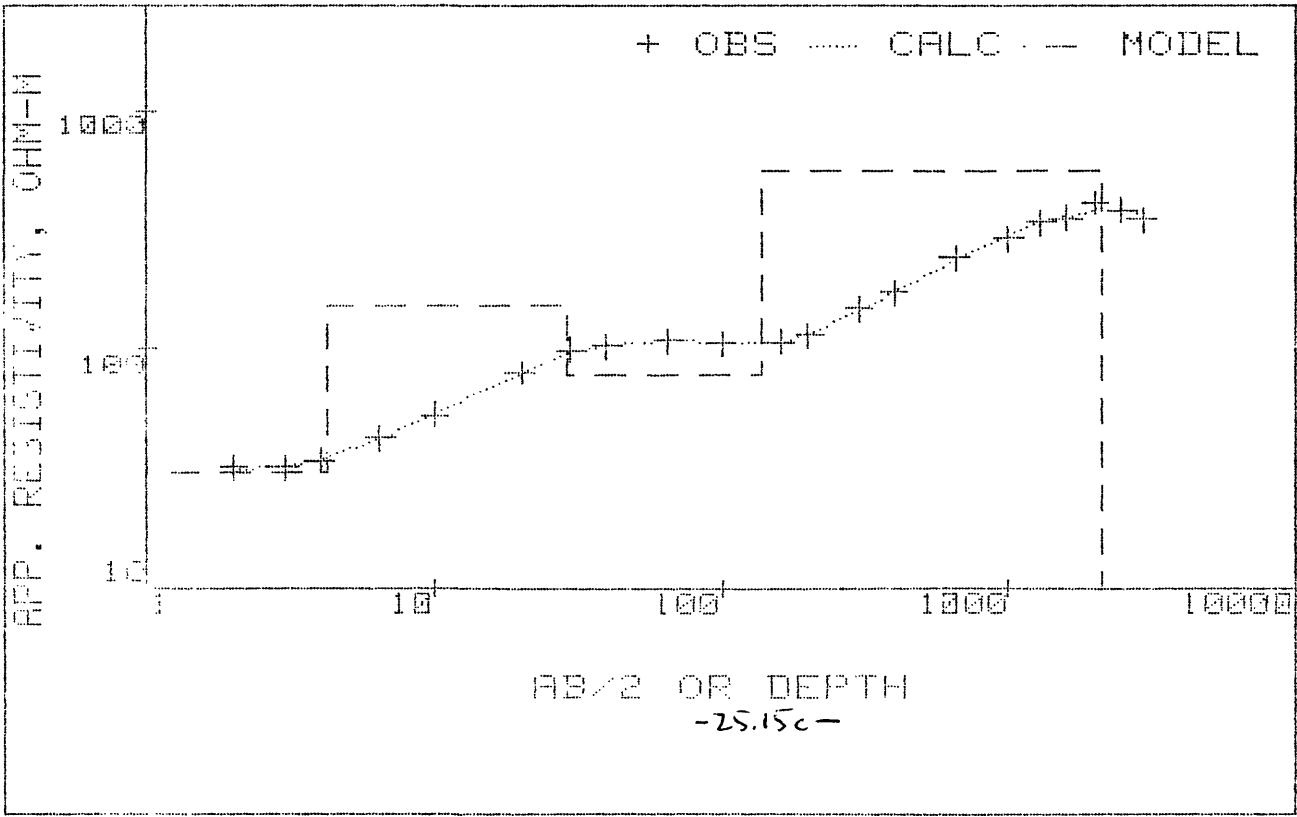
FINAL UNSCALED PARAMETERS--
(* denotes fixed value)

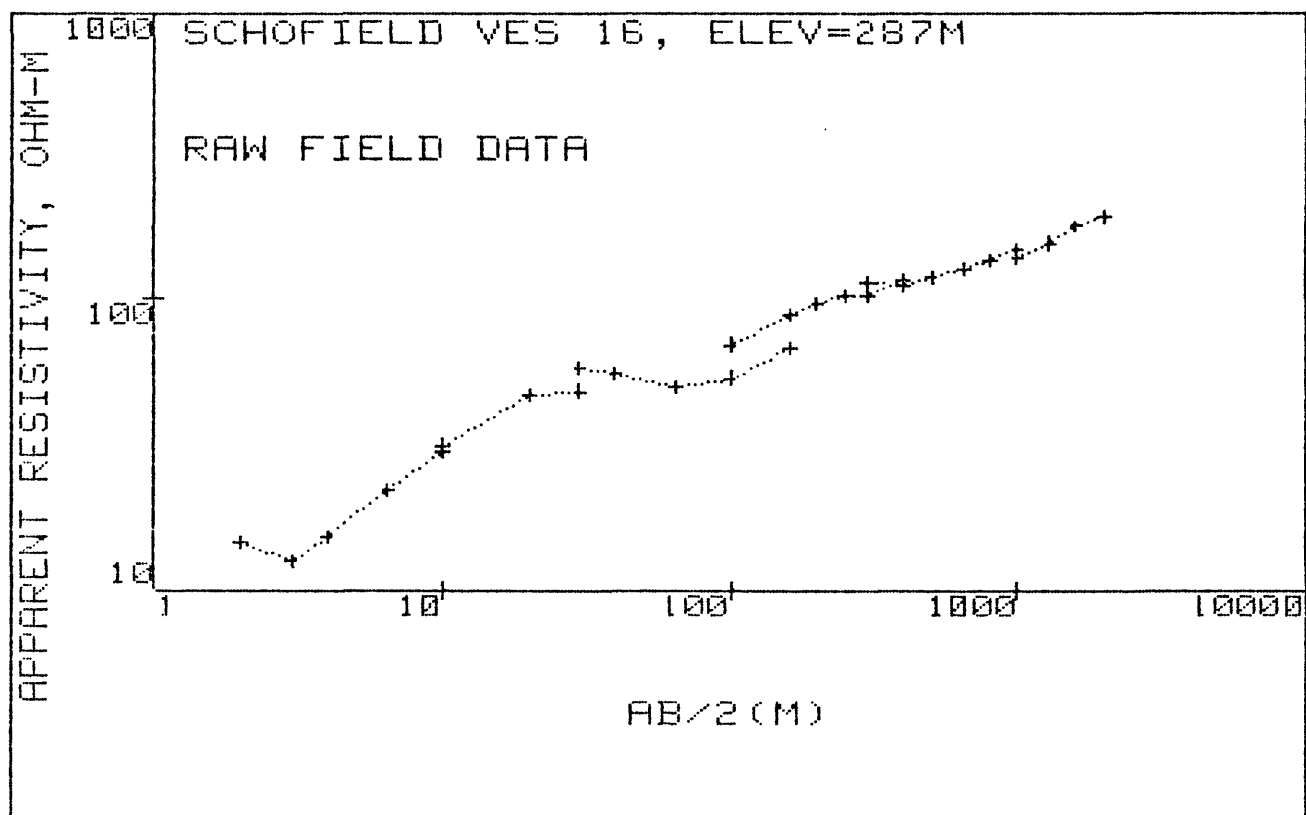
RESISTIVITY

DEPTH

1	3.07604974E+01	1	3.07604974E+01
2	1.54218765E+02	2	1.54218765E+02
3	7.74437488E+01	3	7.74437488E+01
4	5.53208404E+02	4	5.53208404E+02
5	1.00000000E+00	5	1.00000000E+00
6	4.22866051E+00	1	4.22866051E+00
7	2.45978059E+01	2	2.88264665E+01
8	1.09556036E+02	3	1.38382502E+02
9	1.97321062E+03	4	2.11159312E+03

SCHOFIELD VES 15, ELEV=413M





AB/2 (M) APP RHO

2.0	14.7
3.0	12.6
4.0	15.3
6.5	22.0
10.0	30.0
10.0	31.5
20.0	47.0
30.0	48.5
30.0	58.5
40.0	56.0
65.0	50.3
100.0	54.0
160.0	68.0
100.0	70.0
160.0	88.0
200.0	96.0
250.0	102.0
300.0	102.0
400.0	117.0
300.0	113.0
400.0	111.4
500.0	118.8
650.0	127.0
800.0	136.0
1000.0	148.0
1000.0	137.0
1300.0	155.0
1600.0	178.0
2000.0	196.0

	X	OBSERVED	PREDICTED	%RESIDUALS	WEIGHT FN
1	+2.0000E+00	+2.2920E+01	+1.6872E+01	+2.6389E+01	+5.4434E-02
2	+3.0000E+00	+1.9650E+01	+1.9778E+01	-6.5007E-01	+7.4058E+00
3	+4.0000E+00	+2.3860E+01	+2.3683E+01	+7.4037E-01	+5.0229E+00
4	+6.5000E+00	+3.4310E+01	+3.4514E+01	-5.9468E-01	+2.4292E+00
5	+1.0000E+01	+4.6790E+01	+4.7629E+01	-1.7939E+00	+1.3061E+00
6	+2.0000E+01	+6.9810E+01	+6.7808E+01	+2.8680E+00	+5.8676E-01
7	+3.0000E+01	+7.2030E+01	+7.1751E+01	+3.8730E-01	+5.5115E-01
8	+4.0000E+01	+6.8960E+01	+6.9321E+01	-5.2305E-01	+6.0132E-01
9	+6.5000E+01	+6.1940E+01	+6.2630E+01	-1.1143E+00	+7.4534E-01
10	+1.0000E+02	+6.6490E+01	+6.6633E+01	-2.1442E-01	+6.4682E-01
11	+1.6000E+02	+8.3730E+01	+8.2310E+01	+1.6964E+00	+4.0788E-01
12	+2.0000E+02	+9.1270E+01	+9.0182E+01	+1.1920E+00	+3.4327E-01
13	+2.5000E+02	+9.6970E+01	+9.6931E+01	+4.0243E-02	+3.0410E-01
14	+3.0000E+02	+9.6970E+01	+1.0141E+02	-4.5838E+00	+3.0410E-01
15	+4.0000E+02	+1.1120E+02	+1.0700E+02	+3.7765E+00	+2.3125E-01
16	+5.0000E+02	+1.1000E+02	+1.1108E+02	-9.7754E-01	+2.3633E-01
17	+6.5000E+02	+1.1760E+02	+1.1751E+02	+7.9332E-02	+2.0677E-01
18	+8.0000E+02	+1.2590E+02	+1.2531E+02	+4.6706E-01	+1.8040E-01
19	+1.0000E+03	+1.3700E+02	+1.3741E+02	-2.9672E-01	+1.5235E-01
20	+1.3000E+03	+1.5500E+02	+1.5674E+02	-1.1253E+00	+1.1902E-01
21	+1.6000E+03	+1.7800E+02	+1.7523E+02	+1.5559E+00	+9.0252E-02
22	+2.0000E+03	+1.9600E+02	+1.9704E+02	-5.3135E-01	+7.4436E-02

CORRELATION MATRIX:

	1	2	3	4	5	6	7	8	9	10	11
1	+1.00	+.82	+.45	+.22	+.13	+.08	+.95	-.77	+.41	-.22	+.18
2	+.82	+1.00	+.75	+.42	+.27	+.15	+.96	-.99	+.70	-.42	+.35
3	+.45	+.75	+1.00	+.80	+.57	+.33	+.61	-.84	+.99	-.80	+.71
4	+.22	+.42	+.80	+1.00	+.89	+.57	+.32	-.52	+.88	-1.00	+.97
5	+.13	+.27	+.57	+.89	+1.00	+.78	+.20	-.34	+.68	-.89	+.97
6	+.08	+.15	+.33	+.57	+.78	+1.00	+.11	-.20	+.41	-.57	+.72
7	+.95	+.96	+.61	+.32	+.20	+.11	+1.00	-.92	+.56	-.32	+.26
8	-.77	-.99	-.84	-.52	-.34	-.20	-.92	+1.00	-.80	+.52	-.45
9	+.41	+.70	+.99	+.88	+.68	+.41	+.56	-.80	+1.00	-.88	+.80
10	-.22	-.42	-.80	-1.00	-.89	-.57	-.32	+.52	-.88	+1.00	-.97
11	+.18	+.35	+.71	+.97	+.97	+.72	+.26	-.45	+.80	-.97	+1.00

REDUCED CHI-SQUARED=6.625

DCLAG: ***** END *****
 COORDINATES: 0 0
 ELEVATION : 287 METER
 AZIMUTH :

SCHOFIELD VES 16, ELEV=287M

B-SD	B	B+SD
1.177E+001	1.519E+001	1.960E+001
2.352E-001	2.967E+002	3.743E+005
3.479E-008	1.756E+001	8.060E+009
8.722E-105	5.245E+002	3.154E+109
4.109E+001	9.794E+001	2.335E+002
2.089E+002	3.603E+002	6.214E+002
1.250E+000	2.476E+000	4.905E+000
5.548E-004	5.661E+000	5.776E+004
4.486E-011	1.829E+001	7.458E+012
1.682E-112	1.949E+001	2.259E+114
1.128E+001	4.472E+002	1.773E+004

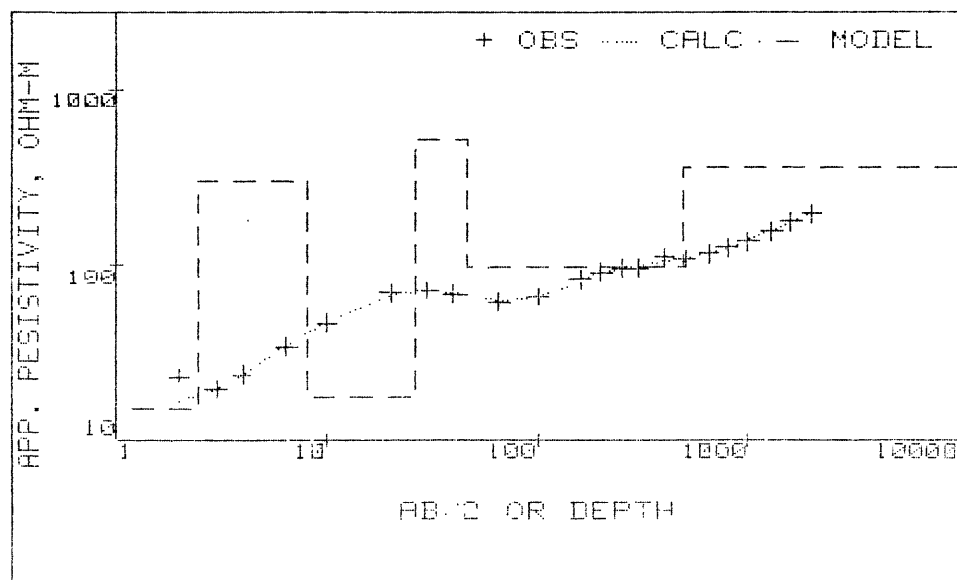
FINAL UNSCALED PARAMETERS---
 (* denotes fixed value)

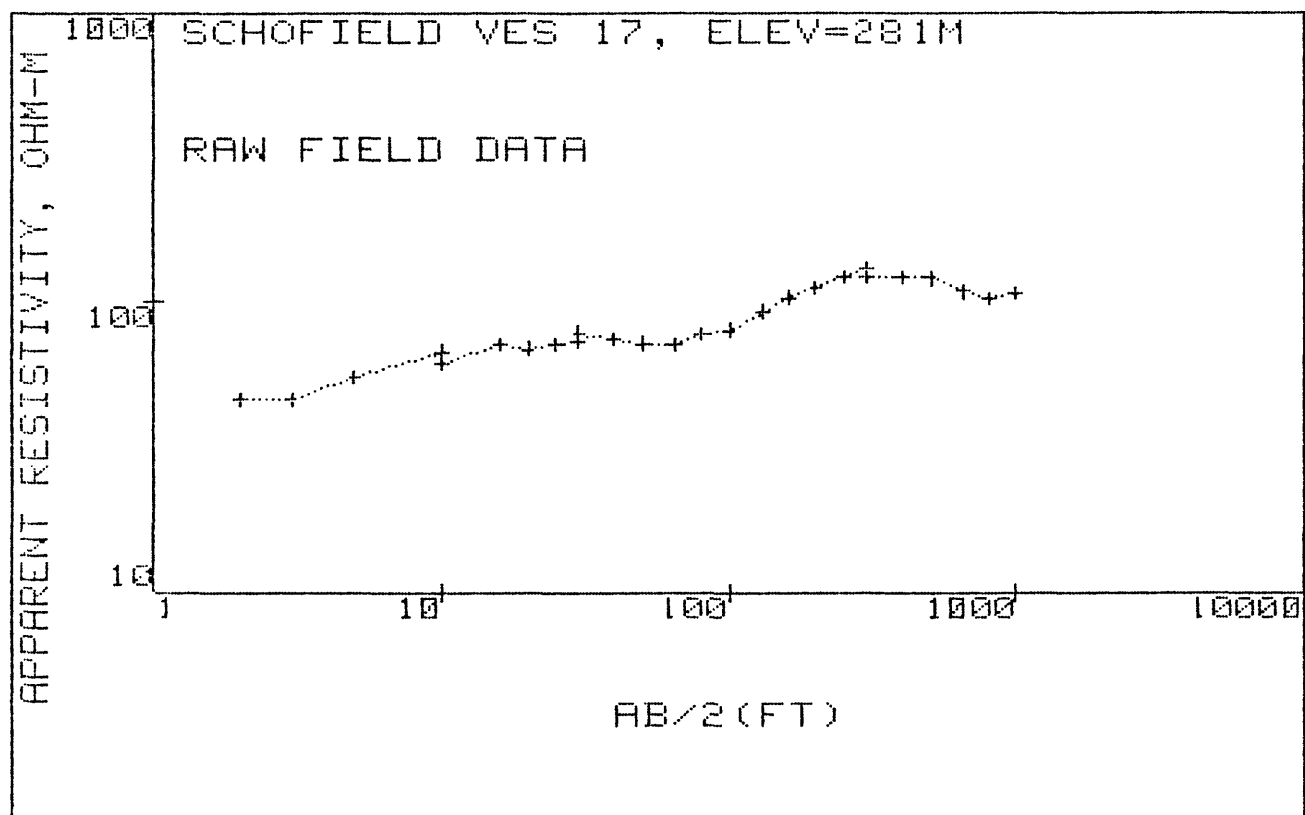
RESISTIVITY

DEPTH

1	1.51861772E+01	1	1.51861772E+01
2	2.96744381E+02	2	2.96744381E+02
3	1.75572740E+01	3	1.75572740E+01
4	5.24471141E+02	4	5.24471141E+02
5	9.79419875E+01	5	9.79419875E+01
6	3.60318152E+02	6	3.60318152E+02
7	2.47579480E+00	1	2.47579480E+00
8	5.66089705E+00	2	8.13669186E+00
9	1.82902085E+01	3	2.64269004E+01
10	1.94916043E+01	4	4.59185047E+01
11	4.47158382E+02	5	4.93076887E+02

SCHOFIELD VES 16, ELEV=287M





AB/2 (M) APP RHO

2.0	46.0
3.0	46.0
5.0	55.0
10.0	67.0
10.0	61.0
16.0	70.5
20.0	68.4
25.0	71.0
30.0	72.8
30.0	77.8
40.0	74.0
50.0	71.5
65.0	70.3
80.0	77.0
100.0	79.0
100.0	79.6
130.0	92.4
160.0	103.0
200.0	112.0
250.0	122.0
300.0	129.0
300.0	121.0
400.0	122.0
500.0	120.0
650.0	108.0
800.0	102.0
1000.0	107.0

	X	OBSERVED	PREDICTED	%RESIDUALS	WEIGHT FN
1	+2.0000E+00	+4.2300E+01	+4.1556E+01	+1.7580E+00	+2.8836E+00
2	+3.0000E+00	+4.2300E+01	+4.3581E+01	-3.0291E+00	+2.8836E+00
3	+5.0000E+00	+5.0580E+01	+4.9508E+01	+2.1195E+00	+2.0168E+00
4	+1.0000E+01	+6.1610E+01	+6.2365E+01	-1.2255E+00	+1.3593E+00
5	+1.6000E+01	+7.1210E+01	+6.9506E+01	+2.3935E+00	+1.0175E+00
6	+2.0000E+01	+6.9090E+01	+7.1354E+01	-3.2764E+00	+1.0809E+00
7	+2.5000E+01	+7.1710E+01	+7.1930E+01	-3.0694E-01	+1.0034E+00
8	+3.0000E+01	+7.3530E+01	+7.1479E+01	+2.7899E+00	+9.5430E-01
9	+4.0000E+01	+6.9940E+01	+6.9631E+01	+4.4201E-01	+1.0548E+00
10	+5.0000E+01	+6.7580E+01	+6.8191E+01	-9.0392E-01	+1.1297E+00
11	+6.5000E+01	+6.6440E+01	+6.8101E+01	-2.5002E+00	+1.1688E+00
12	+8.0000E+01	+7.2770E+01	+7.0344E+01	+3.3335E+00	+9.7434E-01
13	+1.0000E+02	+7.4660E+01	+7.5721E+01	-1.4215E+00	+9.2563E-01
14	+1.3000E+02	+8.6670E+01	+8.5865E+01	+9.2861E-01	+6.8688E-01
15	+1.6000E+02	+9.6610E+01	+9.5827E+01	+8.1046E-01	+5.5280E-01
16	+2.0000E+02	+1.0510E+02	+1.0669E+02	-1.5115E+00	+4.6710E-01
17	+2.5000E+02	+1.1440E+02	+1.1571E+02	-1.1470E+00	+3.9424E-01
18	+3.0000E+02	+1.2100E+02	+1.2042E+02	+4.7781E-01	+3.5241E-01
19	+4.0000E+02	+1.2200E+02	+1.2135E+02	+5.3439E-01	+3.4665E-01
20	+5.0000E+02	+1.2000E+02	+1.1678E+02	+2.6866E+00	+3.5831E-01
21	+6.5000E+02	+1.0800E+02	+1.0855E+02	-5.0765E-01	+4.4235E-01
22	+8.0000E+02	+1.0200E+02	+1.0369E+02	-1.6563E+00	+4.9592E-01
23	+1.0000E+03	+1.0700E+02	+1.0409E+02	+2.7238E+00	+4.5066E-01

CORRELATION MATRIX:

	1	2	3	4	5	6	7	8	9	10	11
1	+1.00	+.51	+.26	+.16	+.10	+.07	+.77	-.37	+.20	-.15	+.10
2	+.51	+1.00	+.73	+.48	+.33	+.23	+.88	-.89	+.59	-.45	+.33
3	+.26	+.73	+1.00	+.86	+.64	+.47	+.53	-.95	+.94	-.82	+.64
4	+.16	+.48	+.86	+1.00	+.91	+.73	+.33	-.73	+.98	-1.00	+.91
5	+.10	+.33	+.64	+.91	+1.00	+.90	+.22	-.52	+.84	-.95	+1.00
6	+.07	+.23	+.47	+.73	+.90	+1.00	+.16	-.38	+.65	-.77	+.91
7	+.77	+.88	+.53	+.33	+.22	+.16	+1.00	-.70	+.42	-.31	+.22
8	-.37	-.89	-.95	-.73	-.52	-.38	-.70	+1.00	-.83	+.69	-.52
9	+.20	+.59	+.94	+.98	+.84	+.65	+.42	-.83	+1.00	-.97	+.84
10	-.15	-.45	-.82	-1.00	-.95	-.77	-.31	+.69	-.97	+1.00	-.94
11	+.10	+.33	+.64	+.91	+1.00	+.91	+.22	-.52	+.84	-.94	+1.00

REDUCED CHI-SQUARED=7.843

DCLAG: ***** END *****
 COORDINATES: 0 0
 ELEVATION : 281 METER
 AZIMUTH :

SCHOFIELD VES 17, ELEV=281M

R-SD	R	R+SD
3.860E+001	4.043E+001	4.234E+001
7.155E+001	8.490E+001	1.008E+002
2.519E+001	5.209E+001	1.077E+002
3.102E-014	5.085E+002	8.337E+018
2.701E-091	1.784E+001	1.178E+093
1.774E-006	6.000E+002	2.029E+011
2.145E+000	2.819E+000	3.703E+000
3.592E+000	1.427E+001	5.668E+001
1.086E+000	5.199E+001	2.490E+003
7.795E-020	7.102E+001	6.471E+022
9.636E-093	1.557E+002	2.517E+096

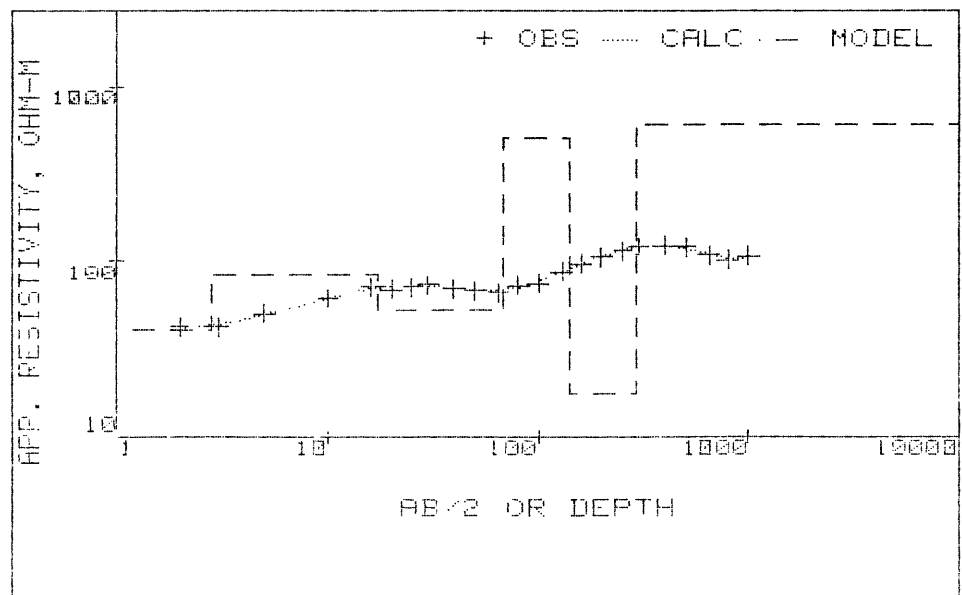
FINAL UNSCALED PARAMETERS--
 (* denotes fixed value)

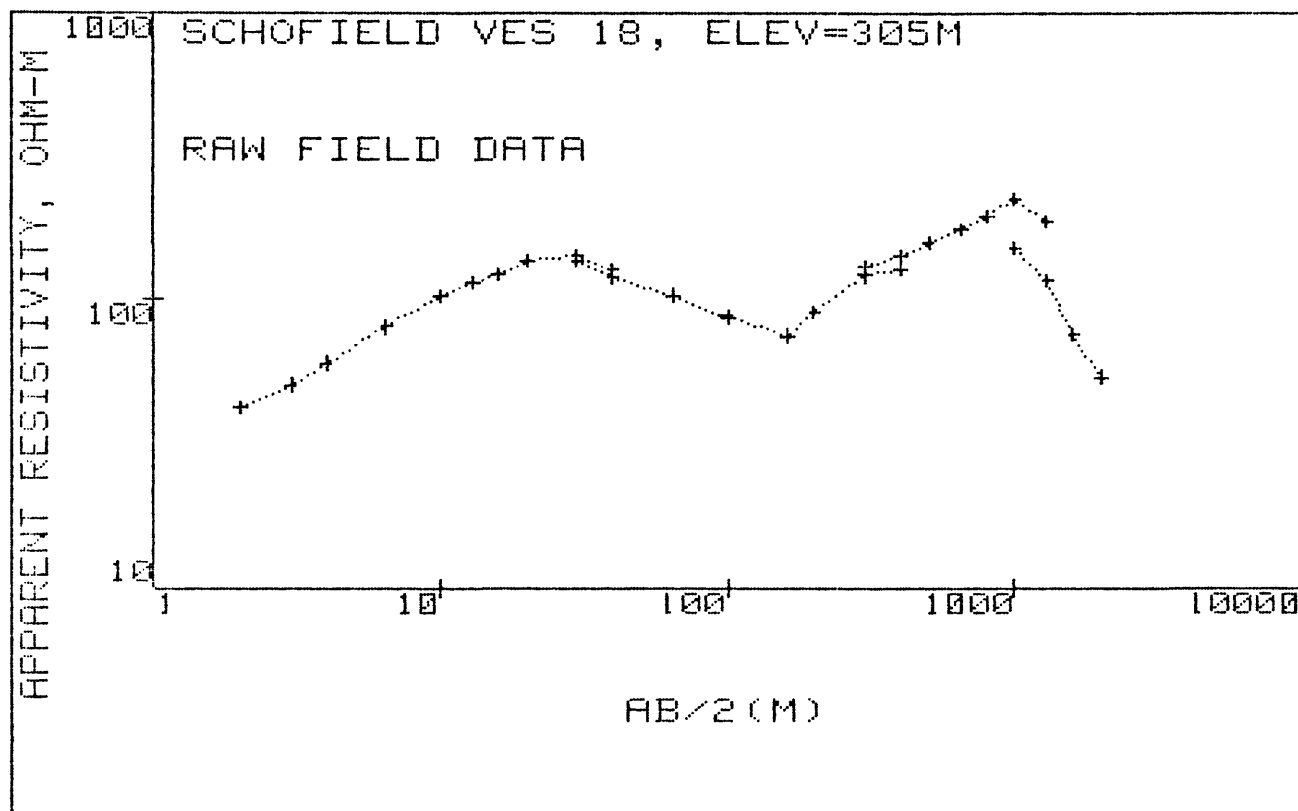
RESISTIVITY

DEPTH

1	4.04277544E+01	1	4.04277544E+01	
2	8.49033478E+01	2	8.49033478E+01	
3	5.20861830E+01	3	5.20861830E+01	
4	5.08542437E+02	4	5.08542437E+02	
5	1.78402342E+01	5	1.78402342E+01	
6	6.00000000E+02	6	6.00000000E+02	
7	2.81852225E+00			1 2.81852225E+00
8	1.42680770E+01			2 1.70865992E+01
9	5.19868017E+01			3 6.90734009E+01
10	7.10225835E+01			4 1.40095984E+02
11	1.55735794E+02			5 2.95831778E+02

SCHOFIELD VES 17, ELEV=281M





AB/2(M) APP RHO

2.0	42.1
3.0	50.6
4.0	60.2
6.5	79.9
10.0	102.0
10.0	102.0
13.0	113.0
16.0	121.0
20.0	134.0
30.0	142.0
40.0	126.0
30.0	134.0
40.0	119.0
65.0	103.0
100.0	86.0
100.0	88.2
160.0	74.5
200.0	89.0
300.0	120.0
400.0	127.0
300.0	130.0
400.0	140.7
500.0	158.0
650.0	176.0
800.0	195.0
1000.0	227.0
1300.0	186.0
1000.0	150.0
1300.0	116.0
1600.0	76.0
2000.0	54.0

	X	OBSERVED	PREDICTED	%RESIDUALS	WEIGHT FN
1	+2.0000E+00	+2.8670E+01	+2.8669E+01	+2.0259E-03	+4.6936E+00
2	+3.0000E+00	+3.4450E+01	+3.4462E+01	-3.5287E-02	+3.2507E+00
3	+4.0000E+00	+4.0990E+01	+4.0872E+01	+2.8847E-01	+2.2962E+00
4	+6.5000E+00	+5.4410E+01	+5.5012E+01	-1.1072E+00	+1.3032E+00
5	+1.0000E+01	+6.9450E+01	+6.9072E+01	+5.4455E-01	+7.9986E-01
6	+1.3000E+01	+7.6940E+01	+7.7345E+01	-5.2644E-01	+6.5171E-01
7	+1.6000E+01	+8.2390E+01	+8.3229E+01	-1.0181E+00	+5.6834E-01
8	+2.0000E+01	+9.1240E+01	+8.8411E+01	+3.1003E+00	+4.6343E-01
9	+3.0000E+01	+9.6690E+01	+9.2892E+01	+3.9285E+00	+4.1266E-01
10	+4.0000E+01	+8.5800E+01	+9.0503E+01	-5.4816E+00	+5.2406E-01
11	+6.5000E+01	+7.4290E+01	+7.5194E+01	-1.2169E+00	+6.9903E-01
12	+1.0000E+02	+6.2030E+01	+5.8930E+01	+4.9983E+00	+1.0027E+00
13	+1.6000E+02	+5.2390E+01	+5.5551E+01	-6.0332E+00	+1.4056E+00
14	+2.0000E+02	+6.2590E+01	+6.0999E+01	+2.5417E+00	+9.8480E-01
15	+3.0000E+02	+8.4390E+01	+7.8827E+01	+6.5918E+00	+5.4172E-01
16	+4.0000E+02	+8.9320E+01	+9.4047E+01	-5.2921E+00	+4.8357E-01
17	+5.0000E+02	+1.0140E+02	+1.0514E+02	-3.6932E+00	+3.7522E-01
18	+6.5000E+02	+1.1300E+02	+1.1482E+02	-1.6089E+00	+3.0213E-01
19	+8.0000E+02	+1.2520E+02	+1.1772E+02	+5.9783E+00	+2.4612E-01
20	+1.0000E+03	+1.4570E+02	+1.1409E+02	+2.1697E+01	+1.8173E-03
21	+1.3000E+03	+1.1940E+02	+9.9505E+01	+1.6663E+01	+2.7061E-03
22	+1.6000E+03	+7.6000E+01	+8.0985E+01	-6.5595E+00	+6.6793E-01
23	+2.0000E+03	+5.4000E+01	+5.7484E+01	-6.4524E+00	+1.3230E+00

CORRELATION MATRIX:

	1	2	3	4	5	6	7	8	9
1	+1.00	+.49	+.20	+.11	+.04	+.93	-.33	+.18	-.10
2	+.49	+1.00	+.57	+.32	+.12	+.71	-.79	+.52	-.30
3	+.20	+.57	+1.00	+.77	+.32	+.31	-.93	+.98	-.74
4	+.11	+.32	+.77	+1.00	+.65	+.17	-.62	+.88	-.99
5	+.04	+.12	+.32	+.65	+1.00	+.06	-.25	+.41	-.74
6	+.93	+.71	+.31	+.17	+.06	+1.00	-.49	+.29	-.16
7	-.33	-.79	-.93	-.62	-.25	-.49	+1.00	-.88	+.59
8	+.18	+.52	+.98	+.88	+.41	+.29	-.88	+1.00	-.85
9	-.10	-.30	-.74	-.99	-.74	-.16	+.59	-.85	+1.00

REDUCED CHI-SQUARED=26.38

DCLAB: ***** END *****
SCHOFIELD VES 18, ELEV=305M

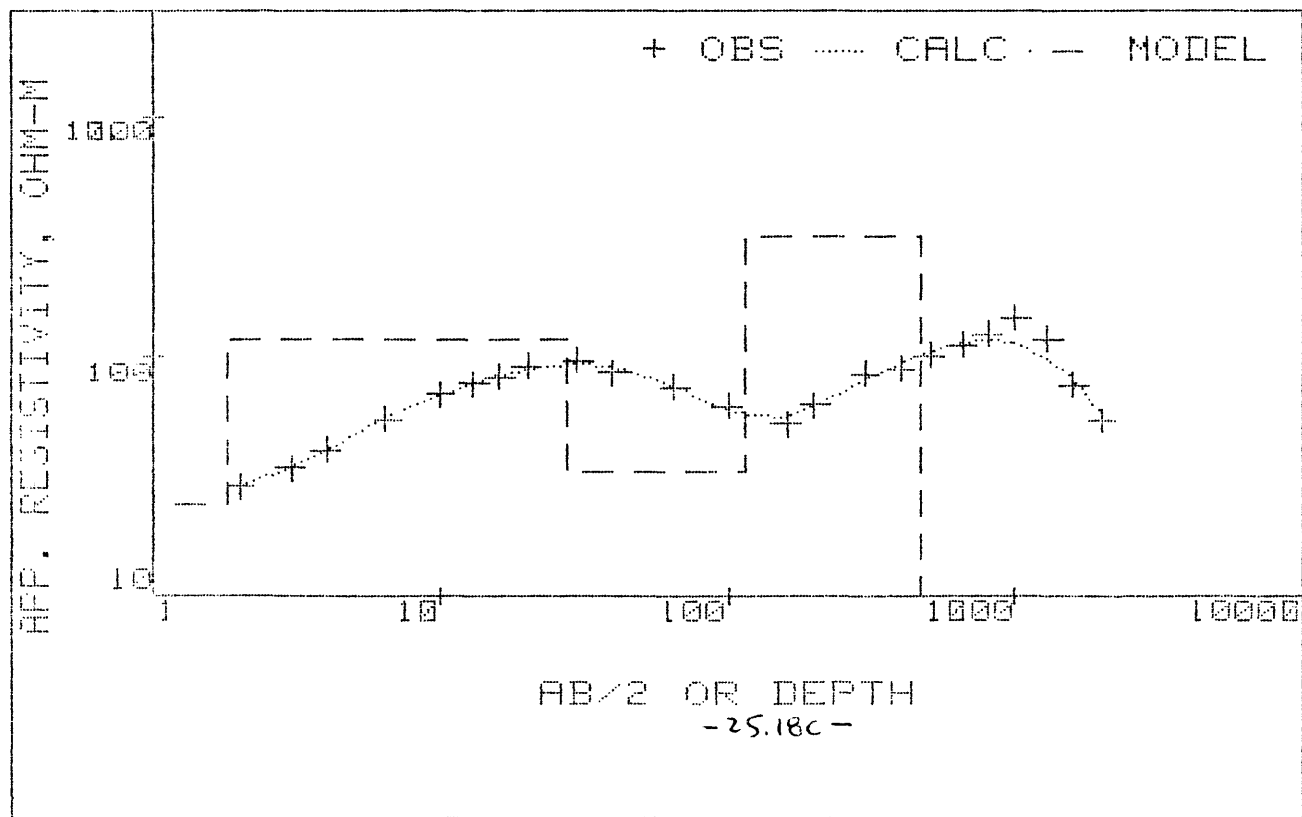
COORDINATES: 0 0
ELEVATION : 305 METER
AZIMUTH :

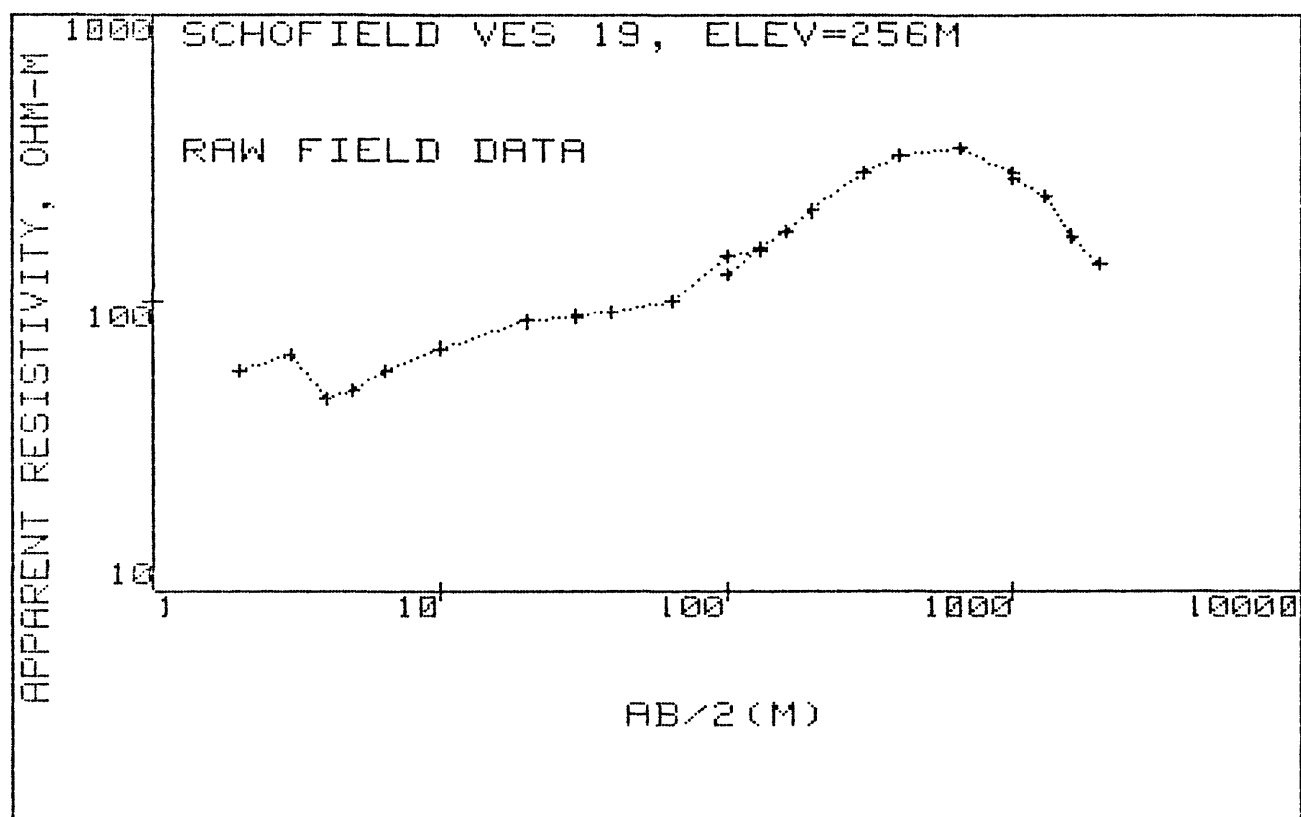
B-SD	B	B+SD
2.053E+001	2.447E+001	2.916E+001
1.016E+002	1.167E+002	1.341E+002
1.452E+001	3.311E+001	7.548E+001
4.145E+001	3.147E+002	2.389E+003
1.765E-015	1.000E+000	5.665E+014
1.336E+000	1.795E+000	2.412E+000
1.524E+001	2.605E+001	4.453E+001
2.284E+001	8.574E+001	3.218E+002
3.414E+001	3.505E+002	3.599E+003

FINAL UNSCALED PARAMETERS--
(* denotes fixed value)

RESISTIVITY		DEPTH	
1	2.44650918E+01	1	2.44650918E+01
2	1.16711700E+02	2	1.16711700E+02
3	3.31067664E+01	3	3.31067664E+01
4	3.14705058E+02	4	3.14705058E+02
5	1.00000000E+00	5	1.00000000E+00
6	1.79516866E+00	1	1.79516866E+00
7	2.60517110E+01	2	2.78468797E+01
8	8.57379062E+01	3	1.13584786E+02
9	3.50503169E+02	4	4.64087955E+02

SCHOFIELD VES 18, ELEV=305M





AB/2(M) APP RHO

2.0	57.3
3.0	65.0
4.0	46.3
5.0	49.1
6.5	57.3
10.0	68.4
10.0	68.2
20.0	85.2
30.0	88.0
30.0	89.0
40.0	91.0
65.0	99.9
100.0	145.0
130.0	151.0
100.0	124.0
130.0	152.0
160.0	174.0
200.0	206.0
300.0	280.0
300.0	279.0
400.0	324.0
650.0	347.0
1000.0	281.0
1000.0	271.0
1300.0	231.0
1600.0	169.0
2000.0	135.0

	X	OBSERVED	PREDICTED	%RESIDUALS	WEIGHT FN
1	+2.0000E+00	+5.1520E+01	+3.6283E+01	+2.9574E+01	+2.9570E-02
2	+3.0000E+00	+5.8440E+01	+3.8448E+01	+3.4209E+01	+2.2982E-02
3	+4.0000E+00	+4.1630E+01	+4.1545E+01	+2.0312E-01	+4.5289E+00
4	+5.0000E+00	+4.4150E+01	+4.5136E+01	-2.2331E+00	+4.0267E+00
5	+6.5000E+00	+5.1520E+01	+5.0646E+01	+1.6961E+00	+2.9570E+00
6	+1.0000E+01	+6.1500E+01	+6.1442E+01	+9.4148E-02	+2.0752E+00
7	+2.0000E+01	+7.6830E+01	+7.6357E+01	+6.1541E-01	+1.3297E+00
8	+3.0000E+01	+7.9350E+01	+8.0091E+01	-9.3392E-01	+1.2466E+00
9	+4.0000E+01	+8.1140E+01	+8.1114E+01	+3.2365E-02	+1.1922E+00
10	+6.5000E+01	+8.9070E+01	+8.9786E+01	-8.0399E-01	+9.8934E-01
11	+1.0000E+02	+1.2930E+02	+1.1762E+02	+9.0298E+00	+4.6947E-01
12	+1.3000E+02	+1.3460E+02	+1.4497E+02	-7.7075E+00	+4.3323E-01
13	+1.6000E+02	+1.6720E+02	+1.7104E+02	-2.2991E+00	+2.8076E-01
14	+2.0000E+02	+1.9800E+02	+2.0237E+02	-2.2049E+00	+2.0021E-01
15	+3.0000E+02	+2.6910E+02	+2.6299E+02	+2.2691E+00	+1.0839E-01
16	+4.0000E+02	+3.1250E+02	+3.0106E+02	+3.6622E+00	+8.0372E-02
17	+6.5000E+02	+3.3470E+02	+3.2585E+02	+2.6441E+00	+7.0064E-02
18	+1.0000E+03	+2.7100E+02	+2.7925E+02	-3.0437E+00	+1.0687E-01
19	+1.3000E+03	+2.3100E+02	+2.2381E+02	+3.1142E+00	+1.4709E-01
20	+1.6000E+03	+1.6900E+02	+1.7636E+02	-4.3573E+00	+2.7481E-01
21	+2.0000E+03	+1.3500E+02	+1.3205E+02	+2.1845E+00	+4.3066E-01

CORRELATION MATRIX:

	1	2	3	4	5	6	7	8	9
1	+1.00	+.72	+.49	+.38	-.40	+.94	-.51	+.49	-.37
2	+.72	+1.00	+.85	+.68	-.67	+.90	-.87	+.85	-.67
3	+.49	+.85	+1.00	+.90	-.73	+.67	-1.00	+1.00	-.89
4	+.38	+.68	+.90	+1.00	-.47	+.52	-.89	+.90	-1.00
5	-.40	-.67	-.73	-.47	+1.00	-.53	+.73	-.73	+.44
6	+.94	+.90	+.67	+.52	-.53	+1.00	-.69	+.67	-.51
7	-.51	-.87	-1.00	-.89	+.73	-.69	+1.00	-1.00	+.88
8	+.49	+.85	+1.00	+.90	-.73	+.67	-1.00	+1.00	-.89
9	-.37	-.67	-.89	-1.00	+.44	-.51	+.88	-.89	+1.00

REDUCED CHI-SQUARED=22.69

DLCLAG: ***** END *****
COORDINATES: 0 0
ELEVATION : 256 METER
AZIMUTH :

SCHOFIELD VES 19, ELEV=256M

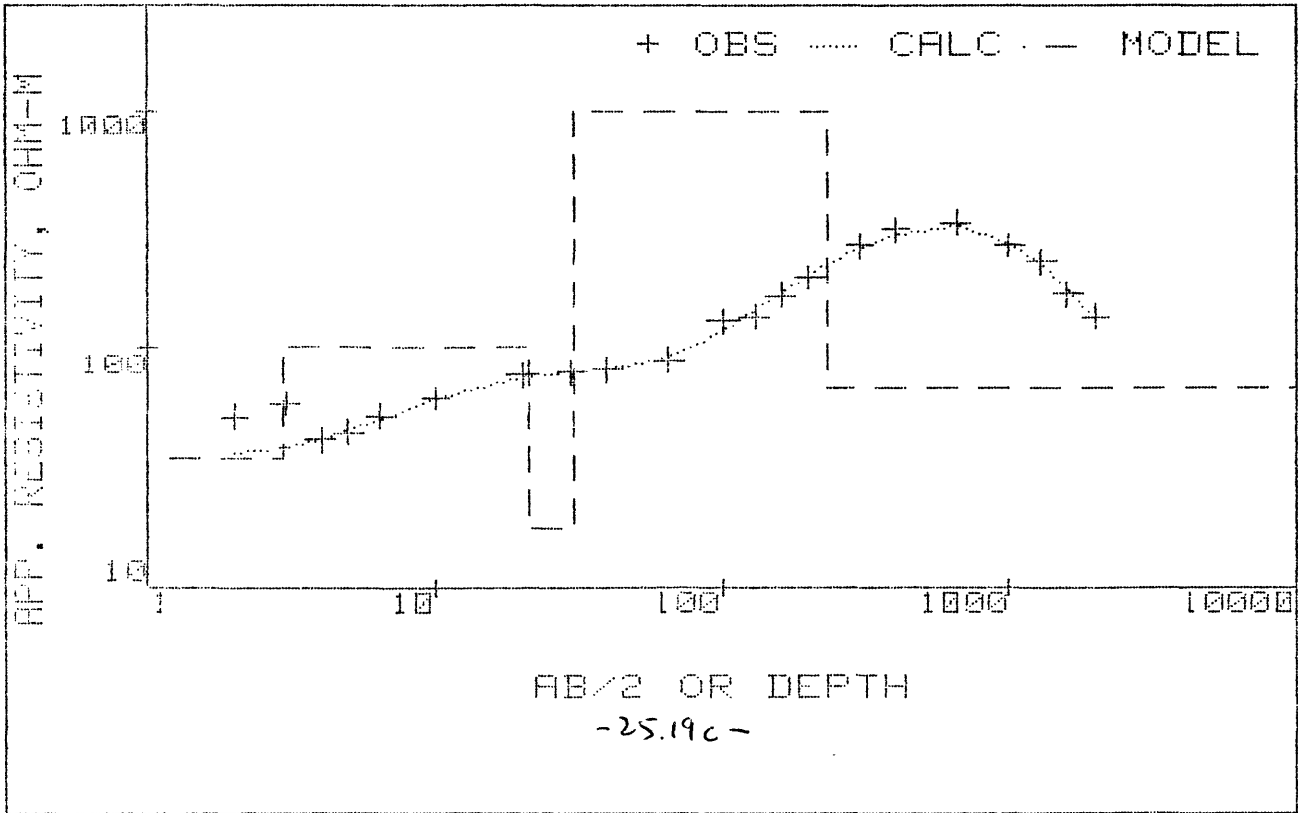
B-SD	B	B+SD
2.854E+001	3.511E+001	4.320E+001
6.188E+001	9.985E+001	1.611E+002
5.439E-076	1.788E+001	5.881E+077
1.329E+002	9.901E+002	7.375E+003
4.678E+001	6.747E+001	9.731E+001
1.643E+000	2.976E+000	5.390E+000
1.923E-004	1.845E+001	1.770E+006
1.884E-078	8.917E+000	4.220E+079
2.472E+001	2.001E+002	1.620E+003

FINAL UNSCALED PARAMETERS--
(% denotes fixed value)

RESISTIVITY DEPTH

1	3.51126705E+01	1	3.51126705E+01
2	9.98513024E+01	2	9.98513024E+01
3	1.78840079E+01	3	1.78840079E+01
4	9.90081576E+02	4	9.90081576E+02
5	6.74696765E+01	5	6.74696765E+01
6	2.97625449E+00	1	2.97625449E+00
7	1.84461670E+01	2	2.14224215E+01
8	8.91651914E+00	3	3.03389406E+01
9	2.00106812E+02	4	2.30445753E+02

SCHOFIELD VES 19, ELEV=256M



ACKNOWLEDGEMENTS

A great many people from the U.S. Geological Survey, Water Resources Division, Hawaii District contributed their time and efforts to the field work phase of this study. We thank Charlie Ewart, Pat Shade, Bill Souza, Isao Yamashiro, Santos Valenciano, Cynthia Miyaji, Marti Ikehara, Lodie Piniol, Salwyn Chinn, Pearl Tam, Kiyoshi Takasaki, Iwao Matsuoka, and Valerie Ige. Special thanks to Ben Jones, district chief during this study, Chip Hunt, overall project chief, Paul Eyre and Bud Sexton, field party organizers.

JK gratefully acknowledges Bob Bisdorf for very helpful comments on the study. KVS would like to thank Dr. Frank Peterson of the University of Hawaii Department of Geology and Geophysics and Dr. Stephen Lau of the Water Resources Research Center at the University.

REFERENCES

- Anderson, W.L., 1979, Program MARQDCLAG -- Marquardt inversion of DC-Schlumberger soundings by lagged-convolution: USGS Open-File Report 79-1432, 58 p.
- Bhattacharya, P.K. and Patra, H.P., 1968, Direct Current Geoelectric Sounding: Elsevier Publishing Co., Amsterdam.
- Dale, R.H. and Takasaki, K. J., 1976, Probable effects of increased pumpage from the Schofield ground-water body, Island of Oahu, Hawaii: USGS Water Resources Investigations 76-47.
- Keller, G.V., and Frischknecht, F.C., 1966, Electrical Methods in Geophysical Prospecting: Pergammon Press, Oxford.
- Mink, J.F., 1981, DBCP and EDB in Soil and Water at Kunia, Oahu, Hawaii: Report submitted to Del Monte Corporation, Oahu.
- Stearns, H.T. and Vaksvik, K.N., 1935, Geology and Ground-water Resources of the Island of Oahu, Hawaii: Div. of Hydrography Bull. 1, Territory of Hawaii, 479 p.
- Swartz, J.H., 1940, Geophysical investigations in the Hawaiian Islands: Trans. Amer. Geophys. Union, 20:292-298.
- Zohdy, A.A.R. and Jackson, D.B., 1969, Application of deep electrical soundings for ground-water exploration in Hawaii: Geophysics, 40:584-600.